Microbial metabolism of food allergens determines the severity of IgE-mediated anaphylaxis

Elisa Sánchez-Martínez[1,x], Liam E. Rondeau[2,x], Manuel Garrido-Romero[1,3], Bruna Barbosa da Luz[2], Dominic A. Haas[2], Gavin Yuen[2], Peter Hall[2], Rebecca Dang[2], Xuan-Yu Wang[2], Lucía Moreno-Serna[1], Celia López-Sanz[1], Emilio Nuñez-Borque[1], Maria Garrido-Arandia[4], Araceli Diaz-Perales[4], Yolanda R. Carrasco[5], Joshua F.E. Koenig[6], Tina D. Walker[6], Manel Jordana[6], Elena F. Verdu[2], Premysl Bercik[2], Giada De Palma[2] Michael G. Surette[2], Pedro Ojeda[7], Francisco Vega[8], Carlos Blanco[8], Lingdi Zhang[9], Supinda Bunyavanich[9], Wayne G. Shreffler[10], Sarita U. Patil[10], F. Javier Moreno[3], Rodrigo Jiménez-Saiz[1,6,11,y,*], Alberto Caminero[2,y,z,*]

[1]Department of Immunology, Instituto de Investigación Sanitaria Hospital Universitario de La Princesa (IIS-Princesa), Universidad Autónoma de Madrid (UAM), Madrid, Spain.

[2]Department of Medicine, Farncombe Family Digestive Health Research Institute, McMaster University, Hamilton, ON, Canada.

[3]Department of Bioactivity and Food Analysis, Instituto de Investigación en Ciencias de la Alimentación (CIAL), CSIC-UAM, CEI, Madrid, Spain.

[4]Centre for Plant Biotechnology and Genomics (CBGP), Universidad Politécnica de Madrid (UPM-INIA), Madrid, Spain.

[5]Department of Immunology and Oncology, Centro Nacional de Biotecnología (CNB)-CSIC, Madrid, Spain.

[6]Department of Medicine, McMaster Immunology Research Centre (MIRC), Schroeder Allergy and Immunology Research Institute (SAIRI), McMaster University, Hamilton, ON, Canada.

[7]Clínica de Asma y Alergia Dres. Ojeda, Madrid, Spain.

[8]Department of Allergy, Hospital Universitario de La Princesa, IIS-Princesa, Madrid, Spain.

[9]Department of Genetics and Genomic Sciences and Department of Pediatrics, Icahn School of Medicine at Mount Sinai, New York, New York, USA.

[10]Food Allergy Center and Center for Immunology and Inflammatory Diseases, Massachusetts General Hospital, Boston, Massachusetts, USA.

[11]Faculty of Experimental Sciences, Universidad Francisco de Vitoria (UFV), Madrid, Spain.

[x]First co-authors who contributed equally to this work.
[y]Senior co-authors.
[z]Lead contact.
*Correspondence: rodrigo.jimenez@ufv.es / @R_JimenezSaiz (R.J.-S); acamine@mcmaster.ca (A.C.) / @LabCaminero

SUMMARY

Anaphylaxis is an acute, potentially life-threatening reaction, often triggered by foods and largely mediated by IgE. Critically important to anaphylaxis are the factors that modulate its severity. The human microbiota is known to influence oral tolerance, but the microbial mechanisms directly involved in IgE-mediated anaphylaxis remain unknown. Here, we demonstrate that human saliva harbors peanut-degrading bacteria that metabolize immunodominant allergens (Ara h 1 and 2) and alter IgE-binding. Additionally, we provide *in vivo* evidence that oral bacteria metabolize peanut allergens, influencing systemic allergen exposure and anaphylaxis severity. Finally, in clinical studies, we observe that common peanut-degrading bacteria, such as *Rothia,* from the oral cavity, are more abundant in peanut-allergic patients who exhibit better tolerance to allergen exposure. Altogether, these results demonstrate that human microbiota modulates IgE-mediated reactions through allergen metabolism. We reveal a novel microbial mechanism with potential to prevent, or reduce, the severity of IgE-mediated anaphylaxis.

KEYWORDS

Allergens, Allergy, Anaphylaxis, IgE, Inflammation, Metabolism, Microbiota, Oral, Peanut, Saliva

INTRODUCTION

Inflammation typically restores homeostasis in response to tissue damage or infection but can cause immunopathology when dysregulated[1]. Anaphylaxis exemplifies this, with acute and potentially fatal outcomes within minutes. The main pathway of anaphylaxis is mediated by immunoglobulin (Ig)E and mast cells: upon allergen binding, mast cell-bound IgE induces the rapid release of inflammatory mediators like tryptase or leukotrienes, which drive the acute clinical manifestations of anaphylaxis[2-4]. Foods are common anaphylaxis triggers, with peanut (PN) being a leading cause of food-induced anaphylaxis and allergy-related deaths among children[5,6]. Food-anaphylaxis, particularly PN-triggered, is most common in North America and Europe and less frequent in the Asia-Pacific[7,8]. The burden of PN allergy is aggravated by its persistence in >70% of individuals, the absence of curative treatments, and the frequent accidental exposures despite patients' avoidance efforts[9-12].

The severity of food-induced anaphylaxis is not solely determined by allergen-specific IgE levels, as clinical reactivity is influenced by a complex interplay of genetic, environmental, dietary, and behavioral factors, as well as co-factors and comorbidities[13,14]. Notably, clinical observations often reveal a disconnect between serum levels of allergen-specific IgE—the key molecule involved in food-induced anaphylaxis—and clinical reactivity[15-17], underscoring the importance of elucidating additional modulators of anaphylaxis[2]. The human microbiota has gained considerable attention in this regard for its capacity to influence both oral tolerance and dietary antigen immunogenicity[18-22]. Indeed, studies have revealed differences in the intestinal microbiota composition of food-allergic patients[23-25]. Nonetheless, the microbial mechanisms involved in food-induced anaphylaxis remain largely unknown.

The oro-gastrointestinal microbiota is often regarded as a "second metabolic organ" capable of breaking down dietary components that are otherwise resistant to human digestive enzymes. Certain food allergens, including the immunodominant PN allergens Ara h 1 and 2[26,27], resist complete digestion by mammalian digestive enzymes[28,29]. Here, we demonstrate that human saliva and the small intestine contain PN-degrading bacteria capable of metabolizing immunodominant allergens and modulating IgE-specific immunity. We also show the *in vivo* capacity of these bacteria to participate in PN-metabolism, thereby modulating systemic allergen access and IgE-mediated anaphylaxis. Finally, in two clinical studies, we describe that common PN-degrading bacteria, such as *Rothia* from the oral cavity, are more abundant in allergic patients who exhibit higher allergen thresholds to controlled allergen exposure. These results demonstrate the human microbiota's ability to modulate IgE-mediated reactions through allergen metabolism and reveal a novel microbial mechanism with translational potential to prevent or mitigate IgE-mediated anaphylaxis.

98 # RESULTS

99 ## Microbiota participates in peanut allergen metabolism

100 To study the role of microbes in PN metabolism, we used C57BL/6 mice with distinct
101 microbiota compositions: germ-free (GF), specific pathogen-free (SPF; diverse), and
102 altered Schaedler flora (ASF; stable with limited species) (**Figure S1**). Mice were gavaged
103 with PN and sacrificed after 40 minutes (**Figure 1A**). The quantities of PN allergens Ara
104 h 1 and 2 were higher in small intestinal content of GF and ASF mice, compared to mice
105 with diverse SPF microbiota (**Figure 1B**). Moreover, microbial alpha-diversity across
106 groups correlated inversely with Ara h 1 and 2 in the small intestine (**Figure S1D**). We
107 also detected variations in the concentrations of these allergens systemically. Compared
108 to SPF mice, GF and ASF mice presented higher serum levels of Ara h 1 but lower serum
109 levels of Ara h 2 (**Figure 1C**). To determine whether these differences were due to
110 variations in the digestive capacity, intestinal contents of PN-naïve mice were incubated
111 with PN (crude PN extract, CPE) *ex vivo*. The intestinal contents of SPF mice degraded
112 Ara h 1 and 2 more effectively than those of GF and ASF mice (**Figure 1D**). We
113 hypothesized that microbial metabolism influenced the differences observed in PN
114 allergen digestion and attempted to isolate PN-degrading bacteria from SPF and ASF
115 mouse intestinal contents. Notably, PN-degrading bacteria were present in the small and
116 large intestines of SPF mice but not found in ASF mice. While various PN-degrading
117 bacterial species were identified, their capacity to digest Ara h 1 and 2 varied by bacterial
118 strain (**Figure 1E**). Together, these results demonstrate that the intestinal microbiota
119 metabolizes PN allergens and influences their systemic availability.

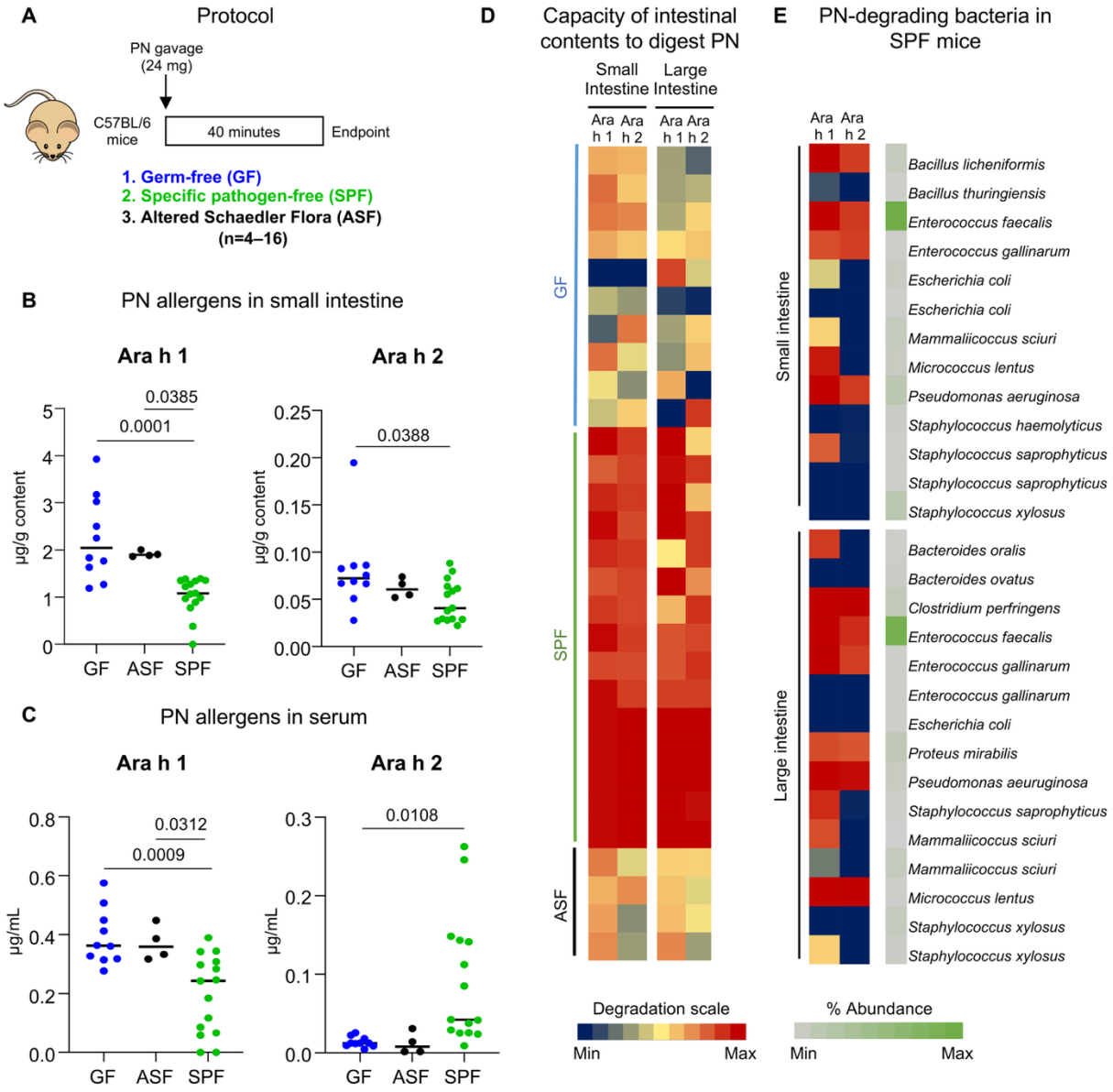

Figure 1. Microbiota participates in allergen metabolism *in vivo*.
(A) Experimental design. Germ-free (GF), specific pathogen-free (SPF), and altered Schaedler flora (ASF) C57BL/6 mice received PN intragastrically (i.g.). Peripheral blood and intestinal contents were collected 40 minutes post-PN delivery. n=4–16 mice per group; 2 independent experiments. (B–C) PN allergens (Ara h 1 and 2) in small intestinal content (B) and serum from peripheral blood (C). Each dot=one mouse. *P* values were calculated using one-way ANOVA with Tukey's post-hoc test. (D) Heatmap showing digestion capacity of GF, ASF, and SPF microbiota against Ara h 1 and 2. PN-naïve intestinal contents were incubated with PN allergens (CPE) *in vitro* and remaining allergens quantified. Each row = one mouse. Degradation capacity is expressed as % degraded relative to control incubations with CPE alone (blue=0%, red=100%). Statistics: one-way ANOVA with Tukey's post-hoc test. Significance levels: Small intestine Ara h 1: GF vs. SPF ($P<0.0001$), ASF vs. SPF ($P=0.0290$). Small intestine Ara h 2: GF vs. SPF ($P<0.0001$), ASF vs. SPF ($P<0.0001$). Large intestine Ara h 1: GF vs. SPF ($P<0.0001$), ASF vs. SPF ($P=0.0289$). Large intestine Ara h 2: GF vs. SPF ($P<0.0001$), ASF vs. SPF ($P<0.0024$). (E) Heatmap of PN-degrading isolates and abundance of bacterial isolates from the small and large intestine of SPF mice. Isolates were obtained by plating SPF intestinal contents on PN-agar and selecting colonies with hydrolytic halos, indicative of PN

degradation. Isolates were incubated in liquid media with CPE to assess Ara h 1 and 2 degradation. Each row=one isolate. Allergen degradation is shown using the same blue-red scale as in (D). Relative abundance is represented on a green scale (low=light, dark=high), based on the frequency of isolation relative to the total number of isolates. See also Figure S1.

Mice with limited peanut-degrading bacteria exhibit stronger mucosal anaphylaxis markers

To investigate the impact of microbial PN metabolism on acute allergic reactions, we used ASF and SPF C3H/HeN mice, a strain more susceptible to type 2 immunity and anaphylaxis upon oral PN challenge[30]. Consistent with our previous findings in C57BL/6 mice, ASF mice exhibited a reduced capacity to metabolize PN compared to SPF C3H/HeN mice (**Figure S2A–C**). ASF and SPF C3H/HeN mice were sensitized to PN with cholera toxin (CT) via intragastric (i.g.) administration once per week for 6 weeks, followed by an i.g. PN-challenge to assess anaphylactic reactions to PN allergens (**Figure 2A**). ASF mice, which present reduced PN-degrading bacteria, had higher serum levels of PN-specific IgE than SPF mice (**Figure 2B**). They also exhibited higher serum levels of mucosal mast cell protease-1 (mMCP-1), indicating local activation of effector cells in the gastrointestinal tract, along with systemic hypothermia following PN challenge (**Figure 2C & Figure S3A**). To bypass the influence of microbial PN metabolism on IgE production, we sensitized SPF and ASF mice with PN + CT via intraperitoneal (i.p.) injection (**Figure 2A**). While both groups exhibited similar serum levels of PN-specific IgE (**Figure 2D**), ASF mice had higher serum mMCP-1 levels and developed hypothermia following PN challenge (**Figure 2E & Figure S3B)**. We further bypassed the endogenous capacity to generate allergen-specific IgE in the sensitization process by passively transferring serum from PN-allergic mice into SPF- and ASF-colonized mice (**Figure 2A**). Both mouse strains presented similar levels of PN-specific IgE in the serum after passive sensitization (**Figure 2F**). However, ASF mice again exhibited higher serum levels of mMCP-1, platelet-activating factor acetylhydrolase (PAF-AH), and hypothermia (**Figure 2G & Figure S3C–D**). These results demonstrate that the presence of certain microbes at the site of allergen challenge can protect from anaphylaxis.

To further investigate how microbiota composition influences anaphylactic outcomes, we characterized bacterial community structure and diversity in ASF and SPF mice across all sensitization protocols (**Figure S4A**). As expected, ASF mice exhibited lower alpha-diversity compared to SPF mice, and this reduction in observed species was associated with increased intestinal levels of Ara h 1 and 2 following PN challenge (**Figure S4B**). Moreover, Ara h 1 and 2 levels inversely correlate with alpha-diversity across sensitization methods (**Figure 2H & Figure S4C**), and serum mMCP-1 concentrations showed similar negative correlations with alpha-diversity in i.g., i.p., and passive models (**Figure S4D**). These findings demonstrate that microbial complexity is linked to enhanced PN degradation and reduced effector responses.

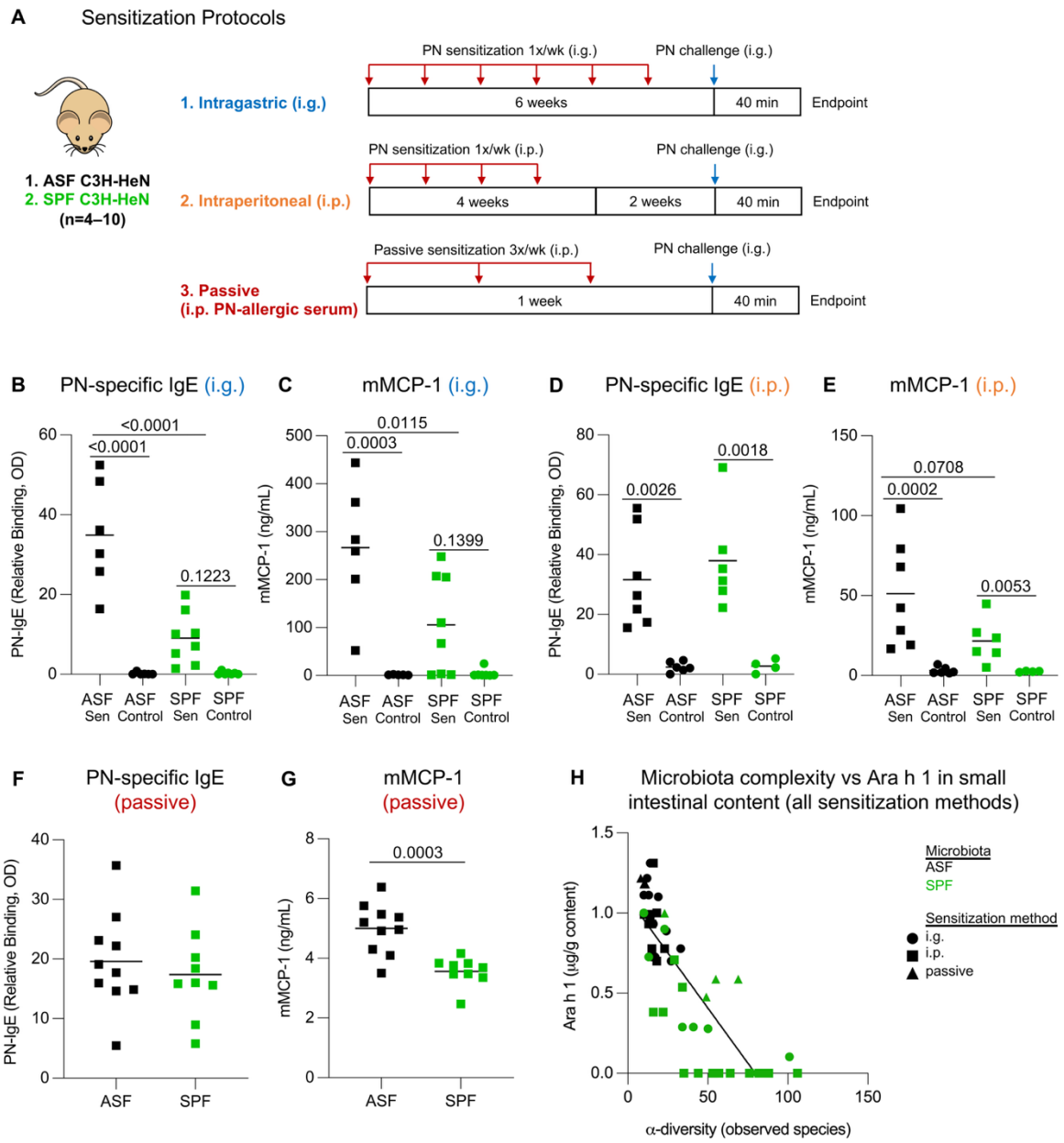

Figure 2. Limited microbial peanut metabolism amplifies mucosal anaphylaxis markers. (A) Experimental design for peanut (PN) sensitization and challenge of C3H-HeN mice colonized with ASF and SPF microbiota. Mice were sensitized (1) intragastrically (i.g.; PN + cholera toxin) once per week for 6 weeks, (2) intraperitoneally (i.p.; PN + cholera toxin) once per week for 4 weeks, and (3) passively (i.p.; serum from PN-allergic mice) once every 48 hours, 3 times. Sensitized mice were challenged with a PN bolus i.g. and sacrificed 40 minutes later. (B–C) Serum PN-specific IgE (B) and serum mucosal mast cell protease 1 (mMCP-1) (C) of i.g. sensitized ASF and SPF mice after PN challenge. (D-E) Serum PN-specific IgE (D) and serum mMCP-1 (E) of i.p. sensitized ASF and SPF mice after PN challenge. (F–G) Serum PN-specific IgE (F), serum mMCP-1 (G) passively sensitized ASF and SPF mice after PN challenge. (H) Correlation plot of Ara h 1 against alpha-diversity in small intestinal content across sensitization methods (y=-0.01375x + 1.095, R^2=0.7053, P<0.0001). n=4–10 mice per group; 2 independent experiments for each sensitization method; each dot=one mouse. P values were calculated using one-way ANOVA with Tukey's post-hoc test (B–E) and Student's t-test (F–G). See also Figures S2-S4.

192 **Human oral cavity and small intestine harbor bacteria with the capacity to digest**
193 **peanut**

194 Food-induced allergic reactions can occur within minutes of allergen exposure. Given this
195 rapid onset, we investigated whether humans harbor PN-degrading bacteria in the oral
196 cavity and the small intestine. We analyzed saliva from 13 volunteers and jejunum
197 aspirates from 5 volunteers with no reported food allergies (**Table S1**). Analysis of the
198 oral and small intestinal microbiota composition via 16S rRNA sequencing revealed
199 donor-specific profiles, with *Prevotella*, *Rothia,* and *Fusobacterium* as the most abundant
200 genera in the saliva and *Streptococcus* as the dominant genus in the jejunum (**Figure**
201 **3A**). Among these taxa, *Rothia* was particularly notable, accounting for up to 43% of the
202 salivary microbiota and as much as 14% of the small intestinal microbiota. We then plated
203 saliva samples on PN-enriched media agar to isolate bacteria with PN-degrading
204 capacity, selecting strains that produced a hydrolytic halo, indicating their ability to
205 degrade PN (**Figure 3B**). PN-degrading bacteria were detected in nearly all donors, with
206 *Rothia, Staphylococcus, Streptococcus,* and *Veillonella* being the most frequently
207 isolated genera. Each isolated bacterial strain was then incubated with CPE to facilitate
208 allergen digestion, and the remaining Ara h 1 and 2 were quantified. Additionally, we
209 screened a well-characterized bacterial collection for PN-degrading potential[31]. While
210 many bacterial strains exhibited PN digestion capabilities on agar plates, their capacity to
211 degrade the allergens varied by taxon and strain (**Figure 3C**). *Rothia*, a dominant oral
212 genus, consistently degraded Ara h 1 and 2 *in vitro*. This activity was observed in all
213 tested *Rothia* strains and a phylogenetically related genus, *Micrococcus*, suggesting a
214 conserved PN-degrading function (**Figure 3C**). In contrast, most strains from other PN-
215 degrading genera such as *Gemella* or *Streptococcus* lacked significant allergen-
216 degrading capacity (**Figure S5A**). While *Staphylococcus* strains showed strong PN-
217 degrading potential, their ability to degrade PN allergens was strain-specific (**Figure 3C**).
218 Like the oral cavity, we identified strains of *Streptococcus*, *Rothia* and *Staphylococcus* in
219 the small intestine of healthy individuals with PN allergen-degrading capacity (**Figure**
220 **S5C**). Altogether, these findings demonstrate that oral and intestinal bacteria degrade PN
221 allergens with genus- and strain-dependent efficiency.

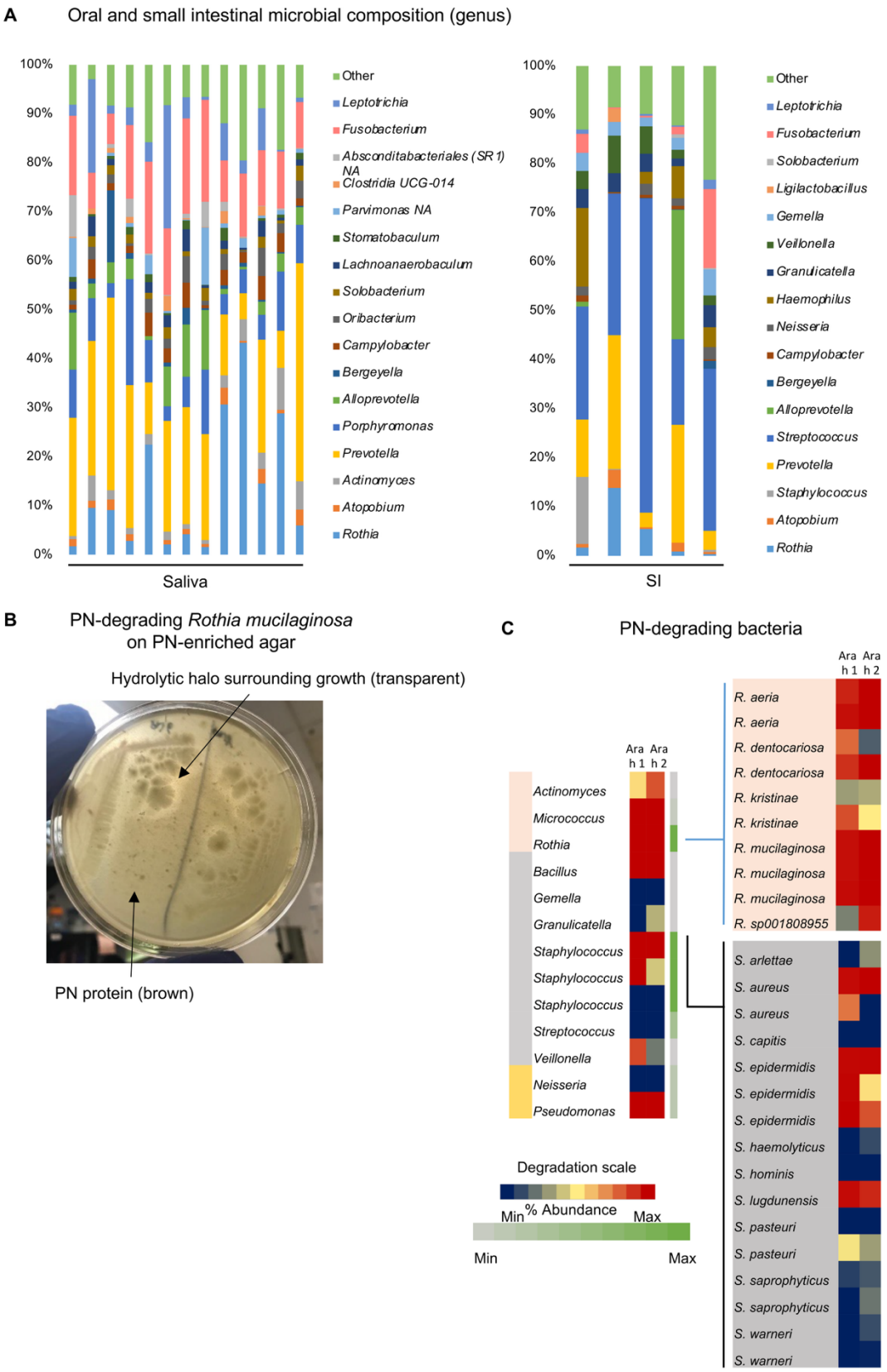
A
Oral and small intestinal microbial composition (genus)
100%
90%
80%
70%
60%
50%
40%
30%
20%
10%
0%
Saliva
SI
Other
Leptotrichia
Fusobacterium
Absconditabacteriales (SR 1) NA
Clostridia UCG-014
Parvimonas NA
Stomatobaculum
Lachnoanaerobaculum
Solobacterium
Oribacterium
Campylobacter
Bergeyella
Alloprevotella
Porphyromonas
Prevotella
Actinomyces
Atopobium
Rothia
Solobacterium
Ligilactobacillus
Gemella
Veillonella
Granulicatella
Haemophilus
Neisseria
Streptococcus
Staphylococcus
B
PN-degrading Rothia mucilaginosa on PN-enriched agar
Hydrolytic halo surrounding growth (transparent)
PN protein (brown)
C
PN-degrading bacteria
Ara h 1
Ara h 2
Actinomyces
Micrococcus
Rothia
Bacillus
Gemella
Granulicatella
Staphylococcus
Staphylococcus
Staphylococcus
Streptococcus
Veillonella
Neisseria
Pseudomonas
R. aeria
R. aeria
R. dentocariosa
R. dentocariosa
R. kristinae
R. kristinae
R. mucilaginosa
R. mucilaginosa
R. mucilaginosa
R. sp001808955
S. arlettae
S. aureus
S. aureus
S. capitis
S. epidermidis
S. epidermidis
S. epidermidis
S. haemolyticus
S. hominis
S. lugdunensis
S. pasteuri
S. pasteuri
S. saprophyticus
S. saprophyticus
S. warneri
S. warneri
Degradation scale
Min
% Abundance
Max
Min
Max

222

223

Figure 3. Human saliva harbors peanut-degrading bacteria.
(A) Genus-level relative abundance of bacteria in saliva (n=13) and jejunal aspirates (n=5) from non-peanut (PN)-allergic individuals. Taxa <1% relative abundance not shown. (B) PN-degrading bacteria (*Rothia mucilaginosa*) from human saliva on PN-agar showing zone of clearance. (C) PN-degrading bacteria isolated from human saliva, identified for whole PN-degradation by growth on PN-agar and assessed for Ara h 1 and 2 degradation. Heatmaps show allergen degradation (blue=0%, red=100% relative to crude peanut extract control) and isolate abundance (green scale, light=low, dark=high). Data presented at the genus and species levels for *Actinomycetota* (pink), *Bacillota* (grey) and *Pseudomonota* (yellow). See also Figure S5.

Peanut allergens are degraded by bacteria

To further study the microbial capacity for PN allergen digestion, we conducted proteomic analyses focusing on key bacterial taxa. We selected two primary genera: *Rothia*, a dominant oral taxon with efficient allergen-digestion capacity, and *Staphylococcus,* which has been previously associated with allergic diseases (**Figure S5B**)[32]. First, we confirmed the capacity of these taxa to degrade the main PN allergens Ara h 1 (64 kDa) and Ara h 2 (17 kDa) using SDS-PAGE (**Figure 4A–B**). To strengthen these data, we performed tandem mass spectrometry analysis on the fraction below 3 kDa, screening for PN-derived peptides after bacterial digestion. Given the low relative abundance of Ara h 2 in the PN matrix (5.9-9.3% of total protein) and the noise introduced by bacterial proteins in the samples, we centered the proteomic analyses on Ara h 1 (12-16% of total protein)[33]. We identified several Ara h 1-derived peptides following PN digestion by strains of *Rothia* and *Staphylococcus*. As expected, we quantified more peptides from bacterial strains that degraded PN more extensively (*Rothia* R3, 9 peptides; S1, 11 peptides; S3, 13 peptides), according to the electrophoretic analysis. Using molecular modelling, we visualized these peptides, marking in yellow peptides digested by bacteria (**Figure 4C–F**). Interestingly, the identified peptides shown in purple have been reported as clinically relevant IgE epitopes recognized by PN-allergic patients[34-45]. These epitopes are distributed across various regions of the 3D structure of Ara h 1, highlighting the lack of localization of the identified peptides to a single structural domain (**Figure 4C–F**). Considering the ability of these *Rothia* and *Staphylococcus* species to degrade PN, we evaluated their impact on human IgE-binding to PN after bacterial digestion by Western blotting. We used a pool of sera from PN-allergic patients with elevated levels of Ara h 1- and Ara h 2-specific IgE (**Table S2**). The analysis showed a substantial reduction in IgE-binding to PN proteins overall, and to Ara h 1 and 2 in particular (**Figure 4G–H**). To precisely define the impact of microbial metabolism on main PN allergens, we mono-sensitized mice to native Ara h 1 or recombinant Ara h 2 and used their sera to analyze IgE recognition of the digested PN fragments via Western blotting (**Figure 4I–J**). *Rothia* digestion of PN reduced IgE-binding to Ara h 1, most notably by strain R3. Similarly, *Staphylococcus* strains (S1 and S3) completely degraded and reduced IgE-binding to Ara h 1, though some residual fragments retained IgE-binding capacity. *Staphylococcus* strains with lower PN-degrading capacity, such as S2, showed less efficacy in reducing binding to Ara h 1 (**Figure 4I)**. On the other hand, sera from mice sensitized with recombinant Ara h 2

267 predominantly recognized a band around ~37 kDa, likely representing its oligomerized
268 forms. Nevertheless, PN-digestion by *Rothia* strains impaired Ara h 2 recognition by IgE,
269 particularly with strain R3. *Staphylococcus* strains S1 and S3 also reduced IgE-binding to
270 Ara h 2, while strain S2 showed little effect (**Figure 4J)**. Altogether, these findings
271 demonstrate the potential of *Rothia* and *Staphylococcus* strains to modify the structure of
272 key PN allergens, including IgE-binding epitopes, thereby altering their recognition by
273 both murine and human IgE.

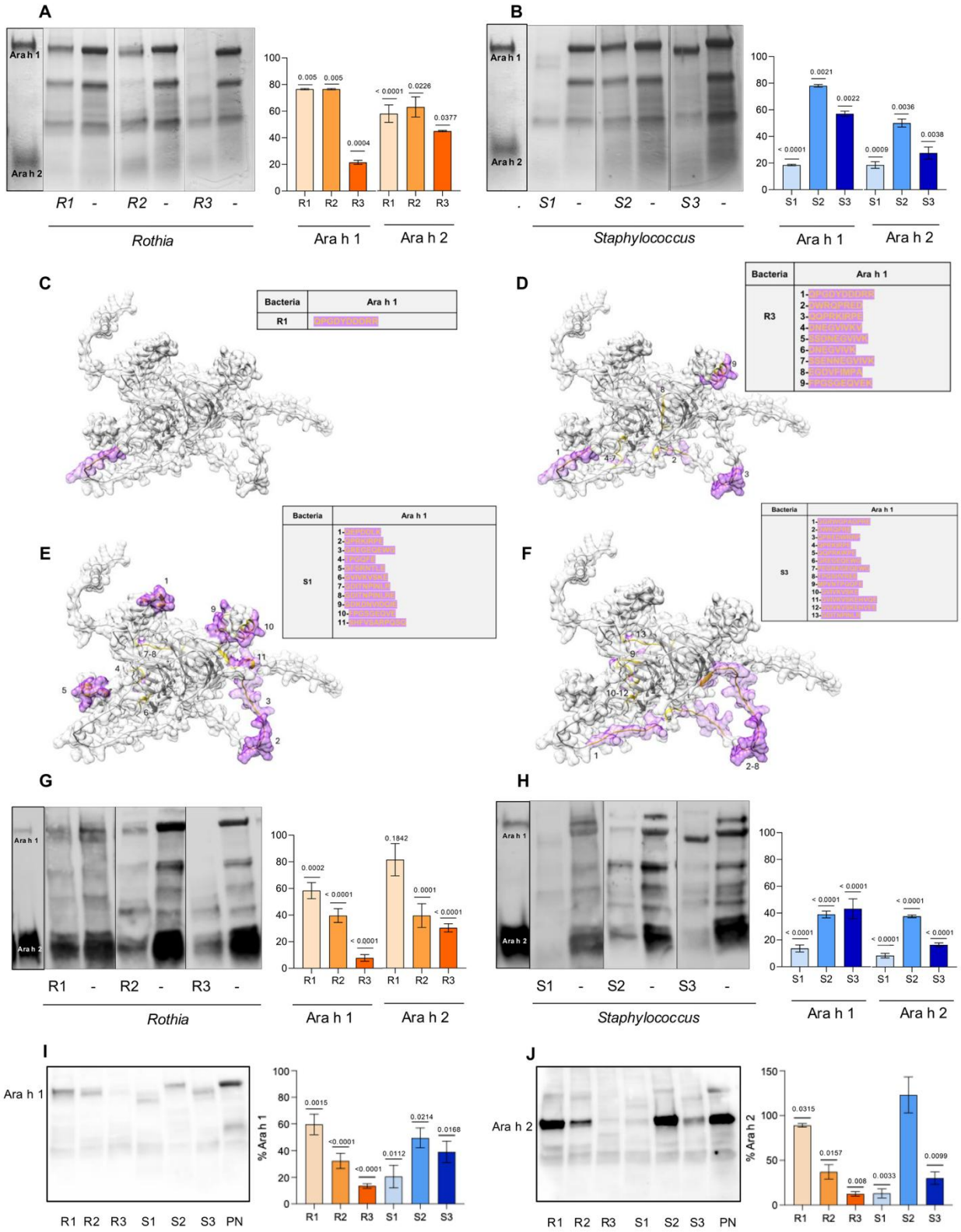

Figure 4. Peanut allergens are degraded by *Rothia* and *Staphylococcus*.
Selected *Rothia* (R1- *R. aeria,* R2- *R. dentacariosa,* and R3- *R. mucilaginosa*) and *Staphylococcus* (S1- *S. epidermidis,* S2- *S. aureus*, and S3- *S. aureus*) strains were incubated with crude peanut extract (CPE) in

liquid media to assess Ara h 1 and 2 degradation. (A–B) SDS-PAGE of Ara h 1 (64 kDa) and Ara h 2 (17 kDa) degradation by *Rothia* (A) and *Staphylococcus* (B) vs. controls. (C–F) Molecular modeling of Ara h 1 (Alphafold database code: AF-P43238-F1): peptides <3 kDa identified by mass spectrometry after digestion by R1 (C), R3 (D), S1 (E), and S3 (F) in yellow; human IgE-recognized epitopes in purple. (G–H) Western blot showing peanut (PN)-allergic human IgE-binding to PN allergens after *Rothia* (G) and *Staphylococcus* (H) digestion relative to controls. (I–J) Western blot showing IgE-binding from Ara h 1 (I) or Ara h 2-sensitized (J) mice after bacterial digestion. Bar charts show allergen quantification after bacterial digestion (mean ± SEM). *P* values calculated using unpaired *t*-test between undigested and bacterially-digested PN.

Microbial metabolism mitigates peanut allergenicity

The structural modifications of Ara h 1 and 2 caused by microbial metabolism affected IgE recognition, prompting us to assess the functional consequences using a mast cell activation assay[46,47]. We sensitized bone marrow-derived mast cells (BMMCs) with sera from mice allergic to either native Ara h 1 or recombinant Ara h 2 and assessed IgE-mediated mast cell activation after challenge with bacterial PN digests. This was done by challenging the BMMCs with either bacterially digested PN or undigested PN, and measuring CD63 and CD107a surface expression, along with β-hexosaminidase activity in the cell supernatants (**Figure 5 & Figure S6A**). Our initial controls confirmed that serum from Ara h 1-allergic mice induced BMMC activation following Ara h 1 or CPE challenge, but not upon Ara h 2 stimulation, and vice versa (**Figure S6B–C**). We then observed that, among the three *Rothia* strains, PN-digestion by strain R2 consistently reduced BMMC activation for both Ara h 1 and 2 (**Figure 5A–B**); while PN-digestion by strains R1 and R3 significantly decreased BMMC responses in Ara h 2-sensitized cells (**Figure 5A–B**). On the other hand, among the three *Staphylococcus* strains, PN-digestion by strain S1 significantly reduced BMMC activation in Ara h 1-sensitized cells **(Figure 5C)**, while BMMC responses to Ara h 2 were impaired by the digestion of the three strains (**Figure 5D**). In sum, these results demonstrate that the metabolism of key PN allergens by human oral bacteria can modulate the ability of these allergens to trigger IgE-mediated mast cell activation.

To further characterize the mechanisms underlying microbial allergen degradation, we performed whole-genome sequencing of the different *Rothia* and *Staphylococcus* species and identified candidate genes encoding protease repertoires (**Figure S7 & Figure S8**). Notably, conserved proteases in *Rothia* include members of the peptidase S8 family of subtilisin-like serine proteases that are secreted extracellularly, which have been previously attributed to degrading recalcitrant dietary proteins such as gluten[48-50], and may likewise contribute to PN allergen degradation. Protease-encoding genes were more variable in *Staphylococcus*, with distinct, non-conserved extracellular proteases identified in each strain. When comparing PN-degrading functionality with annotated protease genes, we observed that potential extracellular proteases including the cysteine protease EcpA, were present in the most efficient degraders against immunodominant allergens. These results confirm the presence of proteolytic machinery potentially involved in PN degradation by bacteria.

A Ara h 1 sensitized

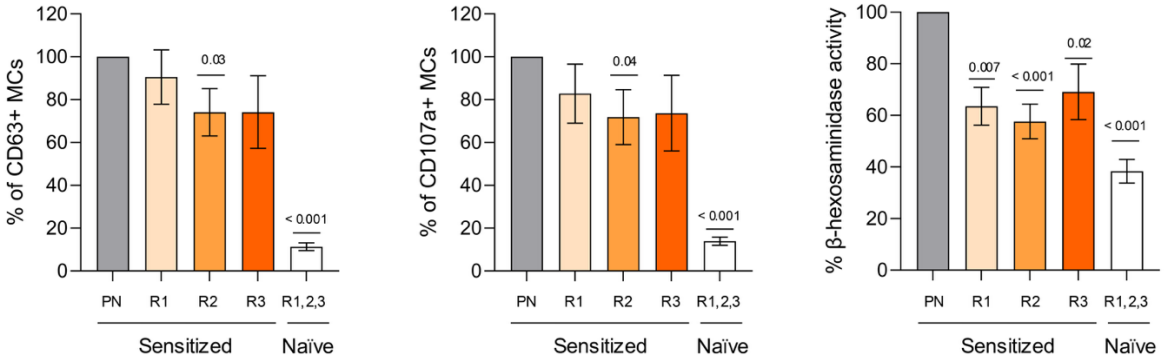

B Ara h 2 sensitized

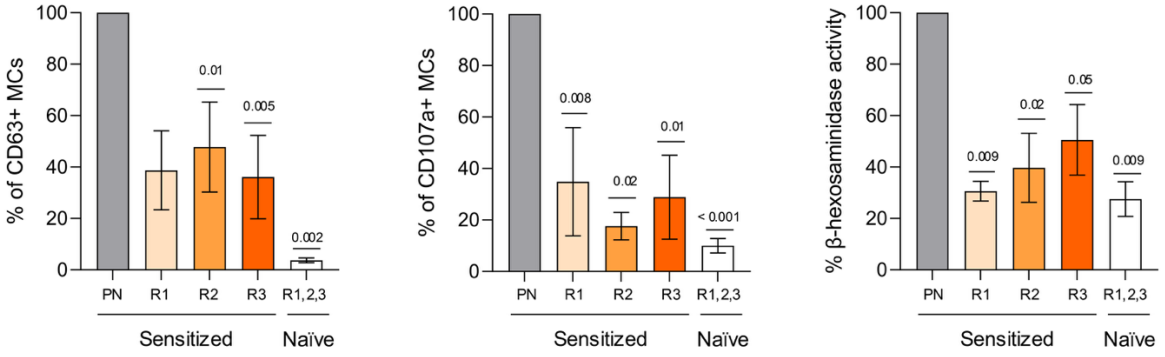

C Ara h 1 sensitized

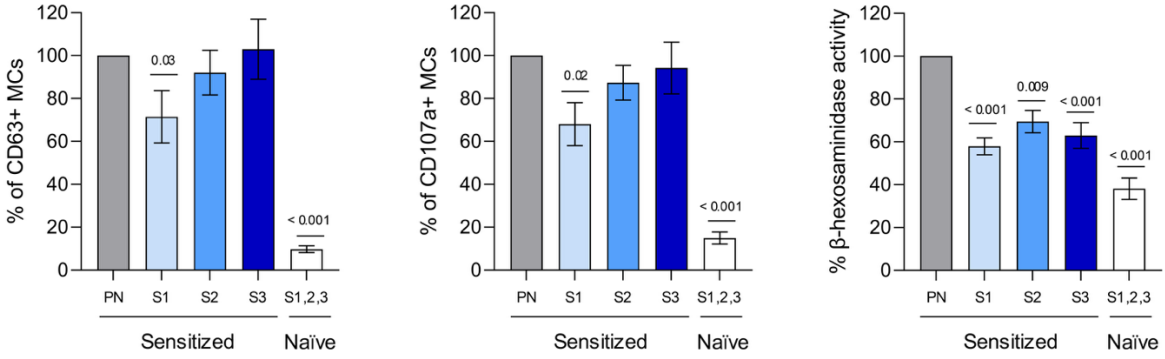

D Ara h 2 sensitized

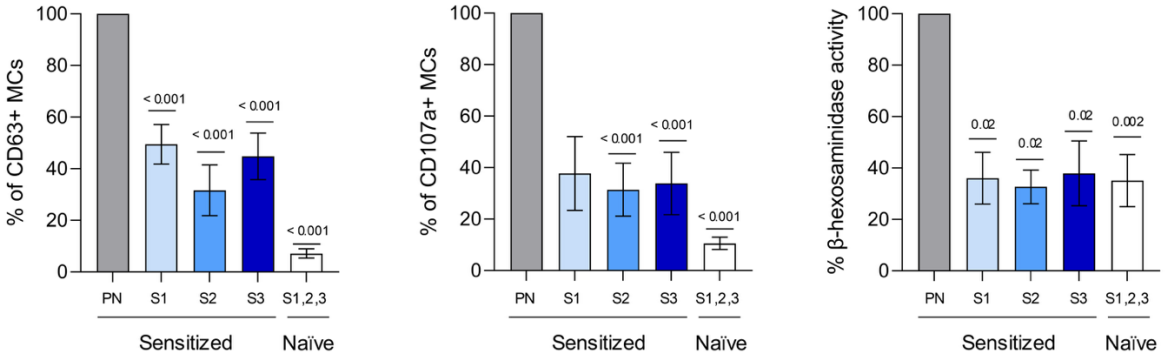

Figure 5. Challenge with bacterially digested peanut impairs mast cell activation. Mast cells (MCs) were sensitized with pooled sera from mice allergic to Ara h 1 or 2 and challenged with undigested peanut (PN; gray, positive control) or PN digested by *Rothia* (orange; R1–*R. aeria*, R2–*R. dentocariosa*, R3–*R. mucilaginosa*; A–B) or *Staphylococcus* (blue; S1–*S. epidermidis,* S2–*S. aureus,* S3–*S. aureus*; C–D). Negative controls (white) were MCs sensitized with sera from non-allergic mice and challenged with pooled bacterially-digested PN from all three *Rothia* or *Staphylococcus* species. Bar graphs indicate CD63 and CD107a expression, and β-hexosaminidase activity, normalized to 100%. Data=mean ± SEM. All three *Rothia* and *Staphylococcus* strains are displayed in the same graphs, but statistical analyses were performed separately for each strain vs. undigested PN. *P* values calculated using one-way ANOVA with Dunnett's post-hoc test, except for specific cases R1-CD63-Ara h 2 (B), S2-CD107a-Ara h 1 (C), and S1-CD107a-Ara h 2 (D), where the Kruskal-Wallis test with Dunn's correction was used. Comparisons with undigested PN used one-way ANOVA with Dunnett's test for β-hexosaminidase activity (D), CD63 (A), and CD107a (A–C), or the Kruskal-Wallis with Dunn's correction for β-hexosaminidase activity (A–C), CD63 (B–D), and CD107a (D). See also Figures S6-S8.

Microbial peanut metabolism alters systemic allergen access

To study the *in vivo* capacity of human oral bacteria to degrade PN allergens, we colonized GF C57BL/6 mice with bacterial strains exhibiting varying allergen-degrading capacities. We selected three *Staphylococcus* strains based on their *in vitro* PN-degrading capacities: one with strong capacity to degrade both Ara h 1 and 2 (S1), one that degrades only Ara h 1 (S3), and one with no detectable allergen-degrading capacity (S2). Additionally, we included a *Rothia* strain (R3) capable of degrading both Ara h 1 and 2. GF mice were used as controls. After colonization, mice were gavaged with PN (**Figure 6A**), as previously described for SPF and ASF mice. Successful transfer of PN-degrading capacity was confirmed in colonized mice (**Figure 6B**). Notably, we observed a reduction in Ara h 1 and 2 levels in the small intestinal content of mice colonized with allergen-degrading bacteria, such as S1 and R3 (**Figure 6C**). Additionally, systemic levels of Ara h 1 and 2 were reduced in these mice (**Figure 6D**). In contrast, Ara h 1—and particularly Ara h 2—showed increased systemic levels in mice colonized with PN-degrading bacteria that had impaired allergen-degrading capacity (S2) (**Figure 6D**). To study whether bacterial metabolism alters allergen passage through the mucosa and subsequent systemic access, we assessed allergen translocation across *ex vivo* mouse small intestinal tissue using Ussing chambers. CPE, pre-incubated with or without the different bacterial strains was applied to the mucosal side of the chamber, and Ara h 1 and 2 levels were quantified on the serosal side of the tissue after 2 hours. We found that PN-degrading bacteria with impaired allergen-degrading capacity facilitated the passage of Ara h 1 and 2 through the intestinal mucosa (**Figure 6E**). These findings suggest that bacteria metabolize PN *in vivo* and control allergen passage through the intestinal mucosal barrier.

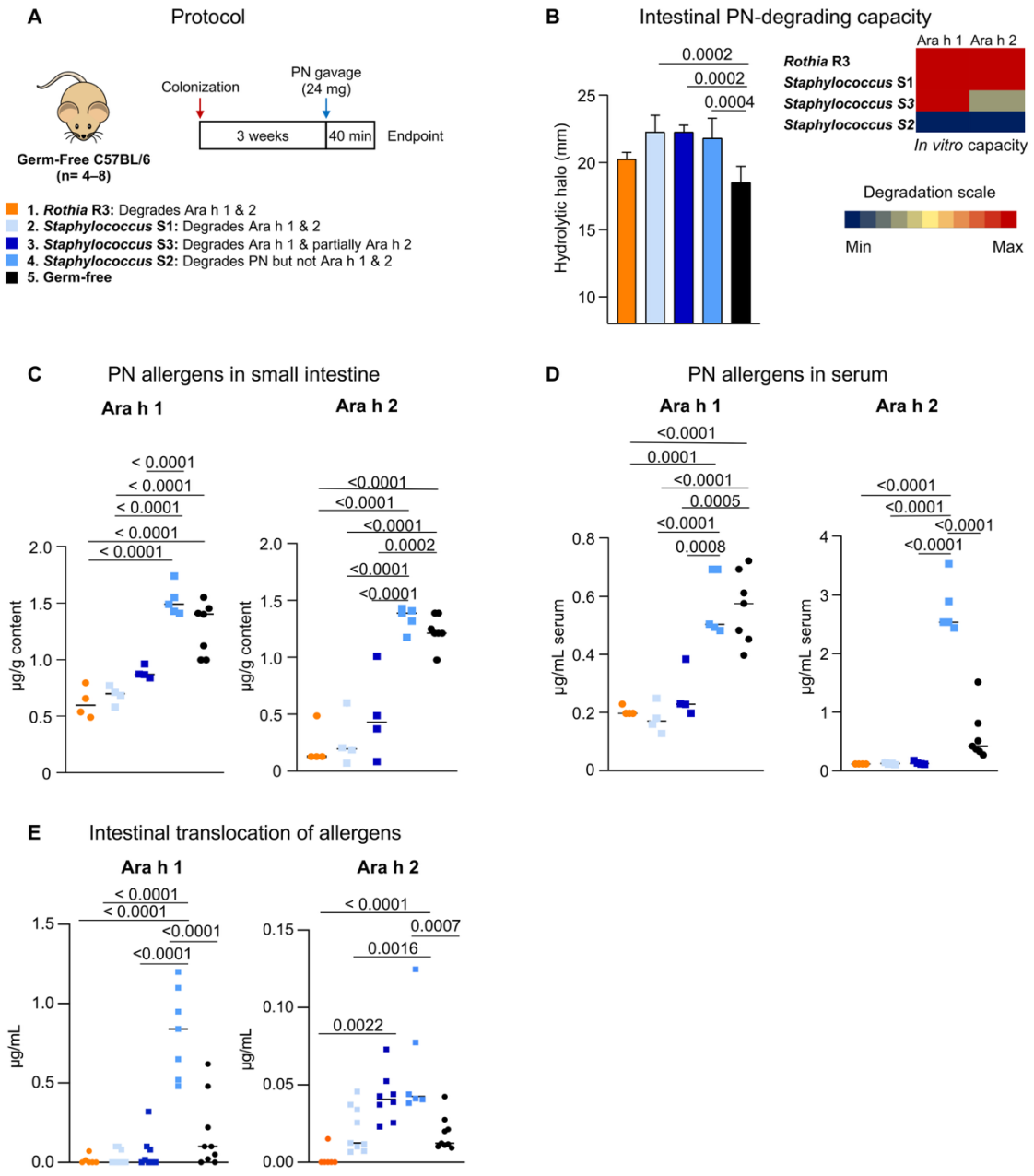

Figure 6. Bacteria dictate systemic access of allergens *in vivo*.
(A) Experimental design. GF C57BL/6 mice were mono-colonized with bacteria (R3–*Rothia mucilaginosa*, S1–*Staphylococcus epidermidis*, S2–*Staphylococcus aureus*, and S3–*Staphylococcus aureus*) for 3 weeks before peanut (PN) gavage; GF mice served as controls. Mice were sacrificed 40 min after PN gavage. (B) PN-degrading capacity of small intestinal contents measured by hydrolytic halo diameter on PN-agar, and degradation of Ara h 1 and 2 (heatmap, blue=0%, red=100% relative to crude peanut extract). (C–D) Ara h 1 and 2 in small intestinal content (C) and serum (D). (E) Translocation of PN allergens digested by bacteria from the mucosal to serosal side of small intestinal tissue in Ussing chambers (R3, orange; S1, light blue; S3, dark blue, S2, medium blue; non-growth control, black). Data are shown as mean + SD (B) and mean where each dot represents an individual mouse (C, D, E). n=4–8 mice/group. *P* values calculated using a one-way ANOVA with Tukey's post-hoc test.

373 **Microbial peanut metabolism dictates anaphylactic reactions *in vivo***

374 To evaluate the impact of microbial PN metabolism on anaphylactic responses, ASF
375 C3H/HeN mice—which have impaired microbial PN metabolism and are susceptible to
376 anaphylactic reactions upon oral exposure—were sensitized to PN via i.p. injection and
377 subsequently challenged with bacterially pre-digested PN (**Figure 7A**). Four groups of
378 mice received an i.g. PN challenge with either untreated PN (control) or PN pre-digested
379 by one of the following bacteria: a) *Rothia* R3, b) *Staphylococcus* S1, or c)
380 *Staphylococcus* S2, each exhibiting distinct allergen-degrading capacities. While all
381 groups showed similar PN-specific IgE levels after sensitization (**Figure 7B**), serum
382 mMCP-1 levels were lower in mice challenged with microbially pre-digested PN (**Figure**
383 **7C**). Notably, mice challenged with PN pre-digested by *Staphylococcus* S2, which has
384 limited allergen-reducing capacity, exhibited higher serum levels of mMCP-1. To evaluate
385 the protective capacity of *Rothia* colonization against food-induced anaphylaxis, ASF
386 C3H/HeN mice were sensitized to PN (i.g.) and then colonized with *Rothia* R3 with
387 efficient PN-degrading capacity (**Figure 7D**). After sensitization, ASF mice with and
388 without PN-degrading bacteria were challenged to PN i.g. Despite having similar PN-
389 specific IgE levels in serum and small intestinal mucosal mast cells (**Figure 7E & Figure**
390 **S9A–E**), mice colonized with *Rothia* R3 (capable of digesting PN allergens) demonstrated
391 significantly reduced serum levels of mMCP-1 (**Figure 7F**) and PAF-AH (**Figure S9B**).
392 Furthermore, PN challenge in ASF mice colonized with or without *Rothia* after i.p.
393 sensitization led to reduced mast cell degranulation in *Rothia*-colonized mice despite
394 similar PN-specific IgE levels and mucosal mast cells (**Figure S9F–J**). Overall, these
395 findings highlight the critical role of microbial allergen metabolism in modulating allergic
396 responses *in vivo*.

397

398 **Peanut-degrading bacteria are increased in allergic patients better tolerating**
399 **peanut**

400 To investigate the role of the oral microbiota in allergic reactions, we collected saliva
401 samples from a small well-defined cohort of PN-allergic patients (**Figure 7G & Table S1)**.
402 Prior to initiating oral immunotherapy (OIT), allergic patients underwent a PN challenge
403 to determine their threshold for reactivity (PN threshold). We analyzed serum levels of
404 IgE and the composition of the oral microbiota. Notably, serum levels of IgE specific to
405 Ara h 1 and 2 showed a poor association with PN threshold **(Figure S10A)**, suggesting
406 the role of additional factors. Examining the oral microbiota, we observed non-significant
407 clustering based on PN threshold (**Figure S10B)**. While PN-degrading taxa were present
408 across patients with varying PN thresholds, individuals with higher PN thresholds
409 exhibited a greater abundance of taxa capable of degrading Ara h 2 **(Figure 7H)**. Notably,
410 *Micrococcales*—a taxon that includes *Rothia* and *Micrococcus*, both efficient at degrading
411 immunodominant Ara h 1 and 2—was reduced in PN-allergic patients with low PN
412 threshold (0–40 mg), independent of serum Ara h 2-specific IgE levels (**Figure 7I**).
413 Interestingly, some high-threshold patients with elevated Ara h 2-specific IgE had

414 increased *Micrococcales*, potentially implicating non-IgE factors in reactivity. To validate
415 our clinical findings, we examined the relative abundance of *Rothia* in saliva of PN-allergic
416 and non-allergic children in an external cohort of 120 children who underwent double-
417 blind, placebo-controlled food challenges[51]. The participants included 23 children with no
418 allergy (controls), 74 with high-threshold PN allergy (reacting to ≥ 443 mg cumulative PN
419 protein), and 23 with low-threshold PN allergy (reacting to <443 mg cumulative PN
420 protein). Notably, *Rothia aeria* ASV14171 was significantly more abundant in the saliva
421 of non-PN-allergic and high PN threshold allergic individuals compared to allergic
422 individuals with low PN thresholds (**Figure 7J**). Other *Rothia* species also showed a trend
423 toward enrichment in the groups (**Figure S10C**). These findings suggest that the oral
424 microbiota could serve as a predictive marker of threshold reactivity to PN, highlighting
425 the potential importance of microbial allergen metabolism in IgE-mediated reactions.

426

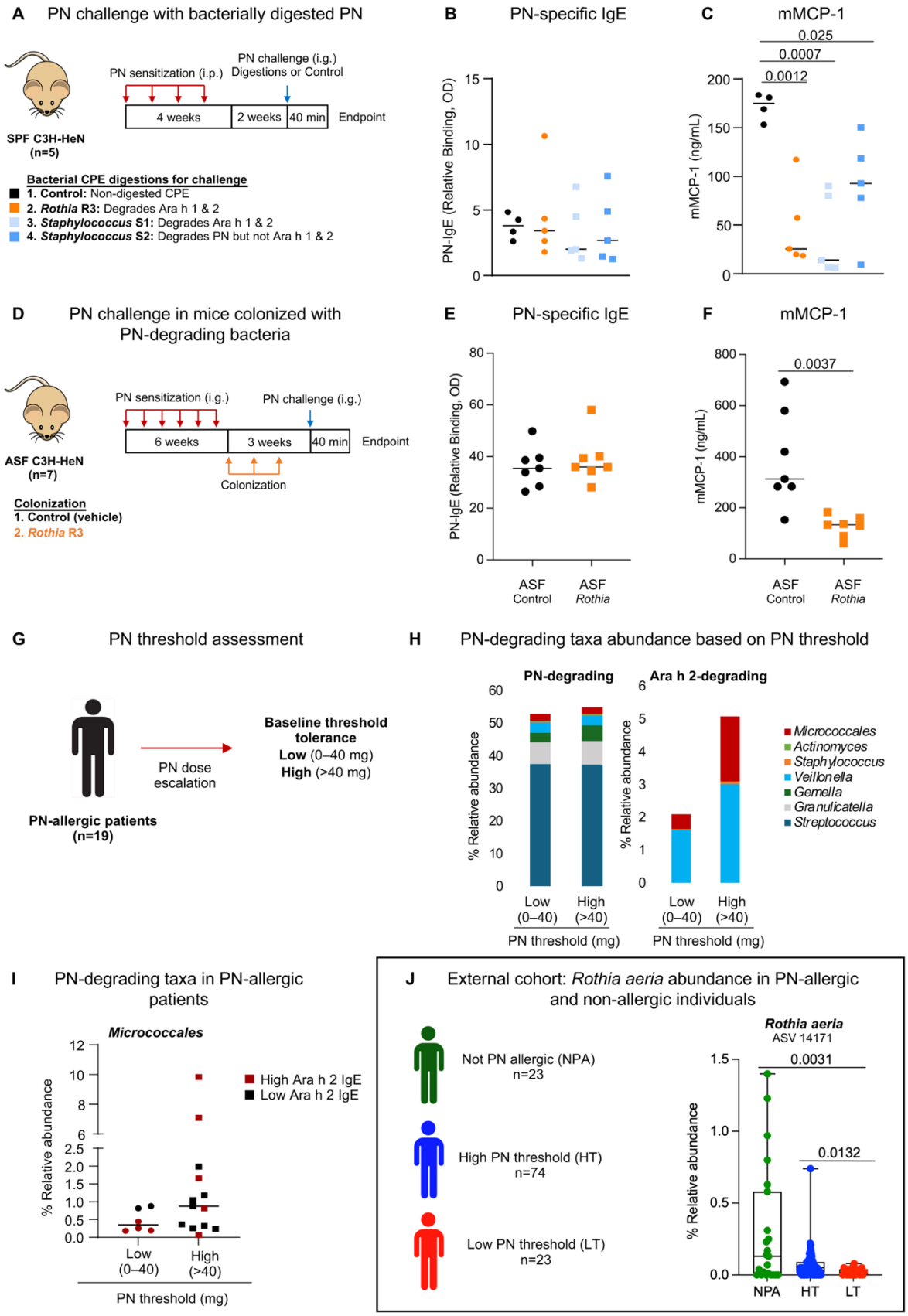
A PN challenge with bacterially digested PN
SPF C3H-HeN (n=5)
PN sensitization (i.p.)
PN challenge (i.g.) Digestions or Control
4 weeks
2 weeks
40 min
Endpoint
Bacterial CPE digestions for challenge
1. Control: Non-digested CPE
2. Rothia R3: Degrades Ara h 1 & 2
3. Staphylococcus S1: Degrades Ara h 1 & 2
4. Staphylococcus S2: Degrades PN but not Ara h 1 & 2
B PN-specific IgE
PN-IgE (Relative Binding, OD)
C mMCP-1
0.025
0.0007
0.0012
mMCP-1 (ng/mL)
D PN challenge in mice colonized with PN-degrading bacteria
ASF C3H-HeN (n=7)
PN sensitization (i.g.)
PN challenge (i.g.)
6 weeks
3 weeks
40 min
Endpoint
Colonization
Colonization
1. Control (vehicle)
2. Rothia R3
E PN-specific IgE
PN-IgE (Relative Binding, OD)
ASF Control
ASF Rothia
F mMCP-1
0.0037
mMCP-1 (ng/mL)
ASF Control
ASF Rothia
G PN threshold assessment
PN-allergic patients (n=19)
PN dose escalation
Baseline threshold tolerance
Low (0–40 mg)
High (>40 mg)
H PN-degrading taxa abundance based on PN threshold
PN-degrading
Ara h 2-degrading
% Relative abundance
Micrococcales
Actinomyces
Staphylococcus
Veillonella
Gemella
Granulicatella
Streptococcus
Low (0–40)
High (>40)
PN threshold (mg)
I PN-degrading taxa in PN-allergic patients
Micrococcales
% Relative abundance
High Ara h 2 IgE
Low Ara h 2 IgE
Low (0–40)
High (>40)
PN threshold (mg)
J External cohort: Rothia aeria abundance in PN-allergic and non-allergic individuals
Not PN allergic (NPA) n=23
High PN threshold (HT) n=74
Low PN threshold (LT) n=23
Rothia aeria
ASV 14171
0.0031
0.0132
% Relative abundance
NPA
HT
LT

427

Figure 7. Microbial peanut metabolism reduces allergic reactions *in vivo* and is associated with allergen tolerance.

(A) Experimental design. SPF C3H-HeN mice were sensitized i.p. to peanut (PN) weekly for 4 weeks and challenged i.g. after 7 weeks with PN digested by *Rothia* (R3), *Staphylococcus epidermidis* (S1), and *Staphylococcus aureus* (S2), or undigested PN. Mice were sacrificed 40 minutes later. n=5 mice/group. (B) Serum PN-specific IgE before challenge. (C) Serum mucosal mast cell protease 1 (mMCP-1) after challenge. (D) Experimental design. ASF C3H-HeN mice were sensitized i.g. to PN weekly for 6 weeks, then colonized with *Rothia* weekly for 3 weeks. PN challenge was given i.g. 3 weeks after the first colonization, followed by sacrifice 40 minutes later. n=7 mice/group. (E) Serum PN-specific IgE before PN challenge. (F) Serum mMCP-1 after PN challenge. (G) Experimental design. PN-allergic patients (n=19) were stratified by PN threshold (low –0-40 mg PN; high–>40 mg PN) prior to oral immunotherapy. (I) Relative abundance (%) of PN- and Ara h 2-degrading bacteria in low vs. high threshold patients. (J) Relative abundance of *Micrococalles* in the saliva of low vs. high PN threshold patients. Dot color represents high (≥20 kUA/mL, red) and low (<20 kUA/mL, black) serum Ara h 2-IgE. (J) *Rothia aeria* ASV 14171 abundance in saliva from 16S rRNA data of an external cohort of 120 children (23 non-PN-allergic controls (NPA), 74 PN-allergic with high PN threshold (HT; >443 mg), and 23 PN-allergic with low PN threshold (LT; <443 mg)) who underwent double-blind, placebo-controlled PN challenges. Data are presented as mean with dots for individual mice or humans (B, C, E, F, H, I), or as interquartile range with whiskers extending to min/max (J). *P* values: one-way ANOVA with Tukey's post-hoc test (C, D), unpaired Student's *t*-test (F, G), and Kruskal-Wallis test with Dunn's post-hoc test (J). See also Figures S9 and S10.

DISCUSSION

The human microbiome is essential for maintaining homeostasis, and disruptions in its composition are associated with immune disorders. The oro-gastrointestinal microbiota has gained attention for its role in influencing oral tolerance and sensitization to food antigens[18-20,22,52]. While studies have reported differences in the intestinal microbiota composition of food-allergic patients[23-25], the microbial mechanisms underlying food-induced anaphylaxis remain largely unknown. In this study, we show that human saliva and small intestinal content harbor allergen-degrading bacteria capable of metabolizing immunodominant PN allergens, thereby modulating IgE-mediated reactions to foods. Identifying the microbes involved in PN metabolism in humans and characterizing the related microbially-mediated IgE-specific immune responses could have implications for reducing the severity of allergic reactions.

The antigenic properties of many foods stem from their resistance to gastrointestinal digestion[28,29]. PN allergens, for example, are poorly metabolized by human digestive enzymes[26,27], whereas the intestinal microbiota encodes diverse metabolic pathways absent in the host that participate in food digestion[53]. For example, the capacity of the intestinal microbiota to degrade other recalcitrant antigenic proteins, such as gluten[54], has been demonstrated[55,56]. Using gnotobiotic mouse models, we demonstrate that microbiota composition and complexity contribute to PN allergen metabolism *in vivo* and the amount of allergen reaching the intestine and circulation. While the intestinal microbiota affects host metabolism and food-dependent immune responses through mechanisms such as altering the intestinal barrier, motility, or immune activation[18,57-59], we confirmed the presence of PN-degrading bacteria capable of digesting Ara h 1 and 2 along the gastrointestinal tract in wild-type SPF mice. These findings reveal the role of

473 the intestinal microbiota in allergen metabolism and raise important questions about how
474 diet-microbiota interactions shape food allergy.

475 Food allergies are primarily IgE-mediated[60], and even minute allergen doses can trigger
476 life-threatening reactions [61]. We hypothesized that microbial metabolism modulates IgE-
477 dependent responses to PN. First, we demonstrated that mice with limited PN-degrading
478 capacity (ASF) developed enhanced allergic reactions to PN than those with efficient PN
479 metabolism (SPF) following i.g. sensitization and challenge. ASF mice exhibited greater
480 mucosal mast cell activation, likely increasing intestinal permeability and facilitating
481 systemic allergen access[62,63]—a critical step in IgE-mediated anaphylaxis[64]. Intriguingly,
482 ASF mice also developed higher titers of antigen-specific IgE than SPF controls,
483 potentially due to their reduced ability to metabolize PN allergens. Similar increases in
484 antigen-specific IgE have been reported in GF mice and mice colonized with limited
485 microbial communities following sensitization[65-67]. Given that food-induced anaphylaxis is
486 largely IgE-dependent[68,69], and the microbiota may influence IgE-mediated food
487 sensitization independently of allergen degradation[18], differences in sensitization
488 between mouse strains could explain the severity of allergic reactions. To bypass local
489 microbial factors, we evaluated the role of microbial metabolism in IgE-mediated food
490 responses using additional models of systemic[70] and passive[47,71] sensitization. Following
491 PN challenge, ASF mice with limited PN-degrading capacity developed enhanced allergic
492 reactions, characterized by increased mast cell degranulation and hypothermia compared
493 to conventional mice, despite similar PN-IgE titers. Altogether, these results indicate that
494 microbial metabolism is a key determinant of IgE-mediated food allergy in mice.

495 Food-induced anaphylaxis usually results from accidental allergen exposure, posing a
496 persistent threat that significantly impacts quality of life[72,73]. Although co-factors such as
497 exercise, estrogen levels, alcohol, and drugs can heighten anaphylaxis risk[14,74], variations
498 in allergen thresholds and susceptibility remain poorly understood. A recent study
499 demonstrated that anaphylaxis severity is independent of the amount of allergen
500 ingested, emphasizing individual sensitivity and the potential role of microbiota in
501 modulating IgE-responses[75]. To explore the potential role of microbial allergen
502 metabolism in humans, we searched for PN-degrading bacteria in healthy donors,
503 focusing on the oral cavity and small intestine where ingested food first interacts with the
504 microbiota. While most microbiota research has centered on the large intestinal lumen
505 due to its ease of sampling and high bacterial density, recent studies have highlighted the
506 stability and complexity of the oral and small intestinal microbiota, as well as their
507 relevance in health and disease[76]. Moreover, the oral microbiota serves as a continuous
508 source of bacteria for the intestinal tract, seeding the small intestine with taxa such as
509 *Rothia* and *Staphylococcus*[77], which may persist and contribute to allergen metabolism
510 as food moves through the upper gut[78]. Using SDS-PAGE, Western blotting, and
511 proteomics, we confirmed the presence of PN-degrading bacteria in the oral cavity with
512 strain-specific capacities to degrade immunodominant PN allergens, disrupt human IgE
513 epitopes, and alter IgE-binding of sera from PN-allergic patients and sensitized mice.

514 Overall, these results confirm the capacity of bacteria to potentially alter allergenicity in
515 the oral cavity and small intestine of humans.

516 Dominant taxa in the oral cavity and small intestine such as *Rothia*, and related genera
517 like *Micrococcus*, consistently digested both Ara h 1 and 2 *in vitro,* altering IgE recognition.
518 The capacity of *Rothia* to degrade other dietary antigens such as gluten proteins has been
519 also suggested[50,79]. Remarkably, impaired IgE recognition of PN upon *Rothia* digestion
520 hampered the activation of the classical pathway of anaphylaxis both *in vitro* (mast cell
521 assays) and *in vivo* (PN-allergic mice challenged with digested PN). In addition, the PN-
522 degrading capacity of *Rothia* was validated *in vivo*, reducing the concentration of major
523 PN allergens reaching the small intestine and circulation. We also tested the capacity of
524 *Rothia* strains to alter IgE-mediated reactions following colonization in a competitive
525 environment. To avoid changes in the adaptive immune response, ASF mice were
526 colonized following either i.g. or i.p. sensitization. ASF mice colonized with *Rothia* had
527 reduced IgE-mediated allergic responses and mucosal mast cell degranulation following
528 challenge compared to ASF controls. These results confirm that the protective effects of
529 allergen metabolism arise by reducing allergen availability in the intestinal environment
530 rather than by altering systemic sensitization. Altogether, our data demonstrate that PN-
531 degrading bacteria can modulate acute allergic responses *in vivo*.

532 Microbial PN metabolism does not always protect against IgE-mediated responses.
533 Certain PN-degrading genera, such as *Gemella* or *Streptococcus,* lacked allergen-
534 degrading capacity *in vitro*, while *Staphylococcus*, a main PN-degrading taxon in the oral
535 cavity*,* displayed strain-specific effects in our work. Others have reported that skin
536 colonization by *Staphylococcus aureus* induces keratinocyte release of IL-36α[80], a pro-
537 inflammatory cytokine linked to allergic sensitization to foods[32]. Additionally,
538 *Staphylococcus* and other microbial proteases such as EcpA can induce immune
539 activation and low-grade inflammation in the colon[81], and promote inflammatory
540 responses to innocuous antigens[82,83]. Our findings revealed that *Staphylococcus* strains
541 vary in their capacity to remove PN allergens and alter IgE-mediated recognition and mast
542 cell activation *in vitro*. In gnotobiotic mice colonized with *Staphylococcus* strains exhibiting
543 differing PN-degrading capacities, efficient strains reduced Ara h 1 and 2 levels in the
544 small intestine and serum. However, these immunodominant peptides increased
545 systemically in mice colonized with a strain lacking efficient PN-degrading capacity.
546 Enhanced passage of Ara h 1 and 2 through the intestinal mucosa after partial digestion
547 of PN by this *Staphylococcus* strain was also confirmed with Ussing chambers,
548 highlighting the role of bacterial activity in systemic allergen access, a critical step in
549 anaphylactic reactions[64]. These results indicate that *Staphylococcus* species, including
550 *Staphylococcus aureus,* may facilitate allergen passage through the mucosal barrier and
551 promote allergic inflammation when allergen degradation is incomplete[84,85]. Some
552 *Staphylococcus* strains can also compromise the epithelial barrier and increase
553 permeability directly[86,87]. Therefore, microbes may have a dual impact on IgE-mediated
554 immune responses, depending on the bacteria's ability to degrade PN allergens,
555 regardless of its taxonomy. Complete microbial degradation of PN allergens reduces IgE

556 responses, while inefficient metabolism may promote anaphylaxis by enhancing the
557 passage of allergens through the mucosa. Altogether, the ability of the microbiota to
558 completely degrade immunodominant allergens and reduce IgE recognition of PN
559 significantly influences subsequent mast cell activation and anaphylactic reactions.

560 Despite these findings, the precise microbial proteases responsible for PN allergen
561 metabolism remain to be fully identified. Whole-genome sequencing of different *Rothia*
562 species revealed diverse protease repertoires, including subtilisin-like serine proteases.
563 Members of this family have been shown to degrade other recalcitrant dietary proteins[48-
564 50], such as gluten, suggesting they may contribute to PN allergen metabolism. Efficient
565 PN-degrading *Staphylococcus* possessed annotated extracellular proteases, including
566 the virulence-associated cysteine protease EcpA[88,89]. However, given the broad
567 proteolytic capacity of the oral microbiota, multiple enzymes could be involved in
568 modulating allergenicity. Future studies integrating genetic modulation will be required to
569 pinpoint the specific microbial enzymes mediating these effects.

570 While our findings consistently support the role of microbial metabolism in modulating PN
571 allergenicity, variability was observed in our results across models and microbial
572 communities. Both technical (*e.g.*, antibody and *ex vivo* assay variability) and biological
573 factors (*e.g.*, postprandial state, vendor-specific SPF microbiota) likely contributed. We
574 used i.g. challenges to focus on mucosal mast cell activation, though these induce weaker
575 clinical anaphylaxis than the i.p. route and add variability. Specifically, immune responses
576 upon i.g. challenge are influenced by factors including allergen delivery, intestinal
577 permeability, gastric emptying, and genetic background. This variability is further
578 amplified after i.g. sensitization that also enhances mast cell recruitment to the small
579 intestinal mucosa and intestinal permeability[90]. GF mice, the gold standard for studying
580 microbially-mediated phenotypes, were used to investigate PN metabolism, but they
581 exhibit altered intestinal barrier function, impaired motility, and increased proteolytic
582 activity, and their underdeveloped immunity can exaggerate sensitization and
583 anaphylaxis[65,67,91-93]. Importantly, sensitization was not the primary focus of this study and
584 allergic responses may be influenced by factors beyond microbial[22], such as the extent
585 of mast cell recruitment to the intestine[90]. To better isolate microbial effects, we used ASF
586 mice, which provide minimal but stable microbiota with limited endogenous PN-degrading
587 activity. ASF mice serve as a stronger comparator for high PN-degrading capacity
588 microbiota or as a model for supplementation with PN-degrading taxa. Colonization of
589 ASF mice with PN-degrading *Rothia* after i.g. or i.p. sensitization to PN reduced
590 anaphylaxis markers and mast cell degranulation. Microbial composition and complexity
591 were key determinants of allergen degradation and IgE-mediated responses, as shown
592 by a negative correlation between alpha-diversity and both intestinal allergen levels and
593 serum mMCP-1 in ASF and SPF mice. This suggests that variability in PN degradation
594 and anaphylaxis observed in our study may be partially attributed to individual differences
595 in microbiota composition and complexity, with some SPF mice potentially harboring
596 fewer PN-degrading bacteria.

The primary recommendation for food allergic patients is strict avoidance of allergens, yet this is a challenge for ubiquitous foods such as egg, wheat, milk or PN, leading to frequent accidental exposures[10,12,94,95]. Allergen thresholds differ among PN-allergic patients, with some individuals experiencing anaphylaxis to trace amounts[96,97]. To investigate the role of microbial allergen metabolism in food-induced anaphylaxis, we characterized the oral microbiota of PN-allergic patients initiating OIT with varying allergen thresholds. Allergen-specific IgE did not correlate well with allergen thresholds in our study, consistent with previous findings[98,99]. However, patients with higher PN thresholds showed greater abundance of *Micrococcales* (an order including PN-degrading *Rothia* and *Micrococcus*), than highly sensitive allergic patients to PN, independent of IgE titers. Consistent with this observation, our analysis of an external pediatric cohort revealed that *Rothia aeria* was significantly more abundant in the saliva of non-PN-allergic and high-threshold PN-allergic individuals compared to allergic individuals with low thresholds, with other *Rothia* species also showing a trend toward enrichment[51]. A previous study also reported an increased relative abundance of *Rothia* in the saliva of PN-allergic children after undergoing OIT[100], and *Veillonella*, an oral taxon with PN-degrading capacity, is increased in those with greater reaction thresholds[101]. Together, these findings suggest that allergen threshold associates with the metabolic activity of oral microbiota against food allergens, and may serve as a marker of reactivity. Still, the mechanistic link between oral microbiota and allergen threshold in humans remains speculative, requiring preclinical and longitudinal validation. Longitudinal assessment of oral microbiota and allergen reactivity during PN OIT in future studies will further inform how microbiota may influence OIT outcomes. Although OIT remains the only allergen-specific treatment with disease-modifying potential, it is associated with limitations such as events that compromise patient adherence, quality of life, and overall effectiveness[73,102,103]. Functional analysis of the oral microbiota may help identify patients with low allergen thresholds less suitable for OIT, while harnessing PN-degrading bacteria may raise allergen thresholds. Characterizing PN-degrading bacteria could also be applied to reduce cross-contamination risks—a leading cause of unintentional allergen exposure and a significant concern in food allergy management[95,104-106]—and improve the formulation of hypoallergenic products. In summary, our findings reveal a novel microbial mechanism of relevance in food-induced anaphylaxis. Our results underscore the role of the human microbiota in dictating the severity of IgE-mediated reactions through allergen metabolism and highlight the therapeutic potential of harnessing bacterial allergen-degrading capabilities for managing food allergies.

RESOURCE AVAILABILITY

Lead contact: Further information and requests for resources and reagents should be directed to the lead contact Alberto Caminero (acamine@mcmaster.ca).

Materials availability: This study did not generate new unique reagents.

Data and code availability: The microbiome sequencing data generated in this study have been deposited in the NCBI BioProject database under the accession number PRJNA1223483. The mass spectrometry proteomics data have been deposited to the ProteomeXchange Consortium via the PRIDE partner repository with the dataset identifier PXD060888 and 10.6019/PXD060888. Any additional information required to reanalyze the data reported in this paper is available from the lead contact upon reasonable request.

ACKNOWLEDGMENTS

We thank the McMaster University AGU staff, Dr. Heather G. Galipeau, Joe Noratangelo, Michael Rosati, and Sarah Armstrong for their assistance with mouse care. We thank the McMaster Genome Facility, Laura Rosati, and Michelle Shah for technical support with 16S rRNA gene sequencing. We thank Gaston Rueda for assistance with clinical samples. We thank the staff of the Proteomics Unit at CNB-CSIC, particularly Dr. Alberto Paradela, for analysis and technical support. We are grateful to Drs. Pablo Rodríguez del Río, Salvador Iborra and Francisco Sánchez-Madrid for their critical review of the manuscript. This work was supported by grants from The Nutricia Research Foundation (NRF-2021-13) and the New Frontiers in Research Fund (NFRFE-2019-00083) to R.J.-S. and A.C.; and by a grant from the European Food Safety Authority (GP/EFSA/ENCO/2020/02-1) to F.J.M. R.J.-S.´s laboratory is supported by the Instituto de Salud Carlos III (ISCIII; CP20/00043; PI22/00236; PI25/00477; RD24/0007/0037) and by the Ministerio de Ciencia, Innovación y Universidades (CNS2024-154194). A.C. holds a Family Douglas Research Chair in Intestinal Research and is funded by the Canadian Institutes of Health Research (CIHR; Project Grant 202010PJT), NSERC (DGECR-2022-00221) and by Crohn's and Colitis Canada (CCC, Grants-In-Aid grant). L.E.R. is supported by a Frederick Banting and Charles Best Canada Graduate Scholarship-Doctoral award from CIHR and a graduate scholarship from the Farncombe Institute. E.S.-M. is supported by a Formación de Profesorado Universitario grant (FPU23/03341) from Ministerio de Universidades. S.U.P. is supported by NIAID NIH R01 grants 1R01AI155630 and 1R01AI182001. L.M.-S. is supported by the Investigo program through the Ministerio de Trabajo y Economía Social, Servicio Público de Empleo (SEPE), which is funded by "Plan de Recuperación, Transformación y Resiliencia" and "NextGenerationEU" of the European Union (2022- C23.I01). C.L.S and E.N.-B are supported by a Río Hortega (CM23/0019) and a Sara Borrell grant (CD23/00125), respectively, from ISCIII. E.F.V. is supported by a CIHR Project Grant (PJT-183881) and holds a Tier 1 Canada Research Chair in Microbial Therapeutics and Nutrition in Gastroenterology. L.Z. and S.B. received funding from NIAID NIH R01 AI147028 and U196053.

AUTHOR CONTRIBUTIONS

Conceptualization, R.J.-S., A.C.; Methodology, R.J.-S., A.C.; Investigation, E.S.-M., L.E.R., M.G.-R., D.H., P.H., B.B., G.Y., R.D., J.F.E.K., T.D.W., L.M.-S., C.L.S., E.N.-B., X.Y.W., G.D.P., L.Z., F.J.M., R.J.-S., A.C.; Resources, M.G.-A., A.D.-P., E.F.V., Y.R.C., P.O., F.V., C.B., J.F.E.K, M.J., W.G.S., S.U.P., F.J.M., M.G.S., S.B., P.B.; Writing – Original Draft Preparation, E.S.-M., L.E.R., R.J.-S., A.C.; Writing – Review & Editing Preparation, E.S.-M., L.E.R., R.J.-S., A.C.; Visualization Preparation, E.S.-M., L.E.R.; Supervision, R.J.-S., A.C.; funding Acquisition, R.J.-S., A.C.

DECLARATION OF INTERESTS

R.J.-S. receives research funds from a collaboration agreement between FIB-Hospital Universitario de La Princesa and Inmunotek S.L., which does not present any conflicts with the data presented. Provisional patent (63/670,312) was filed in the United States Patent and Trademark office based on data presented in this manuscript ("Microbial metabolism of peanut allergens and uses thereof).

SUPPLEMENTAL INFORMATION INDEX

Figures S1-S10 and their legends, as well as Tables S1 and S2 are in a PDF.

References

1. Meizlish, M.L., Franklin, R.A., Zhou, X., and Medzhitov, R. (2021). Tissue Homeostasis and Inflammation. Annu Rev Immunol *39*, 557-581. 10.1146/annurev-immunol-061020-053734.
2. Nunez-Borque, E., Dribin, T.E., Rodriguez Del Rio, P., Camargo, C.A., Jr., Esteban, V., du Toit, G., Jimenez-Saiz, R., and Giovannini, M. (2025). Anaphylaxis: Spotlight on Inflammation. Clin Exp Allergy *55*, 8-10. 10.1111/cea.14610.
3. Bachtel, N.D., Cullen, J.L., Liu, M., Erickson, S.A., Kutyavin, V.I., El-Naccache, D.W., Florsheim, E.B., Lim, J., Sullivan, Z.A., Imaeda, R., et al. (2025). Intestinal mast cell-derived leukotrienes mediate the anaphylactic response to ingested antigens. Science *389*, eadp0246. 10.1126/science.adp0246.
4. Hoyt, L.R., Liu, E., Olson, E.C., Jacobsen, D.R., Siniscalco, E.R., Krier-Burris, R.A., Greenfield, K.G., McBride, C.D., Alfajaro, M.M., Amat, J.A.R., et al. (2025). Cysteinyl leukotrienes stimulate gut absorption of food allergens to promote anaphylaxis in mice. Science *389*, eadp0240. 10.1126/science.adp0240.
5. Dyer, A.A., Rivkina, V., Perumal, D., Smeltzer, B.M., Smith, B.M., and Gupta, R.S. (2015). Epidemiology of childhood peanut allergy. Allergy Asthma Proc *36*, 58-64. 10.2500/aap.2015.36.3819.
6. Cianferoni, A., and Muraro, A. (2012). Food-induced anaphylaxis. Immunol Allergy Clin North Am *32*, 165-195. 10.1016/j.iac.2011.10.002.
7. Muraro, A., Sublett, J.W., Haselkorn, T., Nilsson, C., and Casale, T.B. (2021). Incidence of anaphylaxis and accidental peanut exposure: A systematic review. Clin Transl Allergy *11*, e12064. 10.1002/clt2.12064.
8. Leung, A.S.Y., Tham, E.H., Pacharn, P., Xing, Y., Trinh, H.K.T., Lee, S., Ahn, K., Chatchatee, P., Sato, S., Ebisawa, M., et al. (2024). Disparities in pediatric anaphylaxis triggers and management across Asia. Allergy *79*, 1317-1328. 10.1111/all.16098.
9. Neuman-Sunshine, D.L., Eckman, J.A., Keet, C.A., Matsui, E.C., Peng, R.D., Lenehan, P.J., and Wood, R.A. (2012). The natural history of persistent peanut allergy. Ann Allergy Asthma Immunol *108*, 326-331 e323. 10.1016/j.anai.2011.11.010.
10. Cherkaoui, S., Ben-Shoshan, M., Alizadehfar, R., Asai, Y., Chan, E., Cheuk, S., Shand, G., St-Pierre, Y., Harada, L., Allen, M., and Clarke, A. (2015). Accidental exposures to peanut in a large cohort of Canadian children with peanut allergy. Clin Transl Allergy *5*, 16. 10.1186/s13601-015-0055-x.
11. Peters, R.L., Guarnieri, I., Tang, M.L.K., Lowe, A.J., Dharmage, S.C., Perrett, K.P., Gurrin, L.C., and Koplin, J.J. (2022). The natural history of peanut and egg allergy in children up to age 6 years in the HealthNuts population-based longitudinal study. J Allergy Clin Immunol *150*, 657-665 e613. 10.1016/j.jaci.2022.04.008.
12. Vasse, M., Moyart, M., Cisterne, C., Thumerelle, C., Drumez, E., Behal, H., Pouessel, G., Lejeune, S., and Deschildre, A. (2025). Children Allergic to Peanut and/or Tree Nuts Are at Risk of Accidental Allergic Reactions. Clin Exp Allergy *n/a*. 10.1111/cea.70132.

741 13. Benede, S., Garrido-Arandia, M., Martin-Pedraza, L., Bueno, C., Diaz-Perales,
742 A., and Villalba, M. (2017). Multifactorial Modulation of Food-Induced
743 Anaphylaxis. Front Immunol *8*, 552. 10.3389/fimmu.2017.00552.
744 14. Munoz-Cano, R., Pascal, M., Araujo, G., Goikoetxea, M.J., Valero, A.L., Picado,
745 C., and Bartra, J. (2017). Mechanisms, Cofactors, and Augmenting Factors
746 Involved in Anaphylaxis. Front Immunol *8*, 1193. 10.3389/fimmu.2017.01193.
747 15. Flinn, A., and Hourihane, J.O. (2013). Allergic reaction to peanuts: can we predict
748 reaction severity in the wild? Curr Allergy Asthma Rep *13*, 645-650.
749 10.1007/s11882-013-0369-5.
750 16. Petek, T., Lajhar, M., Krasovec, B., Homsak, M., Kavalar, M., Korosec, P., Koren,
751 B., Tomazin, M., Hojnik, T., and Berce, V. (2023). Risk Factors for Anaphylaxis in
752 Children Allergic to Peanuts. Medicina (Kaunas) *59*. 10.3390/medicina59061037.
753 17. Turner, P.J., Baumert, J.L., Beyer, K., Boyle, R.J., Chan, C.H., Clark, A.T.,
754 Crevel, R.W., DunnGalvin, A., Fernandez-Rivas, M., Gowland, M.H., et al.
755 (2016). Can we identify patients at risk of life-threatening allergic reactions to
756 food? Allergy *71*, 1241-1255. 10.1111/all.12924.
757 18. Caminero, A., Meisel, M., Jabri, B., and Verdu, E.F. (2019). Mechanisms by
758 which gut microorganisms influence food sensitivities. Nat Rev Gastroenterol
759 Hepatol *16*, 7-18. 10.1038/s41575-018-0064-z.
760 19. Stephen-Victor, E., Crestani, E., and Chatila, T.A. (2020). Dietary and Microbial
761 Determinants in Food Allergy. Immunity *53*, 277-289.
762 10.1016/j.immuni.2020.07.025.
763 20. Cerovic, V., Pabst, O., and Mowat, A.M. (2025). The renaissance of oral
764 tolerance: merging tradition and new insights. Nat Rev Immunol *25*, 42-56.
765 10.1038/s41577-024-01077-7.
766 21. Stephen-Victor, E., Kuziel, G.A., Martinez-Blanco, M., Jugder, B.E., Benamar,
767 M., Wang, Z., Chen, Q., Lozano, G.L., Abdel-Gadir, A., Cui, Y., et al. (2025).
768 RELMbeta sets the threshold for microbiome-dependent oral tolerance. Nature
769 *638*, 760-768. 10.1038/s41586-024-08440-7.
770 22. Caminero, A., Sanchez-Martinez, E., Wulczynski, M., Moreno-Serna, L., Verdu,
771 E.F., and Jimenez-Saiz, R. (2025). Potential role of microbes in antigen-based
772 food sensitivities. Semin Immunol *79*, 101982. 10.1016/j.smim.2025.101982.
773 23. Azad, M.B., Konya, T., Guttman, D.S., Field, C.J., Sears, M.R., HayGlass, K.T.,
774 Mandhane, P.J., Turvey, S.E., Subbarao, P., Becker, A.B., et al. (2015). Infant
775 gut microbiota and food sensitization: associations in the first year of life. Clin
776 Exp Allergy *45*, 632-643. 10.1111/cea.12487.
777 24. De Filippis, F., Paparo, L., Nocerino, R., Della Gatta, G., Carucci, L., Russo, R.,
778 Pasolli, E., Ercolini, D., and Berni Canani, R. (2021). Specific gut microbiome
779 signatures and the associated pro-inflamatory functions are linked to pediatric
780 allergy and acquisition of immune tolerance. Nature Communications *12*.
781 10.1038/s41467-021-26266-z.
782 25. Bao, R., Hesser, L.A., He, Z., Zhou, X., Nadeau, K.C., and Nagler, C.R. (2021).
783 Fecal microbiome and metabolome differ in healthy and food-allergic twins. J Clin
784 Invest *131*. 10.1172/JCI141935.
785 26. Koppelman, S.J., Hefle, S.L., Taylor, S.L., and de Jong, G.A. (2010). Digestion of
786 peanut allergens Ara h 1, Ara h 2, Ara h 3, and Ara h 6: a comparative in vitro

787 study and partial characterization of digestion-resistant peptides. Mol Nutr Food
788 Res *54*, 1711-1721. 10.1002/mnfr.201000011.
789 27. Kopper, R.A., Odum, N.J., Sen, M., Helm, R.M., Steve Stanley, J., and Wesley
790 Burks, A. (2004). Peanut protein allergens: gastric digestion is carried out
791 exclusively by pepsin. J Allergy Clin Immunol *114*, 614-618.
792 10.1016/j.jaci.2004.05.012.
793 28. Jimenez-Saiz, R., Benede, S., Molina, E., and Lopez-Exposito, I. (2015). Effect of
794 processing technologies on the allergenicity of food products. Critical reviews in
795 food science and nutrition *55*, 1902-1917. 10.1080/10408398.2012.736435.
796 29. Moreno, F.J. (2007). Gastrointestinal digestion of food allergens: effect on their
797 allergenicity. Biomed Pharmacother *61*, 50-60. 10.1016/j.biopha.2006.10.005.
798 30. Gertie, J.A., Zhang, B., Liu, E.G., Hoyt, L.R., Yin, X., Xu, L., Long, L.L.,
799 Soldatenko, A., Gowthaman, U., Williams, A., and Eisenbarth, S.C. (2022). Oral
800 anaphylaxis to peanut in a mouse model is associated with gut permeability but
801 not with Tlr4 or Dock8 mutations. J Allergy Clin Immunol *149*, 262-274.
802 10.1016/j.jaci.2021.05.015.
803 31. Whelan, F.J., Waddell, B., Syed, S.A., Shekarriz, S., Rabin, H.R., Parkins, M.D.,
804 and Surette, M.G. (2020). Culture-enriched metagenomic sequencing enables in-
805 depth profiling of the cystic fibrosis lung microbiota. Nat Microbiol *5*, 379-390.
806 10.1038/s41564-019-0643-y.
807 32. Tsilochristou, O., du Toit, G., Sayre, P.H., Roberts, G., Lawson, K., Sever, M.L.,
808 Bahnson, H.T., Radulovic, S., Basting, M., Plaut, M., et al. (2019). Association of
809 Staphylococcus aureus colonization with food allergy occurs independently of
810 eczema severity. J Allergy Clin Immunol *144*, 494-503.
811 10.1016/j.jaci.2019.04.025.
812 33. Koppelman, S.J., Vlooswijk, R.A., Knippels, L.M., Hessing, M., Knol, E.F., van
813 Reijsen, F.C., and Bruijnzeel-Koomen, C.A. (2001). Quantification of major
814 peanut allergens Ara h 1 and Ara h 2 in the peanut varieties Runner, Spanish,
815 Virginia, and Valencia, bred in different parts of the world. Allergy *56*, 132-137.
816 10.1034/j.1398-9995.2001.056002132.x.
817 34. Burks, A.W., Shin, D., Cockrell, G., Stanley, J.S., Helm, R.M., and Bannon, G.A.
818 (1997). Mapping and mutational analysis of the IgE-binding epitopes on Ara h 1,
819 a legume vicilin protein and a major allergen in peanut hypersensitivity. Eur J
820 Biochem *245*, 334-339. 10.1111/j.1432-1033.1997.t01-1-00334.x.
821 35. Shin, D.S., Compadre, C.M., Maleki, S.J., Kopper, R.A., Sampson, H., Huang,
822 S.K., Burks, A.W., and Bannon, G.A. (1998). Biochemical and structural analysis
823 of the IgE binding sites on ara h1, an abundant and highly allergenic peanut
824 protein. J Biol Chem *273*, 13753-13759. 10.1074/jbc.273.22.13753.
825 36. Jiang, S., Wang, S., Sun, Y., Zhou, Z., and Wang, G. (2011). Molecular
826 characterization of major allergens Ara h 1, 2, 3 in peanut seed. Plant Cell Rep
827 *30*, 1135-1143. 10.1007/s00299-011-1022-1.
828 37. Cong†, Y., Lou†, F., Xue, W., Li, L., and Chena, M. (2008). Characterisation of
829 the IgE-binding immunodominant epitopes on Ara h1. Food and Agricultural
830 Immunology *19*, 175-185. 10.1080/09540100802172599.
831 38. Bogh, K.L., Nielsen, H., Madsen, C.B., Mills, E.N., Rigby, N., Eiwegger, T.,
832 Szepfalusi, Z., and Roggen, E.L. (2012). IgE epitopes of intact and digested Ara

833 h 1: a comparative study in humans and rats. Molecular immunology *51*, 337-
834 346. 10.1016/j.molimm.2012.04.002.
835 39. Bogh, K.L., Nielsen, H., Eiwegger, T., Madsen, C.B., Mills, E.N., Rigby, N.M.,
836 Szepfalusi, Z., and Roggen, E.L. (2014). IgE versus IgG4 epitopes of the peanut
837 allergen Ara h 1 in patients with severe allergy. Molecular immunology *58*, 169-
838 176. 10.1016/j.molimm.2013.11.014.
839 40. Hansen, C.S., Dufva, M., Bogh, K.L., Sullivan, E., Patel, J., Eiwegger, T.,
840 Szepfalusi, Z., Nielsen, M., and Christiansen, A. (2016). Linear epitope mapping
841 of peanut allergens demonstrates individualized and persistent antibody-binding
842 patterns. J Allergy Clin Immunol *138*, 1728-1730. 10.1016/j.jaci.2016.06.019.
843 41. Shreffler, W.G., Beyer, K., Chu, T.H., Burks, A.W., and Sampson, H.A. (2004).
844 Microarray immunoassay: association of clinical history, in vitro IgE function, and
845 heterogeneity of allergenic peanut epitopes. J Allergy Clin Immunol *113*, 776-
846 782. 10.1016/j.jaci.2003.12.588.
847 42. Rambo, I.M., Kronfel, C.M., Rivers, A.R., Swientoniewski, L.T., McBride, J.K.,
848 Cheng, H., Simon, R.J., Ryan, R., Tilles, S.A., Nesbit, J.B., et al. (2023). IgE and
849 IgG4 epitopes of the peanut allergens shift following oral immunotherapy. Front
850 Allergy *4*, 1279290. 10.3389/falgy.2023.1279290.
851 43. Suarez-Farinas, M., Suprun, M., Bahnson, H.T., Raghunathan, R., Getts, R.,
852 duToit, G., Lack, G., and Sampson, H.A. (2021). Evolution of epitope-specific IgE
853 and IgG(4) antibodies in children enrolled in the LEAP trial. J Allergy Clin
854 Immunol *148*, 835-842. 10.1016/j.jaci.2021.01.030.
855 44. Chen, G., Shrock, E.L., Li, M.Z., Spergel, J.M., Nadeau, K.C., Pongracic, J.A.,
856 Umetsu, D.T., Rachid, R., MacGinnitie, A.J., Phipatanakul, W., et al. (2021).
857 High-resolution epitope mapping by AllerScan reveals relationships between IgE
858 and IgG repertoires during peanut oral immunotherapy. Cell Rep Med *2*, 100410.
859 10.1016/j.xcrm.2021.100410.
860 45. Suarez-Farinas, M., Lee, K.W., Suprun, M., Bahnson, H.T., Foong, R.X., Du Toit,
861 G., Lack, G., and Sampson, H.A. (2025). Kinetics of epitope-specific IgE and
862 IgG(4) in early peanut allergy development and resolution. J Allergy Clin
863 Immunol. 10.1016/j.jaci.2025.06.022.
864 46. Lopez-Sanz, C., Sanchez-Martinez, E., and Jimenez-Saiz, R. (2022). Protocol to
865 desensitize human and murine mast cells after polyclonal IgE sensitization.
866 STAR Protoc *3*, 101755. 10.1016/j.xpro.2022.101755.
867 47. Fernandez-Gallego, N., Castillo-Gonzalez, R., Moreno-Serna, L., Garcia-Civico,
868 A.J., Sanchez-Martinez, E., Lopez-Sanz, C., Fontes, A.L., Pimentel, L.L.,
869 Gradillas, A., Obeso, D., et al. (2024). Allergic inflammation triggers dyslipidemia
870 via IgG signalling. Allergy *79*, 2680-2699. 10.1111/all.16187.
871 48. Helmerhorst, E.J., Zamakhchari, M., Schuppan, D., and Oppenheim, F.G. (2010).
872 Discovery of a novel and rich source of gluten-degrading microbial enzymes in
873 the oral cavity. PLoS One *5*, e13264. 10.1371/journal.pone.0013264.
874 49. Wei, G., Darwish, G., Oppenheim, F.G., Schuppan, D., and Helmerhorst, E.J.
875 (2020). Commensal Bacterium Rothia aeria Degrades and Detoxifies Gluten via
876 a Highly Effective Subtilisin Enzyme. Nutrients *12*. 10.3390/nu12123724.
877 50. Wei, G., Tian, N., Siezen, R., Schuppan, D., and Helmerhorst, E.J. (2016).
878 Identification of food-grade subtilisins as gluten-degrading enzymes to treat

879 celiac disease. Am J Physiol Gastrointest Liver Physiol *311*, G571-580.
880 10.1152/ajpgi.00185.2016.
881 51. Zhang, L., Chun, Y., Grishina, G., Lo, T., Reed, K., Wang, J., Sicherer, S., Berin,
882 M.C., and Bunyavanich, S. (2025). Oral and Gut Microbial Hubs Associated With
883 Reaction Threshold Interact With Circulating Immune Factors in Peanut Allergy.
884 Allergy. 10.1111/all.16481.
885 52. Gomez de Aguero, M., Ganal-Vonarburg, S.C., Fuhrer, T., Rupp, S., Uchimura,
886 Y., Li, H., Steinert, A., Heikenwalder, M., Hapfelmeier, S., Sauer, U., et al.
887 (2016). The maternal microbiota drives early postnatal innate immune
888 development. Science *351*, 1296-1302. 10.1126/science.aad2571.
889 53. Caminero, A., Guzman, M., Libertucci, J., and Lomax, A.E. (2023). The emerging
890 roles of bacterial proteases in intestinal diseases. Gut Microbes *15*, 2181922.
891 10.1080/19490976.2023.2181922.
892 54. Shan, L., Molberg, O., Parrot, I., Hausch, F., Filiz, F., Gray, G.M., Sollid, L.M.,
893 and Khosla, C. (2002). Structural basis for gluten intolerance in celiac sprue.
894 Science *297*, 2275-2279. 10.1126/science.1074129.
895 55. Caminero, A., Galipeau, H.J., McCarville, J.L., Johnston, C.W., Bernier, S.P.,
896 Russell, A.K., Jury, J., Herran, A.R., Casqueiro, J., Tye-Din, J.A., et al. (2016).
897 Duodenal Bacteria From Patients With Celiac Disease and Healthy Subjects
898 Distinctly Affect Gluten Breakdown and Immunogenicity. Gastroenterology *151*,
899 670-683. 10.1053/j.gastro.2016.06.041.
900 56. Caminero, A., McCarville, J.L., Zevallos, V.F., Pigrau, M., Yu, X.B., Jury, J.,
901 Galipeau, H.J., Clarizio, A.V., Casqueiro, J., Murray, J.A., et al. (2019).
902 Lactobacilli Degrade Wheat Amylase Trypsin Inhibitors to Reduce Intestinal
903 Dysfunction Induced by Immunogenic Wheat Proteins. Gastroenterology *156*,
904 2266-2280. 10.1053/j.gastro.2019.02.028.
905 57. Tremaroli, V., and Backhed, F. (2012). Functional interactions between the gut
906 microbiota and host metabolism. Nature *489*, 242-249. 10.1038/nature11552.
907 58. Thomson, C.A., Morgan, S.C., Ohland, C., and McCoy, K.D. (2022). From germ-
908 free to wild: modulating microbiome complexity to understand mucosal
909 immunology. Mucosal Immunol *15*, 1085-1094. 10.1038/s41385-022-00562-3.
910 59. Jimenez-Saiz, R., Anipindi, V.C., Galipeau, H., Ellenbogen, Y., Chaudhary, R.,
911 Koenig, J.F., Gordon, M.E., Walker, T.D., Mandur, T.S., Abed, S., et al. (2020).
912 Microbial Regulation of Enteric Eosinophils and Its Impact on Tissue Remodeling
913 and Th2 Immunity. Front Immunol *11*, 155. 10.3389/fimmu.2020.00155.
914 60. Jutel, M., Agache, I., Zemelka-Wiacek, M., Akdis, M., Chivato, T., Del Giacco, S.,
915 Gajdanowicz, P., Gracia, I.E., Klimek, L., Lauerma, A., et al. (2023).
916 Nomenclature of allergic diseases and hypersensitivity reactions: Adapted to
917 modern needs: An EAACI position paper. Allergy *78*, 2851-2874.
918 10.1111/all.15889.
919 61. Galli, S.J., and Tsai, M. (2012). IgE and mast cells in allergic disease. Nat Med
920 *18*, 693-704. 10.1038/nm.2755.
921 62. Leyva-Castillo, J.M., Galand, C., Kam, C., Burton, O., Gurish, M., Musser, M.A.,
922 Goldsmith, J.D., Hait, E., Nurko, S., Brombacher, F., et al. (2019). Mechanical
923 Skin Injury Promotes Food Anaphylaxis by Driving Intestinal Mast Cell
924 Expansion. Immunity *50*, 1262-1275 e1264. 10.1016/j.immuni.2019.03.023.

925 63. Jacob, C., Yang, P.C., Darmoul, D., Amadesi, S., Saito, T., Cottrell, G.S.,
926 Coelho, A.M., Singh, P., Grady, E.F., Perdue, M., and Bunnett, N.W. (2005).
927 Mast cell tryptase controls paracellular permeability of the intestine. Role of
928 protease-activated receptor 2 and beta-arrestins. J Biol Chem *280*, 31936-31948.
929 10.1074/jbc.M506338200.
930 64. Strait, R.T., Mahler, A., Hogan, S., Khodoun, M., Shibuya, A., and Finkelman,
931 F.D. (2011). Ingested allergens must be absorbed systemically to induce
932 systemic anaphylaxis. J Allergy Clin Immunol *127*, 982-989 e981.
933 10.1016/j.jaci.2011.01.034.
934 65. Cahenzli, J., Koller, Y., Wyss, M., Geuking, M.B., and McCoy, K.D. (2013).
935 Intestinal microbial diversity during early-life colonization shapes long-term IgE
936 levels. Cell Host Microbe *14*, 559-570. 10.1016/j.chom.2013.10.004.
937 66. Wyss, M., Brown, K., Thomson, C.A., Koegler, M., Terra, F., Fan, V., Ronchi, F.,
938 Bihan, D., Lewis, I., Geuking, M.B., and McCoy, K.D. (2019). Using Precisely
939 Defined in vivo Microbiotas to Understand Microbial Regulation of IgE. Front
940 Immunol *10*, 3107. 10.3389/fimmu.2019.03107.
941 67. Stefka, A.T., Feehley, T., Tripathi, P., Qiu, J., McCoy, K., Mazmanian, S.K.,
942 Tjota, M.Y., Seo, G.Y., Cao, S., Theriault, B.R., et al. (2014). Commensal
943 bacteria protect against food allergen sensitization. Proc Natl Acad Sci U S A
944 *111*, 13145-13150. 10.1073/pnas.1412008111.
945 68. Arias, K., Chu, D.K., Flader, K., Botelho, F., Walker, T., Arias, N., Humbles, A.A.,
946 Coyle, A.J., Oettgen, H.C., Chang, H.D., et al. (2011). Distinct immune effector
947 pathways contribute to the full expression of peanut-induced anaphylactic
948 reactions in mice. J Allergy Clin Immunol *127*, 1552-1561 e1551.
949 10.1016/j.jaci.2011.03.044.
950 69. Gowthaman, U., Chen, J.S., Zhang, B., Flynn, W.F., Lu, Y., Song, W., Joseph, J.,
951 Gertie, J.A., Xu, L., Collet, M.A., et al. (2019). Identification of a T follicular helper
952 cell subset that drives anaphylactic IgE. Science *365*, eaaw6433.
953 10.1126/science.aaw6433.
954 70. Chu, D.K., Jimenez-Saiz, R., Verschoor, C.P., Walker, T.D., Goncharova, S.,
955 Llop-Guevara, A., Shen, P., Gordon, M.E., Barra, N.G., Bassett, J.D., et al.
956 (2014). Indigenous enteric eosinophils control DCs to initiate a primary Th2
957 immune response in vivo. J Exp Med *211*, 1657-1672. 10.1084/jem.20131800.
958 71. Jimenez-Saiz, R., Chu, D.K., Mandur, T.S., Walker, T.D., Gordon, M.E.,
959 Chaudhary, R., Koenig, J., Saliba, S., Galipeau, H.J., Utley, A., et al. (2017).
960 Lifelong memory responses perpetuate humoral T(H)2 immunity and anaphylaxis
961 in food allergy. J Allergy Clin Immunol *140*, 1604-1615 e1605.
962 10.1016/j.jaci.2017.01.018.
963 72. Knibb, R.C., Jones, C.J., Herbert, L.J., and Screti, C. (2024). Psychological
964 support needs for children with food allergy and their families: A systematic
965 review. Pediatr Allergy Immunol *35*, e14108. 10.1111/pai.14108.
966 73. Mori, F., Giovannini, M., Barni, S., Jimenez-Saiz, R., Munblit, D., Biagioni, B.,
967 Liccioli, G., Sarti, L., Liotti, L., Ricci, S., et al. (2021). Oral Immunotherapy for
968 Food-Allergic Children: A Pro-Con Debate. Front Immunol *12*, 636612.
969 10.3389/fimmu.2021.636612.

970 74. Niggemann, B., and Beyer, K. (2014). Factors augmenting allergic reactions.
971 Allergy *69*, 1582-1587. 10.1111/all.12532.
972 75. Piletta-Zanin, A., Scherl, A., Benhamou, A., Braendle, G., Caubet, J.C., Graham,
973 F., Grosgurin, O., Harr, T., Manzano, S., Nigolian, H., et al. (2025). The Severity
974 of Allergic Reactions in a Real-World Environment Is Independent of the Eliciting
975 Amounts of Foods. Allergy *80*, 238-247. 10.1111/all.16413.
976 76. Baker, J.L., Mark Welch, J.L., Kauffman, K.M., McLean, J.S., and He, X. (2024).
977 The oral microbiome: diversity, biogeography and human health. Nat Rev
978 Microbiol *22*, 89-104. 10.1038/s41579-023-00963-6.
979 77. Constante, M., Libertucci, J., Galipeau, H.J., Szamosi, J.C., Rueda, G., Miranda,
980 P.M., Pinto-Sanchez, M.I., Southward, C.M., Rossi, L., Fontes, M.E., et al.
981 (2022). Biogeographic Variation and Functional Pathways of the Gut Microbiota
982 in Celiac Disease. Gastroenterology *163*, 1351-1363 e1315.
983 10.1053/j.gastro.2022.06.088.
984 78. Kunath, B.J., De Rudder, C., Laczny, C.C., Letellier, E., and Wilmes, P. (2024).
985 The oral-gut microbiome axis in health and disease. Nat Rev Microbiol *22*, 791-
986 805. 10.1038/s41579-024-01075-5.
987 79. Zamakhchari, M., Wei, G., Dewhirst, F., Lee, J., Schuppan, D., Oppenheim, F.G.,
988 and Helmerhorst, E.J. (2011). Identification of Rothia bacteria as gluten-
989 degrading natural colonizers of the upper gastro-intestinal tract. PLoS One *6*,
990 e24455. 10.1371/journal.pone.0024455.
991 80. Patrick, G.J., Liu, H., Alphonse, M.P., Dikeman, D.A., Youn, C., Otterson, J.C.,
992 Wang, Y., Ravipati, A., Mazhar, M., Denny, G., et al. (2021). Epicutaneous
993 Staphylococcus aureus induces IL-36 to enhance IgE production and ensuing
994 allergic disease. J Clin Invest *131*. 10.1172/JCI143334.
995 81. Rondeau, L.E., Da Luz, B.B., Santiago, A., Bermudez-Brito, M., Hann, A., De
996 Palma, G., Jury, J., Wang, X., Verdu, E.F., Galipeau, H.J., et al. (2024).
997 Proteolytic bacteria expansion during colitis amplifies inflammation through
998 cleavage of the external domain of PAR2. Gut Microbes *16*, 2387857.
999 10.1080/19490976.2024.2387857.
1000 82. Agaronyan, K., Sharma, L., Vaidyanathan, B., Glenn, K., Yu, S., Annicelli, C.,
1001 Wiggen, T.D., Penningroth, M.R., Hunter, R.C., Dela Cruz, C.S., and Medzhitov,
1002 R. (2022). Tissue remodeling by an opportunistic pathogen triggers allergic
1003 inflammation. Immunity *55*, 895-911 e810. 10.1016/j.immuni.2022.04.001.
1004 83. Caminero, A., McCarville, J.L., Galipeau, H.J., Deraison, C., Bernier, S.P.,
1005 Constante, M., Rolland, C., Meisel, M., Murray, J.A., Yu, X.B., et al. (2019).
1006 Duodenal bacterial proteolytic activity determines sensitivity to dietary antigen
1007 through protease-activated receptor-2. Nat Commun *10*, 1198. 10.1038/s41467-
1008 019-09037-9.
1009 84. Jimenez-Saiz, R., Ellenbogen, Y., Koenig, J.F.E., Gordon, M.E., Walker, T.D.,
1010 Rosace, D., Spill, P., Bruton, K., Kong, J., Monteiro, K., et al. (2019). IgG1(+) B-
1011 cell immunity predates IgE responses in epicutaneous sensitization to foods.
1012 Allergy *74*, 165-175. 10.1111/all.13481.
1013 85. Kong, J., Chalcraft, K., Mandur, T.S., Jimenez-Saiz, R., Walker, T.D.,
1014 Goncharova, S., Gordon, M.E., Naji, L., Flader, K., Larche, M., et al. (2015).

1015 Comprehensive metabolomics identifies the alarmin uric acid as a critical signal
1016 for the induction of peanut allergy. Allergy *70*, 495-505. 10.1111/all.12579.
1017 86. Kwak, Y.K., Vikstrom, E., Magnusson, K.E., Vecsey-Semjen, B., Colque-Navarro,
1018 P., and Mollby, R. (2012). The Staphylococcus aureus alpha-toxin perturbs the
1019 barrier function in Caco-2 epithelial cell monolayers by altering junctional
1020 integrity. Infect Immun *80*, 1670-1680. 10.1128/IAI.00001-12.
1021 87. Moran, M.C., Brewer, M.G., Schlievert, P.M., and Beck, L.A. (2023). S. aureus
1022 virulence factors decrease epithelial barrier function and increase susceptibility to
1023 viral infection. Microbiol Spectr *11*, e0168423. 10.1128/spectrum.01684-23.
1024 88. Martinez-Garcia, S., Rodriguez-Martinez, S., Cancino-Diaz, M.E., and Cancino-
1025 Diaz, J.C. (2018). Extracellular proteases of Staphylococcus epidermidis: roles
1026 as virulence factors and their participation in biofilm. APMIS : acta pathologica,
1027 microbiologica, et immunologica Scandinavica *126*, 177-185.
1028 10.1111/apm.12805.
1029 89. Cau, L., Williams, M.R., Butcher, A.M., Nakatsuji, T., Kavanaugh, J.S., Cheng,
1030 J.Y., Shafiq, F., Higbee, K., Hata, T.R., Horswill, A.R., and Gallo, R.L. (2021).
1031 Staphylococcus epidermidis protease EcpA can be a deleterious component of
1032 the skin microbiome in atopic dermatitis. J Allergy Clin Immunol *147*, 955-966
1033 e916. 10.1016/j.jaci.2020.06.024.
1034 90. Forbes, E.E., Groschwitz, K., Abonia, J.P., Brandt, E.B., Cohen, E., Blanchard,
1035 C., Ahrens, R., Seidu, L., McKenzie, A., Strait, R., et al. (2008). IL-9- and mast
1036 cell-mediated intestinal permeability predisposes to oral antigen hypersensitivity.
1037 J Exp Med *205*, 897-913. 10.1084/jem.20071046.
1038 91. Hayes, C.L., Dong, J., Galipeau, H.J., Jury, J., McCarville, J., Huang, X., Wang,
1039 X.Y., Naidoo, A., Anbazhagan, A.N., Libertucci, J., et al. (2018). Commensal
1040 microbiota induces colonic barrier structure and functions that contribute to
1041 homeostasis. Scientific reports *8*, 14184. 10.1038/s41598-018-32366-6.
1042 92. Li, Y., Watanabe, E., Kawashima, Y., Plichta, D.R., Wang, Z., Ujike, M., Ang,
1043 Q.Y., Wu, R., Furuichi, M., Takeshita, K., et al. (2022). Identification of trypsin-
1044 degrading commensals in the large intestine. Nature *609*, 582-589.
1045 10.1038/s41586-022-05181-3.
1046 93. Santiago, A., Hann, A., Constante, M., Rahmani, S., Libertucci, J., Jackson, K.,
1047 Rueda, G., Rossi, L., Rithwick, R., Ruf, W., et al. (2023). Crohn's disease
1048 proteolytic microbiota enhances inflammation through PAR2 pathway in
1049 gnotobiotic mice. Gut Microbes *15*, 2205425. 10.1080/19490976.2023.2205425.
1050 94. Rotella, K., and Oriel, R.C. (2022). Accidental Reactions to Foods: Frequency,
1051 Causes, and Severity. Curr Treat Options Allergy *9*, 157-168. 10.1007/s40521-
1052 022-00314-5.
1053 95. Hsu, C., Hosakoppal, S., Yong, M., Gupta, R., Makhija, M., and Singh, A.M.
1054 (2024). Prevalence and Characteristics of Accidental Ingestions Among Pediatric
1055 Food Allergy Patients. J Allergy Clin Immunol Pract *12*, 3089-3095 e3082.
1056 10.1016/j.jaip.2024.08.006.
1057 96. Li, J.C., Rotter, N.S., Stieb, E.S., Stockbridge, J.L., Theodorakakis, M.D., and
1058 Shreffler, W.G. (2024). Utility of food allergy thresholds. Ann Allergy Asthma
1059 Immunol *132*, 321-327. 10.1016/j.anai.2023.12.012.

1060 97. Patel, N., Adelman, D.C., Anagnostou, K., Baumert, J.L., Blom, W.M., Campbell,
1061 D.E., Chinthrajah, R.S., Mills, E.N.C., Javed, B., Purington, N., et al. (2021).
1062 Using data from food challenges to inform management of consumers with food
1063 allergy: A systematic review with individual participant data meta-analysis. J
1064 Allergy Clin Immunol *147*, 2249-2262 e2247. 10.1016/j.jaci.2021.01.025.
1065 98. Santos, A.F., Barbosa-Morais, N.L., Hurlburt, B.K., Ramaswamy, S., Hemmings,
1066 O., Kwok, M., O'Rourke, C., Bahnson, H.T., Cheng, H., James, L., et al. (2020).
1067 IgE to epitopes of Ara h 2 enhance the diagnostic accuracy of Ara h 2-specific
1068 IgE. Allergy *75*, 2309-2318. 10.1111/all.14301.
1069 99. Patil, S.U., Steinbrecher, J., Calatroni, A., Smith, N., Ma, A., Ruiter, B., Virkud,
1070 Y., Schneider, M., and Shreffler, W.G. (2019). Early decrease in basophil
1071 sensitivity to Ara h 2 precedes sustained unresponsiveness after peanut oral
1072 immunotherapy. J Allergy Clin Immunol *144*, 1310-1319 e1314.
1073 10.1016/j.jaci.2019.07.028.
1074 100. Blackman, A.C., Thapa, S., Venkatachalam, A., Horvath, T.D., Runge, J.K.,
1075 Haidacher, S.J., Hoch, K.M., Haag, A.M., Luna, R.A., and Anagnostou, A. (2022).
1076 Insights into Microbiome and Metabolic Signatures of Children Undergoing
1077 Peanut Oral Immunotherapy. Children (Basel) *9*. 10.3390/children9081192.
1078 101. Zhang, L., Chun, Y., Ho, H.E., Arditi, Z., Lo, T., Sajja, S., Rose, R., Jones, D.,
1079 Wang, J., Sicherer, S., and Bunyavanich, S. (2022). Multiscale study of the oral
1080 and gut environments in children with high- and low-threshold peanut allergy. J
1081 Allergy Clin Immunol *150*, 714-720 e712. 10.1016/j.jaci.2022.04.026.
1082 102. Chu, D.K., Wood, R.A., French, S., Fiocchi, A., Jordana, M., Waserman, S.,
1083 Brozek, J.L., and Schunemann, H.J. (2019). Oral immunotherapy for peanut
1084 allergy (PACE): a systematic review and meta-analysis of efficacy and safety.
1085 Lancet *393*, 2222-2232. 10.1016/S0140-6736(19)30420-9.
1086 103. Barshow, S., Tirumalasetty, J., Sampath, V., Zhou, X., Seastedt, H., Schuetz, J.,
1087 and Nadeau, K. (2024). The Immunobiology and Treatment of Food Allergy.
1088 Annu Rev Immunol *42*, 401-425. 10.1146/annurev-immunol-090122-043501.
1089 104. Fierstein, J.L., Brown, D., Gupta, R., and Bilaver, L. (2021). Understanding Food-
1090 Related Allergic Reactions Through a US National Patient Registry. J Allergy Clin
1091 Immunol Pract *9*, 206-215 e201. 10.1016/j.jaip.2020.08.011.
1092 105. Taylor, S.L., and Baumert, J.L. (2010). Cross-contamination of foods and
1093 implications for food allergic patients. Curr Allergy Asthma Rep *10*, 265-270.
1094 10.1007/s11882-010-0112-4.
1095 106. Miller, T.A., Koppelman, S.J., Bird, J.A., Hernandez-Trujillo, V., Thyagarajan, A.,
1096 Mack, D., Chalil, J.M., Green, T.D., and Baumert, J.L. (2022). Peanut cross-
1097 contamination in randomly selected baked goods. Ann Allergy Asthma Immunol
1098 *128*, 439-442. 10.1016/j.anai.2022.01.037.
1099 107. Dewhirst, F.E., Chien, C.C., Paster, B.J., Ericson, R.L., Orcutt, R.P., Schauer,
1100 D.B., and Fox, J.G. (1999). Phylogeny of the defined murine microbiota: altered
1101 Schaedler flora. Appl Environ Microbiol *65*, 3287-3292. 10.1128/AEM.65.8.3287-
1102 3292.1999.
1103 108. Burton, O.T., Stranks, A.J., Tamayo, J.M., Koleoglou, K.J., Schwartz, L.B., and
1104 Oettgen, H.C. (2017). A humanized mouse model of anaphylactic peanut allergy.
1105 J Allergy Clin Immunol *139*, 314-322 e319. 10.1016/j.jaci.2016.04.034.

1106 109. Whelan, F.J., and Surette, M.G. (2017). A comprehensive evaluation of the sl1p
1107 pipeline for 16S rRNA gene sequencing analysis. Microbiome *5*, 100.
1108 10.1186/s40168-017-0314-2.
1109 110. Pazos-Castro, D., Gonzalez-Klein, Z., Montalvo, A.Y., Hernandez-Ramirez, G.,
1110 Romero-Sahagun, A., Esteban, V., Garrido-Arandia, M., Tome-Amat, J., and
1111 Diaz-Perales, A. (2022). NLRP3 priming due to skin damage precedes LTP
1112 allergic sensitization in a mouse model. Sci Rep *12*, 3329. 10.1038/s41598-022-
1113 07421-y.
1114 111. Wang, Y., Matsushita, K., Jackson, J., Numata, T., Zhang, Y., Zhou, G., Tsai, M.,
1115 and Galli, S.J. (2021). Transcriptome programming of IL-3-dependent bone
1116 marrow-derived cultured mast cells by stem cell factor (SCF). Allergy *76*, 2288-
1117 2291. 10.1111/all.14808.
1118 112. Kechin, A., Boyarskikh, U., Kel, A., and Filipenko, M. (2017). cutPrimers: A New
1119 Tool for Accurate Cutting of Primers from Reads of Targeted Next Generation
1120 Sequencing. J Comput Biol *24*, 1138-1143. 10.1089/cmb.2017.0096.
1121 113. Martin, M. (2011). Cutadapt removes adapter sequences from high-througput
1122 sequencing reads. EMBnet.journal *17*, 10-12.
1123 https://doi.org/10.14806/ej.17.1.200.
1124 114. Callahan, B.J., McMurdie, P.J., Rosen, M.J., Han, A.W., Johnson, A.J., and
1125 Holmes, S.P. (2016). DADA2: High-resolution sample inference from Illumina
1126 amplicon data. Nat Methods *13*, 581-583. 10.1038/nmeth.3869.
1127 115. Quast, C., Pruesse, E., Yilmaz, P., Gerken, J., Schweer, T., Yarza, P., Peplies,
1128 J., and Glockner, F.O. (2013). The SILVA ribosomal RNA gene database project:
1129 improved data processing and web-based tools. Nucleic Acids Res *41*, D590-
1130 596. 10.1093/nar/gks1219.
1131 116. Price, M.N., Dehal, P.S., and Arkin, A.P. (2010). FastTree 2--approximately
1132 maximum-likelihood trees for large alignments. PLoS One *5*, e9490.
1133 10.1371/journal.pone.0009490.
1134 117. McMurdie, P.J., and Holmes, S. (2013). phyloseq: an R package for reproducible
1135 interactive analysis and graphics of microbiome census data. PLoS One *8*,
1136 e61217. 10.1371/journal.pone.0061217.
1137 118. Derakhshani, H., Bernier, S.P., Marko, V.A., and Surette, M.G. (2020).
1138 Completion of draft bacterial genomes by long-read sequencing of synthetic
1139 genomic pools. BMC genomics *21*, 519. 10.1186/s12864-020-06910-6.
1140 119. Chen, S., Zhou, Y., Chen, Y., and Gu, J. (2018). fastp: an ultra-fast all-in-one
1141 FASTQ preprocessor. Bioinformatics *34*, i884-i890.
1142 10.1093/bioinformatics/bty560.
1143 120. Chen, S. (2023). Ultrafast one-pass FASTQ data preprocessing, quality control,
1144 and deduplication using fastp. Imeta *2*, e107. 10.1002/imt2.107.
1145 121. Wick, R.R., Judd, L.M., Gorrie, C.L., and Holt, K.E. (2017). Unicycler: Resolving
1146 bacterial genome assemblies from short and long sequencing reads. PLoS
1147 Comput Biol *13*, e1005595. 10.1371/journal.pcbi.1005595.
1148 122. Schwengers, O., Jelonek, L., Dieckmann, M.A., Beyvers, S., Blom, J., and
1149 Goesmann, A. (2021). Bakta: rapid and standardized annotation of bacterial
1150 genomes via alignment-free sequence identification. Microb Genom *7*.
1151 10.1099/mgen.0.000685.

1152 123. Page, A.J., Cummins, C.A., Hunt, M., Wong, V.K., Reuter, S., Holden, M.T.,
1153 Fookes, M., Falush, D., Keane, J.A., and Parkhill, J. (2015). Roary: rapid large-
1154 scale prokaryote pan genome analysis. Bioinformatics *31*, 3691-3693.
1155 10.1093/bioinformatics/btv421.

1156

1157

1158

1159

1160

1161

1162 # STAR PROTOCOLS

1163 ## RESOURCE AVAILABILITY

1164 Lead contact

1165 Requests for further information or resources should be directed to the lead contact
1166 Alberto Caminero (acamine@mcmaster.ca).

1167 Materials availability

1168 This study did not generate new unique reagents.

1169 Data and code availability

1170 The microbiome sequencing data generated in this study have been deposited in the
1171 NCBI BioProject database under the accession number PRJNA1223483. The mass
1172 spectrometry proteomics data have been deposited to the ProteomeXchange Consortium
1173 via the PRIDE partner repository with the dataset identifier PXD060888 and
1174 10.6019/PXD060888.

1175 ## EXPERIMENTAL MODEL AND STUDY PARTICIPANT DETAILS

1176 Human samples
1177 Human saliva from peanut (PN) allergic patients entering oral immunotherapy (OIT; n=19)
1178 were collected. These samples were obtained from children aged 1-14 years who
1179 participated in a standard clinical oral food challenge to establish PN threshold prior to
1180 clinical management with PN OIT at Massachusetts General Hospital. Saliva was
1181 collected with the SalivaBio Children's Swab (Salimetrics) following the manufacturer's
1182 protocol, and samples were stored at -80°C until further use. PN- and antigen-specific Ig
1183 levels in plasma from patients undergoing OIT were measured using a Phadia
1184 ImmunoCAP 1000 instrument (ThermoFisher) according to the manufacturer's
1185 instructions. Saliva samples from healthy volunteers (n=13) were collected at McMaster
1186 University under BUP#423. All patients and healthy volunteers provided written informed
1187 consent as per local institutional review board guidelines. Supportive and demographics
1188 data can be found in Table S1.
1189
1190 To complement oral sampling, small intestinal aspirate samples (mid-jejunal washes)
1191 were obtained from non-allergic control individuals without any chronic gastrointestinal or
1192 metabolic conditions (n=5). These samples were collected under an ongoing clinical
1193 protocol led by Dr. Premysl Bercik at McMaster University (HIREB #15311). Push
1194 enteroscopy was performed following an overnight fast, and jejunal washes (15–20 mL)
1195 were collected as previously described[77]. Briefly, sterile saline was applied using a water
1196 jet to dislodge mucus-associated and luminal bacteria from the mid-jejunum and samples
1197 were frozen with or without 20% glycerol for further use. Small intestinal microbiota was

analyzed by 16S rRNA sequencing, and samples were cultured for isolation and identification of PN-degrading bacteria. Supportive and demographics data can be found in Table S1.

Human sera for Western blotting were provided by the Allergology Service at Hospital Universitario de La Princesa (Madrid, Spain). The Research Ethics Committee of Hospital Universitario de La Princesa approved the study protocol (reference 4460). All the donors provided written informed consent with no conflict of interest. Donor sera characterization is detailed in Table S2.

Mice

Age-, sex-, and strain-matched controls were used in all experiments. Specific pathogen-free (SPF) C57BL/6 mice were purchased from Charles River and Taconic, while SPF C3H-HeN mice were purchased from Taconic. Germ-free (GF) C57BL/6 mice used for colonization experiments were originally purchased from Taconic and derived GF by two-stage embryo transfer. They were bred in flexible-film gnotobiotic isolators at McMaster University's Farncombe Family Digestive Health Research Institute Axenic Gnotobiotic Unit (AGU). C3H-HeN mice with altered Schaedler flora (ASF) microbiota, a simple and stable microbiota[81,107], were bred and housed in GF conditions at the AGU. The C3H-HeN ASF mice were originally purchased from Taconic and have been maintained in the AGU for over 20 generations. All mice were maintained on a 12-h light-dark cycle and fed an autoclaved chow diet and sterile water *ad libitum*. Eight-to-12-week-old mice were used throughout. All procedures were approved by the Environmental Council of the Community of Madrid with PROEX references 45.2/20 and 9.7/23, and the McMaster University Animal Care Committee and McMaster University Animal Research Ethics Board in accordance with the Animal Utilization Protocol #22-26. Ethical regulations for animal research were strictly followed.

Food allergy and anaphylaxis model

To study the impact of microbes on PN metabolism and anaphylaxis, C3H-HeN mice with different microbiota were sensitized to PN using distinct techniques. 1. Intra-gastric sensitization: mice were provided 3.25 mg of crude PN extract (CPE; Greer Laboratories Inc) and 0.625 µg of cholera toxin (List Biological Laboratories) in 0.1 mL of PBS by oral gavage once a week for 6 weeks; 2. Intra-peritoneal sensitization: mice were provided 3.25 mg of CPE and 6.25 µg of cholera toxin in 0.1 mL of PBS intra-peritoneally once a week for 4 weeks; 3. Passive sensitization- mice were subjected to 3 intra-peritoneal injections (0.1, 0.2, and 0.4 mL) of serum obtained from intra-peritoneally sensitized PN-allergic mice as described[47]. After sensitization, mice were challenged with a 24 mg bolus of CPE in 0.8 mL of PBS by oral gavage. In some experiments, CPE was pre-digested with PN allergen-degrading bacteria (*Rothia* R3, *Staphylococcus* S1, or S2), or mice were colonized with PN-degrading bacteria (*Rothia* R3), prior to the oral challenge to evaluate

1237 the impact of bacterial PN metabolism on allergenicity and anaphylaxis. Serum was
1238 collected 48 h before challenge. Mice were monitored for 40 min after challenge for
1239 changes in rectal (core) body temperature. Peripheral blood was collected, and mice were
1240 euthanized 40 min after the oral challenge. Mucosal mast cell protease 1 (mMCP-1) was
1241 quantified in serum after the PN challenge, as it is a key biomarker of anaphylaxis in mice,
1242 serving a similar role to serum tryptase for indicating mast cell activation in humans[108].
1243 Platelet-activating factor acetylhydrolase (PAF-AH) was quantified in serum as a marker
1244 of mast cell activation.
1245
1246 Microbiota model for studying microbial PN metabolism
1247 To investigate the role of microbiota in PN metabolism, we used two colonization
1248 approaches: 1. We studied PN metabolism in mice colonized with ASF and SPF
1249 microbiota, and GF controls; 2. GF C57BL/6 mice were mono-colonized with selected
1250 PN-degrading bacteria (*Rothia* R3 or *Staphylococcus* S1, S2, or S3). After colonization,
1251 mice were administered 24 mg of CPE in 0.8 mL of PBS by oral gavage. Small and large
1252 intestinal contents and serum from peripheral blood were collected 40 minutes post-
1253 administration for quantification of PN allergens Ara h 1 and 2 in biological samples by
1254 ELISA (Indoor Biotechnologies) as described below. Additionally, small intestinal
1255 contents were incubated *ex vivo* with CPE overnight (o/n), and remaining Ara h 1 and 2
1256 levels were quantified by ELISA (Indoor Biotechnologies). C57BL/6 mice were used in
1257 these experiments because of difficulties generating C3H-HeN mice under GF conditions.
1258
1259 Characterization of bacterial PN-degradation and immune activation
1260 To assess bacterial degradation of PN allergens and its impact on immune activation, we
1261 performed *in vitro* digestions, proteomic characterization, and mast cell activation assays.
1262 Bacterial isolates were incubated with CPE and degradation of Ara h 1 and Ara h 2 was
1263 quantified by ELISA. Then, *Rothia* (R1, R2, and R3) and *Staphylococcus* (S1, S2, and
1264 S3) candidates were selected for further characterization by SDS-PAGE, and Western
1265 blotting. Western blotting was performed using sera from PN-allergic patients as well as
1266 sera from mice allergic to Ara h 1 or to Ara h 2, to identify IgE-binding epitopes in the
1267 digested PN allergens. Proteomic analysis using nano liquid chromatography coupled to
1268 mass spectroscopy was used to characterize the degradation products and PN-specific
1269 epitopes. For immune activation studies, bone marrow-derived mast cells (BMMCs) were
1270 cultured and sensitized to PN with sera from PN-allergic mice. These cells were
1271 challenged with bacterially digested PN to evaluate BMMC activation by β-
1272 hexosaminidase release and flow cytometry analysis of degranulation markers (CD63,
1273 CD107a)[46].
1274
1275

1276 **METHOD DETAILS**

1277 Mouse colonization procedures

1278 For colonization of GF C57BL/6 mice with ASF and SPF microbiota, fresh cecal and colon
1279 contents were harvested from SPF C57BL/6 mice (Taconic) or ASF C3H-HeN mice,
1280 diluted 1:10 in sterile PBS in anaerobic conditions, and 0.2 mL of each cecal/fecal
1281 suspension was orally gavaged to mice.
1282
1283 For mono-colonization of GF C57BL/6 mice with PN-degrading bacteria, *Rothia* R3 or
1284 *Staphylococcus* S1, S2, or S3 were grown o/n in brain heart infusion broth (BHI; Research
1285 products International Corp.) and 10^9 colony forming units (CFU) from the culture were
1286 provided by oral gavage with PBS as a vehicle. GF controls were provided PBS by oral
1287 gavage.
1288
1289 For the PN anaphylaxis model, ASF C3H-HeNTac mice received 10^9 CFU total of *Rothia*
1290 R3, by oral gavage, administered once per week for three weeks after sensitization and
1291 before PN challenge. Sterile PBS was used as a vehicle and served as a non-colonization
1292 control.
1293
1294 Colonization was confirmed by culturing intestinal content combined with PCR of the 16S
1295 rRNA gene and Sanger sequencing to verify bacterial identity (methods detailed below).
1296 These checks were performed throughout the experiments and at endpoint. Mice with
1297 evidence of contamination or failed colonization were excluded from the analysis. For
1298 selected experiments, 16S rRNA microbiota analysis was also performed to confirm
1299 overall microbial community composition.
1300

1301 PN-specific IgE determination

1302 Peripheral blood was collected by retro-orbital bleeding 48 h before the PN challenge.
1303 Serum PN-specific IgE was measured using a sandwich ELISA adapted from previously
1304 described methods[47]. Briefly, 96-well plates (high-binding, flat-bottom, polystyrene;
1305 Corning, USA) were coated o/n at 4°C with 2 µg/mL rat anti-mouse IgE antibody diluted
1306 in PBS. Plates were washed with PBS/0.05% Tween-20 (PBS-T; Sigma Aldrich), then
1307 blocked with 1% BSA in PBS-T for 2 h at room temperature (RT). Plates were washed
1308 thoroughly with PBS-T, then serum samples were incubated on the plate at 1/2 dilution
1309 o/n at 4°C. To detect PN-specific IgE, plates were incubated with biotinylated-CPE (biot-
1310 CPE; 0.1518 µg/mL in blocking solution) for 90 min at RT. Biot-CPE was generated using
1311 the EZ-Link Sulfo-NHS-LC-Biotinylation kit (Thermo Scientific). A standard curve, to
1312 which no capture antibody or sera was added, was generated using biot-CPE, serially
1313 diluted from 75 ng/mL to 0.6 ng/mL in PBS. Plates were washed thoroughly, then
1314 incubated with streptavidin-HRP (1:250 dilution in blocking solution; Thermo Scientific)
1315 and tetramethylbenzidine substrate (TMB; Thermo Scientific or Biolegend). The reaction

1316 was stopped with 1 N H_2SO_4. OD was measured at 450 nm, and the values were
1317 interpolated against the biot-CPE standard curve to determine relative PN-specific IgE-
1318 binding. Results are expressed as PN-IgE (Relative Binding, OD), reflecting the ability of
1319 serum PN-specific IgE to bind PN allergens.
1320
1321 mMCP-1 quantification
1322 Peripheral blood was collected by retro-orbital bleeding 40 min after the PN challenge.
1323 The concentration of mMCP-1 was quantified using a Mouse mMCPT-1 ELISA kit
1324 (Thermo Scientific) following the manufacturer's instructions. Briefly, serum samples were
1325 diluted by 1/25 and incubated on the capture antibody (anti-mouse mMCPT-1)-coated
1326 plate for 2 h at RT. After washing, a biotin-conjugated anti-mouse mMCPT-1 antibody
1327 was added to the plate and incubated for 1 h at RT. The reaction was developed with
1328 avidin-HRP and TMB, stopped with 1N H_2SO_4 and OD was measured at 450 nm. The
1329 results are expressed as ng of mMCP-1 per mL of serum and multiplied by the dilution
1330 factor of the sample.
1331
1332 ELISA detection of PN allergens in biological samples
1333 Ara h 1 and 2 were detected in samples harvested 40 min following intra-gastric
1334 administration of 24 mg of CPE in 0.8 mL of PBS. Serum from peripheral blood was
1335 collected by retro-orbital bleeding and analyzed undiluted. Whole small and large
1336 intestinal content was analyzed after dilution by 1/5 and 1/10 in PBS. The quantification
1337 of PN allergens was performed using proprietary ELISA kits for Ara h 1 and 2 following
1338 the manufacturer's instructions (Indoor Biotechnologies). Briefly, for Ara h 1 detection by
1339 ELISA (Indoor Biotechnologies): Plates pre-coated with a monoclonal anti-Ara h 1
1340 antibody were washed with wash buffer, and biological samples and Ara h 1 standards
1341 were added and incubated for 1 h. The plates were washed, and a second monoclonal
1342 anti-Ara h 1 antibody conjugated to peroxidase was added and incubated for 1 h. After a
1343 final wash, TMB substrate was added, and the reaction was stopped with 0.5 N H_2SO_4.
1344 OD was measured at 450 nm, and results were expressed as the concentration of Ara h
1345 1 in biological samples, multiplied by the dilution factor. For Ara h 2 detection by ELISA
1346 (Indoor Biotechnologies): Plates pre-coated with a monoclonal anti-Ara h 2 antibody were
1347 washed with wash buffer, and biological samples and Ara h 2 standards were added and
1348 incubated for 1 h. After washing, a rabbit anti-Ara h 2 polyclonal detection antibody was
1349 added and incubated for 1 h. This was followed by the addition of a peroxidase-
1350 conjugated anti-rabbit IgG for 1 h. After the final wash, TMB substrate was added, and
1351 the reaction was stopped with 0.5 N H_2SO_4. OD was measured at 450 nm, and results
1352 were expressed as the concentration of Ara h 2 in biological samples, multiplied by the
1353 dilution factor.
1354
1355

1356

1357 Detection of PN degradation by microbes isolated from human saliva and mouse and
1358 human intestinal content

1359 Whole human saliva samples from healthy individuals (n=13), human small intestinal
1360 aspirates (jejunum) (n=5), and mouse small and large intestinal contents (10 mg/mL in
1361 PBS) were plated on agar media plates designed to isolate PN-degrading bacteria. BHI
1362 media enriched with powdered PN (organic partially defatted PN; PB&Me, Sahah
1363 Naturals) or agar supplemented with powered PN were used. Plates were incubated with
1364 samples for 48 h in aerobic and anaerobic conditions (Bactron IV anaerobic chamber).
1365 The bacteria were isolated based on their capacity to generate a visible hydrolytic halo in
1366 the media, which is indicative of the breakdown of PN components in the media. Isolated
1367 bacteria demonstrating PN hydrolytic activity were incubated in liquid BHI with CPE (0.5
1368 mg/mL). After 48 h of incubation under aerobic or anaerobic conditions, the amount of
1369 Ara h 1 and 2 in media was quantified by ELISA as described above. Allergen degradation
1370 was calculated as the percentage of allergen degraded relative to the initial concentration
1371 in non-growth controls (CPE). These values were visualized in heatmaps using a blue-
1372 red color scale, where blue represents no degradation (0%) and red indicates complete
1373 degradation (100%).

1374 Relative abundance of each bacterial isolate was determined by calculating the proportion
1375 of times each taxon was isolated across all samples. These values were expressed as
1376 percentages and displayed using a green color scale, ranging from light green (low
1377 relative abundance) to dark green (high relative abundance).

1378 Salivary and intestinal microbes were identified using Sanger sequencing technology.
1379 Briefly, DNA from isolates was extracted by picking single bacterial colonies into water,
1380 boiling, and centrifuging at 2,000 RCF for 2 min. The 8F-926R region of the 16S rRNA
1381 gene was amplified by PCR using the extracted DNA and sequences were determined
1382 using Sanger sequencing (FW primer: 5'- AGAGTTTGATCCTGGCTCAG-3', RV primer:
1383 5'-CCGTCAATTCCT-TTRAGTTT-3'). The resulting sequences for the isolates were
1384 taxonomically assigned using the NCBI nucleotide collection database[109].

1385

1386 PAF-AH quantification

1387 Serum levels of platelet-activating factor acetylhydrolase (PAF-AH) were quantified using
1388 a mouse PAF-AH/PLA2G7/Lp-PLA2 ELISA kit (Novus Biologicals) according to the
1389 manufacturer's instructions. Briefly, serum samples were diluted 1:10 in PBS and
1390 incubated capture antibody coated plates. After washing, a biotin-conjugated detection
1391 antibody was added for 1 h at RT, followed by HRP conjugate for 30 min. The reaction
1392 was developed with TMB, stopped with 1N H_2SO_4, and OD was measured at 450nm.
1393 Results were expressed as ng/mL serum and corrected for the dilution factor.

1394

1395

1396 Quantification of mucosal tryptase-positive mast cells

1397 Paraffin-embedded small intestinal sections were deparaffinized in xylene and
1398 redhydrated through a graded ethanol series. Antigen retrieval was performed by heat in
1399 citric acid buffer, and non-specific binding was blocked with 3% BSA in PBS for 45 min.
1400 Sections were incubated o/n at 4°C with a rabbit monoclonal anti-mast cell tryptase
1401 antibody (1:200, Abcam). Immunoreactive cells were visualized using 3,3-
1402 diaminobenzidiene (DAB; Dako). Negative controls were performed by omitting the
1403 primary antibody. Tryptase positive mast cells were quantified in the mucosa and
1404 normalized to mucosal area using an Axio Imager Z2 microscope (Carl Zeiss, Jena,
1405 Germany). The data are expressed as tryptase-positive cells/μm^2.

1406

1407 Microbial digestion of PN for challenge

1408 Selected bacteria (*Rothia aeria* (R3), *Staphylococcus epidermidis* (S1), and
1409 *Staphylococcus aureus* (S3)) were grown o/n on BHI agar plates enriched with 1%
1410 powdered PN to confirm PN degradation capability (visible PN hydrolytic halo). For each
1411 strain, a 10 mL pre-inoculum was prepared by o/n culture in liquid BHI. Then, 10 µL of
1412 pre-inoculum was transferred into 5 mL of OptiMEM medium containing 30 mg/mL CPE
1413 and incubated for 6 h to complete the PN digestion process. The resulting digests were
1414 boiled for 5 min to kill the bacteria, and 800 µL of the digests, containing 24 mg of digested
1415 PN, was administered by oral gavage at the time of challenge as described above.
1416 OptiMEM medium served as the vehicle for non-digested CPE challenge.

1417

1418 Measurement of *ex vivo* intestinal PN-degrading capacity

1419 The ability of the intestinal content from mice colonized with PN-degrading bacteria to
1420 degrade PN was assessed using ELISA and a bioassay with agar media enriched with
1421 PN. Solid BHI agar enriched with 1% powdered PN was prepared, and a 50 µL aliquot of
1422 diluted (1/2 in PBS) small intestinal content was placed into wells created in the agar. The
1423 plates were then incubated for 24 h. The PN-degrading capacity was determined by
1424 measuring the diameter of the clear halo around the inoculation site, indicating
1425 degradation, and the results were expressed in millimeters. In addition, the intestinal
1426 contents were also incubated with CPE (0.5 mg/mL). After 48 h of incubation, the quantity
1427 of Ara h 1 and 2 in media was analyzed by ELISA as described above. The data for Ara
1428 h 1 and 2 degradation are represented as blue-red color scales showing the percentage
1429 of allergen degradation relative to the control incubations (CPE), with blue indicating no
1430 degradation (0%) and red indicating complete degradation (100%).

1431

1432 Ussing chamber detection of PN translocation after bacterial digestion

1433 Translocation of PN allergens after digestion by bacteria was evaluated *ex vivo* using
1434 small intestinal sections of SPF C3H-HeN mice and the Ussing chamber technique. For

1435 preparation of bacterial PN allergen digestions, *Rothia mucilaginosa* (R3),
1436 *Staphylococcus epidermidis* (S1), and *Staphylococcus aureus* (S2 & S3) were grown for
1437 16 h in BHI liquid medium. Bacteria were then incubated in BHI with 5 mg/mL CPE for 4
1438 h to allow for bacterial digestion of the PN allergens. After incubation, samples were boiled
1439 for 15 min. Bacterial digestions were performed in triplicate, with a negative control
1440 containing no bacterial inoculum. For the Ussing chamber technique, 1.5 cm sections of
1441 proximal small intestine were collected, opened along the mesenteric border, and
1442 mounted on the sliders of Ussing chambers. Each chamber exposed 0.25 cm^2 of tissue
1443 surface area to 4 mL of circulating oxygenated Krebs buffer containing 10 mM glucose
1444 (serosal side) and 10 mM mannitol (mucosal side), maintained at 37°C and aerated with
1445 95% O_2 and 5% CO_2. Then, 0.2 mL of each bacterial digestion was placed into 4 mL of
1446 Krebs buffer on the mucosal side of the chamber. The experiment was run for 2 h, after
1447 which the total mucosal and serosal volumes were collected. The concentrations of PN
1448 allergens Ara h 1 and Ara h 2 on the serosal side were quantified by ELISA and expressed
1449 as intestinal translocation of allergens. The Ussing chamber system was from Physiologic
1450 Instruments.
1451
1452 <u>Microbial digestion of PN for proteomic and immune activation assays</u>
1453 *Rothia* (R1- *Rothia aeria* R2- *Rothia dentacariosa* R3- *Rothia mucilaginosa*) and
1454 *Staphylococcus* (S1- *Staphylococcus epidermidis,* S2- *Staphylococcus aureus,* S3-
1455 *Staphylococcus aureus*) species were selected for characterization of PN allergen
1456 degradation and allergenicity. Bacteria were grown o/n in BHI (10 mL), then 10 µL of
1457 bacterial culture was taken and used to inoculate 1 mL of OptiMem with 0.5 mg/mL CPE.
1458 The bacteria were incubated in the media with CPE for 4 h at 37ºC. After the incubation,
1459 the digestion was stopped by boiling for 5 min. Subsequently, the digestion of Ara h 1 and
1460 2 were detected using ELISA, SDS-PAGE and Western blotting, and BMMC activation
1461 assays.
1462
1463 <u>SDS-PAGE and Western blotting</u>
1464 To assess PN degradation profiles produced by degradation by *Rothia* and
1465 *Staphylococcus* species we performed SDS-PAGE and Western blotting. Bacteria were
1466 grown in 0.5 mg/mL as mentioned above. Undigested PN and Ara h 1 and 2 were used
1467 as controls. Then Laemmli sample buffer (Bio-Rad) with β-mercaptoethanol (Sigma-
1468 Aldrich) at 1/10 was added at 1/4 in a final volume of 50 µL. Before loading the gel (Any
1469 kD™ Mini-PROTEAN® TGX™ Precast Protein Gels, Bio Rad), samples were heat-
1470 denatured at 100ºC for 5 min. Moreover, a protein molecular weight marker was added
1471 (ThermoFischer). The gel was run in 1X running buffer (*i.e.*, SDS/Tris/Glycine 10X, Bio-
1472 Rad) for 1-1.5 h at 100 V using an electrophoretic cell and a power supply Mini-Protean
1473 System Bio-Rad (Bio-Rad).
1474

1475 For SDS-PAGE, after running, the gel was placed in staining solution (45% of methanol
1476 and 10% of acetic acid in distilled water, plus 0.2% w/v of Coomassie blue, Bioscience)
1477 for 1 h in agitation. Then, the staining solution was removed using destaining solution
1478 (20% methanol and 10% acetic acid, Sigma-Aldrich, in distilled water) in constant
1479 agitation, the process was repeated every 15 min until the background was eliminated.
1480 Then, the gel was photographed using a molecular imaging system (Amersham
1481 ImageQuant™ 800).
1482
1483 For Western blotting, after running the gel, the bands of the gel were transferred to a
1484 nitrocellulose membrane (Bio-Rad) using a transfer system (fiber pad, filter paper,
1485 membrane, gel, filter paper and fiber pad) and transfer buffer (20% methanol and 10% of
1486 Tris-Glycine 1X in distilled water). The transference was run for 1 h at 400 mA. Then, to
1487 check that bands were transferred correctly, the membrane was stained with Ponceau S
1488 Staining solution (ThermoScientific). After cleaning with water and 3 washes with TBS-T
1489 solution, the membrane was blocked in constant agitation for at least 1 h with 3% BSA
1490 (NZYtech) in TBS-T. Then, the membrane was incubated with sera from PN-allergic
1491 donors, or sera from mice allergic to Ara h 1 or to Ara h 2 (diluted in 3% BSA at different
1492 dilutions depending on the amount of IgE) as primary antibody, at 4ºC o/n with smooth
1493 agitation. Sera from non PN-allergic donors (Table S2) and non PN-allergic mice were
1494 used as negative control. During day 2, after performing 6 washes with TBS-T every 10
1495 min with agitation, the membrane was incubated with anti-human IgE-HRP (Invitrogen)
1496 1:10,000 or anti-mouse IgE-HRP (SouthernBiotech) 1:1,000 as secondary antibody for 1
1497 h at RT with agitation. Then, 6 washes with TBS-T every 10 min with agitation were
1498 performed before revealing the membrane According to the instructions of the
1499 manufacturer (Cytiva-Merck), 1:1 of peroxide and luminol and 1 mL of the mixture was
1500 added to the membrane. The chemiluminescent signal of the gel was captured in a
1501 chemiluminescent imaging system (Amersham ImageQuant™ 800). SDS-PAGE and
1502 Western blots were analyzed using Fiji ImageJ.
1503
1504 Proteomics
1505 Proteomics was performed to identify bacterial degradation products of PN allergens and
1506 to map PN-specific epitopes. Microbial PN digestions (above) by *Rothia* (R1, R2, and R3)
1507 and *Staphyloccocus* (S1, S2, and S3) were ultra-filtered using microcon filter units with a
1508 3 kD cutoff that were previously equilibrated and washed with water. The peptides of the
1509 flow-through were selected (<3 kD) and they were cleaned with ZipTip with 0.6 µL
1510 C18 resin (Merck Millipore) to avoid the presence of elements that could interfere with the
1511 mass spectrometry, and they were drained in a SpeedVac Vacuum Concentrator. The
1512 samples, resuspended in a volume of 14 µL and 2 µL LC-MS grade water containing 2%
1513 (v/v) acetonitrile and 0.1% (v/v) formic acid, were used for the quantification with the QBIT
1514 method, analyzing around 0.8 µg per sample. The peptides were analyzed by nano liquid

1515 chromatography coupled to mass spectrometry in data-dependent-acquisition mode
1516 using an UltiMate 3000 High Pressure Liquid Chromatograph (Fisher Scientific) and a
1517 Orbitrap Exploris™ 240 Mass Spectrometer (Fisher Scientific). The flow of the
1518 chromatograph was 250 nL/min for 60 min, and an Easy-spray PepMap C18 analytical
1519 column 50 cm × 75 µm (Fisher Scientific) was used.
1520 The obtained MS1 and MS2 spectra were analyzed using the Peaks
1521 (https://www.bioinfor.com/peaksdb/) search engine against an *Arachis hypogaea*
1522 proteome database obtained from UniprotKB (https://www.uniprot.org/) combined with a
1523 list of typical laboratory contaminants, using a tolerance of 10 ppm and 0.02 Da for the
1524 precursor ions and fragments, respectively. Carbamidomethylation in cysteines was used
1525 as fixed modification and acetyl in the N-terminal end of the protein and methionine
1526 oxidation were used as variable modifications. The search was performed without
1527 restrictions to any proteases and the results were shown as proteins identified with at
1528 least a unique peptide with a False Discovery Rate ≤1%.
1529 The unique peptides obtained after the analysis were located and identified in the
1530 sequences of Ara h 1, which were downloaded from the Protein Data Bank
1531 (https://www.rcsb.org/). The most common human IgE-binding epitopes of Ara h 1 were
1532 found in the following allergen databases: Allergen Nomenclature (https://allergen.org/);
1533 Allergen Online (http://allergenonline.org/); Compare Database
1534 (https://db.comparedatabase.org/); and The Immune Epitope Database (
1535 https://www.iedb.org/). The following studies were considered to specify
1536 immunodominant IgE-binding epitopes[34-45]. Ara h 1 peptides that were contiguous or
1537 overlapping were considered distinct if their cut-off points differed. Peptides not fully
1538 aligned with the canonical sequence were required to have at least 75% alignment and a
1539 minimum of four consecutive identical amino acids Molecular structure analysis was
1540 performed with Chimera v1.17.3 for tridimensional visualization of allergens and relevant
1541 epitopes before and after bacterial digestion.
1542
1543 Mice sensitization to Ara h 1 and Ara h 2
1544 Mice were sensitized to immunodominant PN allergens to generate sera specific to Ara
1545 h 1 or Ara h 2 specific IgE to be used in mast cell degranulation assays (above). To
1546 sensitize mice against native Ara h 1 (InBio) or recombinant Ara h 2 (prepared as
1547 reported[110] using Uniprot reference Q6PSU2-1 without the signal peptide), 3 i.p. injections
1548 with 10 µg of the allergen plus 1 mg aluminum hydroxide (Alhydrogel® adjuvant 2%,
1549 InvivoGen) were performed. Previously, aluminum hydroxide and allergen were mixed at
1550 4ºC during 30 min in a ferris wheel. Between the first and second injection, 2 weeks were
1551 left; and 1 week between the second and third injection. Blood samples were collected
1552 and centrifuged at 16,000 RCF to obtain sera for mast cell activation assays (see below)
1553 and Western blot analysis. Control sera from PN-allergic mice were generated following
1554 immunization with a classical model of food allergy.[47,71]

1555

1556 Bone marrow-derived mast cell culture

1557 BMMCs were cultured to assess mast cell activation by bacterially digested PN allergens.
1558 Bone marrow from femur and tibia of C57BL/6 (Charles River) mice were used to obtain
1559 BMMCs as described[111]. In short, bone marrow was flushed out inserting a 23-gauge
1560 needle (BD Microlance) attached to the 10 mL syringe filled with PBS (Gibco) at the knee
1561 side of both types of bone. Then, the cell suspension collected was filtered with a 40 µm
1562 filter (Falcon). After centrifugating 5 min at 286 RCF and RT, the pellet was lysed with
1563 ACK lysing buffer (Lonza). Erythrocyte-lysed bone marrow cells were cultured for 4 weeks
1564 in Petri dishes at 37ºC and 5% CO_2 in Iscoves´s Modified Dulbecco´s Medium (IMDM,
1565 Gibco) supplemented with 10% fetal bovine serum (FBS, Cytiva), 1% minimal essential
1566 medium (MEM, Gibco), 1% sodium pyruvate (Biowest), 1% penicillin/streptomycin (P/S,
1567 Gibco), 1% non-essential amino acids (Biowest), 0.01% recombinant murine stem cell
1568 factor (SCF, PeproTech) and 0.05% recombinant murine Interleukin (IL-3, PeproTech),
1569 until they differentiated into mature BMMCs. Cell growth and viability were monitored
1570 using the trypan blue exclusion test. The culture media was changed weekly, and the
1571 cellularity was kept below 0.5×10^6 cells/mL.

1572

1573 BMMC activation

1574 BMMC activation was conducted as reported[46,47]. In brief, BMMCs were sensitized o/n at
1575 37ºC and 5% CO_2 with sera at a concentration range of 15–40 ng/mL from Ara h 1- or
1576 Ara h 2-sensitized mice. Culture media was changed 1-2 days previous sensitization. PN-
1577 allergic mice sera were used as a positive control. BMMC sensitization was done at a cell
1578 density of 1×10^6 cells/mL. The next day, BMMCs were washed to eliminate unbound Igs
1579 (cells were spun at 265 RCF for 5 min and low break) and resuspended in supplemented
1580 IMDM without cytokines, nor FBS, at a cell density of 1×10^6 cells/mL. For BMMC
1581 activation, bacteria with PN-degrading potential isolated from saliva and gut of healthy
1582 donors were selected. Then, 0.1×10^6 BMMCs per condition were placed in a U/V bottom
1583 96-well culture plate (Falcon) and challenged with bacterially digested PN (Stallergenes
1584 Greer) at 25 µg/mL and 100 µg/mL in Ara h 1-sensitized BMMCs, or at 50 µg/mL and 200
1585 µg/mL in Ara h 2-sensitized BMMCs. Media and undigested PN were used as negative
1586 and positive controls, respectively. After 20 min at 37ºC and 5% CO_2, the reaction was
1587 stopped on ice and BMMC activation was determined via β-hexosaminidase activity in
1588 the supernatants, and phenotypically (CD63 and CD107a expression) by flow
1589 cytometry[46].

1590

1591 β-hexosaminidase activity assay

1592 BMMCs were centrifugated as above described to recover cell-free supernatants. A
1593 volume of supernatant of 45 µL was added in duplicates to 45 µL of β-hexosaminidase
1594 substrate solution (2 mM p nitrophenyl N-acetyl β-D-glucosamine, Sigma-Aldrich) diluted

in 0.1 M citrate buffer (45 mM dehydrated sodium citrate, 55 Mm citric acid, Sigma-Aldrich, in distilled H_2O) in a flat-bottom 96-well plate. After incubation at 37ºC for 45 min in the dark, 45 µL NaOH 1 M (1M sodium hydroxide, Sigma-Aldrich, in distilled H_2O) were added to stop the reaction. OD was measured at 405 nm with a microplate reader. Buffers alone and BMMC lysates (0.5% Triton X-100, Sigma Aldrich, was used for cell lysis) were used as control, absorbance background (B) and total lysis, respectively. The percentage of BMMC degranulation, based on β-hexosaminidase activity, was calculated as follows:

$$\text{Degranulation (\%)}=\frac{\text{OD supernatant-B}}{\text{OD total lysis-B}}\times 100$$

Flow cytometry

BMMCs were resuspended in ice-cold FACS buffer (2.5 mM EDTA, PanReacAppliChem, 0.5% BSA in PBS). BMMCs were blocked with 1:50 Fc block (purified anti-mouse CD16/32, BioLegend) for 15 min on ice to prevent non-specific antibody binding. Then, BMMCs were incubated with BV421 rat anti-CD117 (c-kit) (BioLegend) 1/200; APC rat anti-CD63 (BioLegend) 1:200; PerCP-Cy5.5 rat anti-CD107a (LAMP-1) (BioLegend) 1:200; PE rat anti-IgE (BioLegend) 1:200; PE-Cy7 rat anti-FcεR1α (BioLegend) 1:200; on ice for 30 min covered from light. Viability was assessed with efluor780 dye (eBioscience) 1:4,000. After washing with FACS buffer to eliminate unbound antibodies, cells were analyzed on a BD FACSCantoll flow cytometer. On average, 10,000 live and single cells were recorded. Data were analyzed with FlowJo v10 software; dead cells and aggregates were excluded and fluorescence minus one (FMO) controls were used for gating.

Microbiota analysis

DNA was extracted from mouse fecal pellets, human saliva, and human jejunal aspirates, and the hypervariable V3-V4 regions of the 16S rRNA gene were amplified with polymerase chain reaction (PCR) using Taq polymerase (Life Technologies), as previously described[81]. Forward barcoded primers targeting the V3 region (v3f_341f-CCTACGGGNGGCWGCAG) and reverse primers targeting the V4 region (v4r_806r-GGACTACNVGGGTWTCTAAT) were used. Forward primers included six-base pair barcodes to allow multiplexing samples. Purified PCR products were sequenced using the Illumina MiSeq platform by the McMaster Genomics facility. Primers were trimmed from the obtained sequences with Cutadapt software[112,113], and processed with Divisive Amplicon Denoising Algorithm 2 (DADA2; version 1.14.0) using the trained SILVA reference database (version 138.1)[114,115]. A phylogenetic tree of the sequences was calculated using FastTree 2[116], and data was explored using the phyloseq package (version 1.30.0) in R (version 3.6.2)[117]. After data cleanup, a total of 292,618 reads were obtained with a minimum of 11,651 and maximum of 60,790 with an average of 32,513 reads per sample for mouse microbiota. For human healthy control salivary microbiota, a total of 273,686 reads were obtained with a minimum of 1,881 and maximum of 48,620 with an average of 16,099 reads per sample. For PN allergic patient salivary microbiota,

a total of 844,167 reads were obtained with a minimum of 3,236 and maximum of 145,324 with an average of 36,702 reads per sample. Alpha-diversity was measured using observed species and Chao1 indices. Beta-diversity was calculated on normalized data and the originated matrices were ordinated using principal coordinate analysis based on Jaccard distance (mouse microbiota) and Bray-Curtis dissimilarity (human microbiota).

For whole genome sequencing of bacterial isolates, genomic DNA was extracted as previously described[81]. Illumina short-read libraries were prepared using the NEBNext Ultra II FS DNA Library Prep Kit for Illumina (NEB, Ipswich, MA, USA). Final libraries were sequenced on an Illumina NextSeq 2000 platform using a P1 flow cell at the McMaster Metagenomics Facility (Hamilton, ON, Canada). The run yielded 3.7 million paired-end (2 × 150 bp) reads per genome. Short reads were processed as previously described[118], with few modifications. Briefly, fastp was used for quality trimming and removal of adapters from Illumina reads[119,120]. Unicycler (v.0.5.1) was then used for de novo assembly[121], followed by Bakta for annotation of the genomes[122]. Genomes were then compared using Roary[123]. The data was further analysed using the MEROPs database and R (4.4.3) to search for proteases. The data are presented as heatmaps where light blue=gene not present and dark blue=present.

Rothia abundance (16S rRNA) data in saliva of non-PN allergic and PN-allergic (high threshold and low threshold) individuals were obtained from a previously published PN allergy cohort described by Zhang *et al*[51]. PN threshold was determined as described in the primary study[51]. In this cohort, amplicon sequence variants (ASVs) belonging to *Rothia* were identified after filtering for low prevalence and low abundance, and relative abundances were quantified following taxonomic assignment against NCBI databases. We used the *Rothia* ASV abundance values as provided by the authors for secondary analysis in the present study.

STATISTICAL ANALYSIS

All variables were analyzed using GraphPad Prism 9 and 10 software (GraphPad Software, USA). Parametric data are depicted as dot plots with each dot representing an individual mouse or biological replicate. Normal distribution was determined by D'Agostino-Pearson omnibus normality test, Shapiro-Wilk test, and Kolmogorov-Smirnov test with Dallal-Wilkinson-Lillie correction. One way analysis of variance (ANOVA) was used to evaluate differences between more than two groups with a parametric distribution and Tukey's or Dunnet's post-hoc corrections were applied. Student's t-test (two-tailed) was performed to evaluate the differences between two independent groups as appropriate. Data with non-normal distribution were evaluated with Kruskal-Wallis test with Dunn's post-hoc test for more than two groups. Correlation analyses were performed using Pearson correlation for parametric data and Spearman correlation for non-

parametric data. A P value of ≤ 0.05 was selected to reject the null hypothesis. Information regarding specific P values, value of n, and how data are presented can be found in figure legends.

KEY RESOURCES TABLE

REAGENT or RESOURCE	SOURCE	IDENTIFIER
Antibodies		
Rat anti-mouse IgE (clone R35-72)	BD Pharmingen	Cat# 553413
Anti-mouse IgE-HRP (clone: 23G3)	SouthernBiotech	Cat#1130-05
Anti-human IgE-HRP	Invitrogen	Cat#A18793
Sera from Ara h 1- or Ara h 2-sensitized mice	This paper	N/A
Purified anti-mouse CD16/32 (clone: 93)	BioLegend	Cat#101302
BV421 rat anti-CD117 (c-kit) (clone: ACK2)	BioLegend	Cat#135124
APC rat anti-CD63 (clone: NVG-2)	BioLegend	Cat#143906
PerCP-Cy5.5 rat anti-CD107a (LAMP-1) (clone: 1D4B)	BioLegend	Cat#121626
PE rat anti-IgE (clone: RME-1)	BioLegend	Cat#406908
PE-Cy7 rat anti-FcεR1α (clone: MAR 1)	BioLegend	Cat#134318
Rabbit anti-mast cell tryptase	Abcam	Cat#ab151757
Bacterial and virus strains		
Rothia aeria	This paper	R1
Rothia dentacariosa	This paper	R2
Rothia mucilagenosa	This paper	R3
Staphylococcus epidermidis	This paper	S1
Staphylococcus aureus	This paper	S2
Staphylococcus aureus	This paper	S3
Biological samples		
Serum from peanut-allergic donors	Hospital Universitario de la Princesa	N/A
Saliva from Healthy controls	McMaster University	N/A
Saliva from peanut-allergic patients	Mass General Hospital	N/A
Chemicals, peptides, and recombinant proteins		
ACK Lysing Buffer	Lonza	Cat#BP10-548E
Iscoves´s Modified Dulbecco´s Medium (IMDM)	Gibco	Cat#12440-053
Fetal Bovine Serum (FBS)	Cytiva	Cat#SV30160.03
Minimal essential medium (MEM)	Gibco	Cat#11120-037
Penicillin/Streptomycin	Gibco	Cat#15140122
Non-essential amino acids	Biowest	Cat#X0557-100
Sodium Pyruvate	Biowest	Cat#L0642
Recombinant Murine Stem Cell Factor (r-mSCF)	PeproTech	Cat#250-03
Recombinant Murine Interleukin 3 (r-mIL-3)	PeproTech	Cat#213-13
Native Ara h 1	InBio	Cat#NA-AH1-1
Native Ara h 2	InBio	Cat#NA-AH2-1
Recombinant Ara h 2	Centre for Plant Biotechnology and Genomics	N/A
Aluminum hydroxide, Alhydrogel® adjuvant 2%	InvivoGen	Cat#21645-51-2
Bovine Serum Albumin (BSA)	NZYtech	Cat#9048-46-8
Tetramethylbenzidine (TMB)	Biolegend	Cat#421101
Peanut (PN; CPE)	Stallergenes Greer	Cat#XPF171D3A25
p nitrophenyl N-acetyl β-D-glucosamine	Sigma-Aldrich	Cat#N9376-100MG
0.5% Triton X-100	Sigma Aldrich	Cat#9036-19-5
Ethylenediaminetetracetic acid (EDTA)	PanReacAppliChem	Cat#131026

Efluor780 viability	eBioscience	Cat#65-0865-14
Any kD™ Mini-PROTEAN® TGX™ Precast Protein Gels	Bio Rad	Cat#4569034
Nitrocelulose membrane	Bio Rad	Cat#1620115
Protein molecular weight marker	ThermoFischer	Cat#26619
Microcon units	Sigma	Cat#UFC5003
Cholera toxin from *Vibrio cholerae* Inaba 5698	List Biological Laboratories	Cat#100B, 9100B
Brain-heart infusion (BHI) broth	Research Products International Corp.	Cat#B11000-1000
Powdered PN	PB & Me, Sahah Naturals	SKU#62845116652
Opti-MEM™ Reduced Serum Medium	Gibco, ThermoScientific	Cat#31985070
3,3-diaminobenzidiene (DAB)	DAKO	Cat#K4065
Critical commercial assays		
Mouse MCpT-1 Uncoated ELISA Kit with Plates	Thermo Scientific	Cat#88-7503-22
Ara h 1 ELISA 2.0	Indoor Biotechnologies	Cat#EPD-AH1-5
Ara h 2 ELISA 2.0	Indoor Biotechnologies	Cat#EPD-AH2-5
EZ-Link Sulfo-NHS-LC-Biotinylation Kit	ThermoScientific	Cat#21435
Mouse PLA2G7/PAF-AH/Lp-PLA2 ELISA Kit	Novus Biologicals	NBP2-81152
Deposited data		
Microbiome and proteomics data (see Star Protocols)		
Experimental models: Cell lines		
Experimental models: Organisms/strains		
Mouse:C57BL/6 (6–12 weeks of age, male or female)	Charles River Laboratory	Strain No.: 027
Mouse:C3H-HeN	Taconic Biosciences	Strain No.: C3H/HeNTac
Mouse:C57BL/6N (germ-free)	Taconic Biosciences	Strain No.: C57BL/6NTac
Oligonucleotides		
Microbiota primers F: (v3f_341f-CCTACGGGNGGCWGCAG) R: (v4r_806r-GGACTACNVGGGTWTCTAAT)	IDT DNA	N/A
Sanger sequencing primers F: (5'- AGAGTTTGATCCTGGCTCAG-3') R: (5'-CCGTCAATTCCT-TTRAGTTT-3')	IDT DNA	N/A
Recombinant DNA		
Software and algorithms		
Graph Pad Prism v 9.0	GraphPad	https://www.graphpad.com/demos/
FlowJo v10	BD	https://www.flowjo.com/solutions/flowjo
Peaks	Bioinformatics Solutions Inc.	https://www.bioinfor.com/peaksdb/
UniprotKB	Uniprot	https://www.uniprot.org/

Protein Data Bank	RCSB PDB	https://www.rcsb.org/
Allergen Nomenclature	Allergen Nomenclature. Financial contributions from IUIS, EAACI, and AAAAI	https://allergen.org/
Allergen Online	AllergenOnline. University of Nebraska-Lincoln	http://allergenonline.org/
Compare Database	Compare	https://db.comparedatabase.org/
Chimera v1.17.3	University of California San Francisco (UCSF)	https://www.cgl.ucsf.edu/chimera/
ImageJ 1.53q	Fiji	https://fiji.sc/
Illumina MiSeq	Illumina Inc.	https://www.illumina.com/
Cutadapt	Marcel Martin[1]	https://cutadapt.readthedocs.io/
DADA2 (version 1.14.0)	Benjamin Callahan[2]	https://benjjneb.github.io/dada2/
SILVA Database (version 138.1)	SILVA Consortium[3]	https://www.arb-silva.de/
FastTree 2	Morgan N. Price et al.[4]	https://www.microbesonline.org/fasttree/
Phyloseq (version1.30.0)	Paul J. McMurdie & Susan Holmes[5]	https://joey711.github.io/phyloseq/
R (version 3.6.2)	R Foundation for Statistical Computing	https://www.r-project.org/
fastp	Chen et al. [6,7]	
Unicycler (v.0.5.1)	Wick RR et al.[8]	
Bakta	Schwengers et al.[9]	
Roary	Page A et al.[10]	
Other		
Sterile Dish 100 mm x 20 mm CC-treated	Corning	Cat#430167
U/V-bottom 96 well TC-treated microplates	Falcon	Cat#353910
Flat-bottom 96 well high binding microplates	Costar	Cat#3590
23-gauge needle	BD Microlance	Cat#300800
40 µm filter	Falcon	Cat#352340
Microplate reader	Promega	GloMax Discover
SalivaBio Children's Swab	Salimetrics	Cat#5001.06
Flow cytometer	BD	FACSCantoII
Ussing chamber system	Physiologic Instruments	Cat#P2400
Imaging system	Amersham	ImageQuant™ 800
ZipTip with 0.6 µL C_{18} resin	Merck Millipore	Cat#ZTC18S008
UltiMate 3000 High Pressure Liquid Chromatograph	Fisher Scientific	Cat# IQLAAAGABHFAPBMBFB
Orbitrap Exploris™ 240 Mass Spectrometer	Fisher Scientific	Cat#BRE725535
Easy-spray PepMap C18 analytical column 50 cm × 75 µm	Fisher Scientific	Cat#ES903
Non-heparinizing microcapillaries (Fisher Scientific),	Fisher Scientific	Cat#11884040

CellPress

References

1. Martin, M. (2011). Cutadapt removes adapter sequences from high-througput sequencing reads. EMBnet.journal *17*, 10-12. https://doi.org/10.14806/ej.17.1.200.
2. Callahan, B.J., McMurdie, P.J., Rosen, M.J., Han, A.W., Johnson, A.J., and Holmes, S.P. (2016). DADA2: High-resolution sample inference from Illumina amplicon data. Nat Methods *13*, 581-583. 10.1038/nmeth.3869.
3. Quast, C., Pruesse, E., Yilmaz, P., Gerken, J., Schweer, T., Yarza, P., Peplies, J., and Glockner, F.O. (2013). The SILVA ribosomal RNA gene database project: improved data processing and web-based tools. Nucleic Acids Res *41*, D590-596. 10.1093/nar/gks1219.
4. Price, M.N., Dehal, P.S., and Arkin, A.P. (2010). FastTree 2--approximately maximum-likelihood trees for large alignments. PLoS One *5*, e9490. 10.1371/journal.pone.0009490.
5. McMurdie, P.J., and Holmes, S. (2013). phyloseq: an R package for reproducible interactive analysis and graphics of microbiome census data. PLoS One *8*, e61217. 10.1371/journal.pone.0061217.
6. Chen, S. (2023). Ultrafast one-pass FASTQ data preprocessing, quality control, and deduplication using fastp. Imeta *2*, e107. 10.1002/imt2.107.
7. Chen, S., Zhou, Y., Chen, Y., and Gu, J. (2018). fastp: an ultra-fast all-in-one FASTQ preprocessor. Bioinformatics *34*, i884-i890. 10.1093/bioinformatics/bty560.
8. Wick, R.R., Judd, L.M., Gorrie, C.L., and Holt, K.E. (2017). Unicycler: Resolving bacterial genome assemblies from short and long sequencing reads. PLoS Comput Biol *13*, e1005595. 10.1371/journal.pcbi.1005595.
9. Schwengers, O., Jelonek, L., Dieckmann, M.A., Beyvers, S., Blom, J., and Goesmann, A. (2021). Bakta: rapid and standardized annotation of bacterial genomes via alignment-free sequence identification. Microb Genom *7*. 10.1099/mgen.0.000685.
10. Page, A.J., Cummins, C.A., Hunt, M., Wong, V.K., Reuter, S., Holden, M.T., Fookes, M., Falush, D., Keane, J.A., and Parkhill, J. (2015). Roary: rapid large-scale prokaryote pan genome analysis. Bioinformatics *31*, 3691-3693. 10.1093/bioinformatics/btv421.

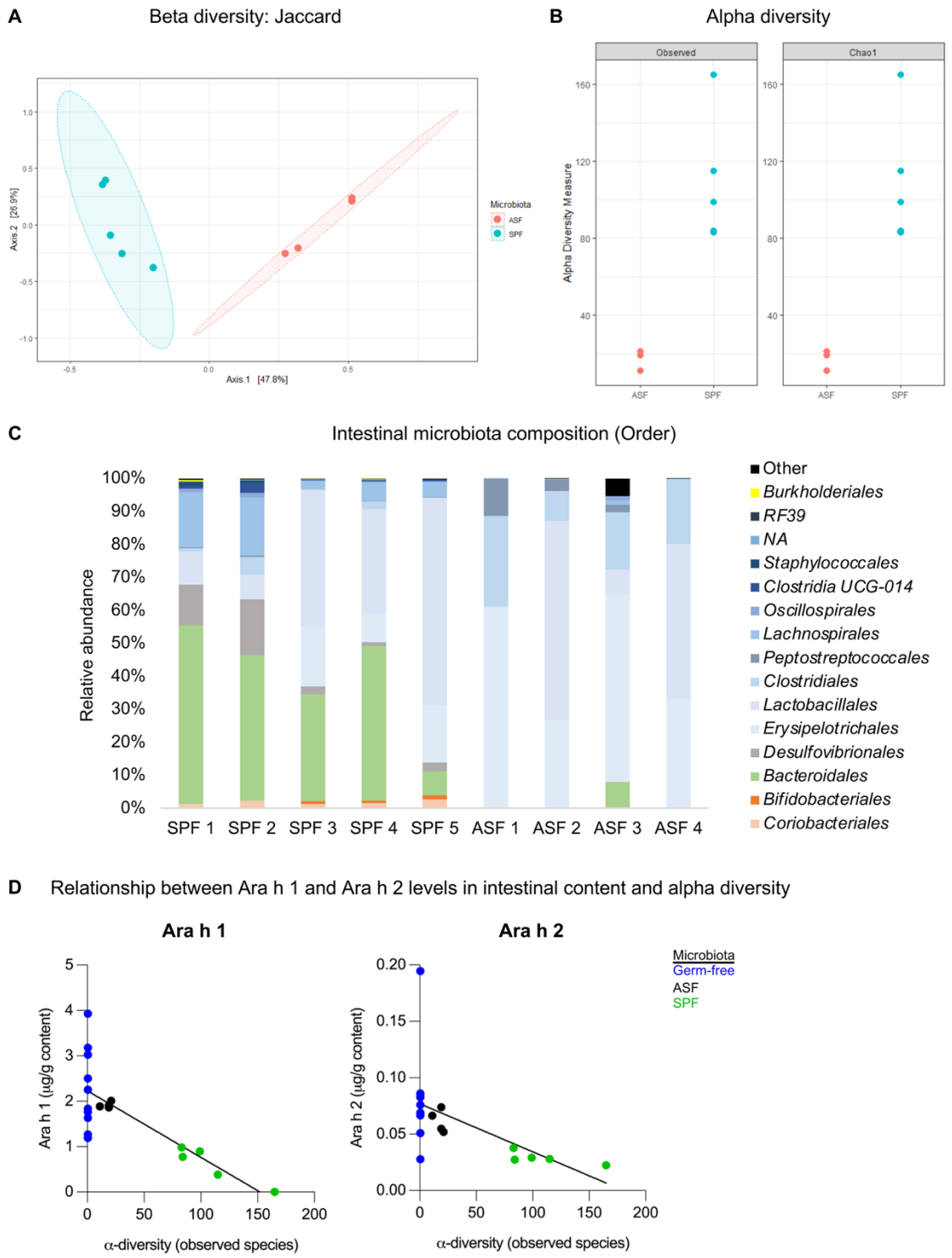

Figure S1. Intestinal microbiota of Altered Schaedler Flora (ASF) and specific pathogen free (SPF) C57BL/6 mice. (A) Beta-diversity (Jaccard index) plot of fecal microbiota of ASF and SPF mice where each dot represents one mouse. (B) Alpha-diversity metrics based on observed species and Chao1 index of ASF and SPF mice where each dot represents one mouse. (C) Order-level relative abundance of the microbial composition of ASF and SPF mice where each bar represents one mouse. (D) Correlation plot of Ara

h 1 (y=-0.01467x + 2.231, R^2=0.5678, P=0.0002) and Ara h 2 (y=-0.0004257x + 0.07693, R^2=0.0137, P=0.0137) against alpha-diversity in small intestinal content of germ free, ASF, and SPF mice. n=4–5 mice per group.

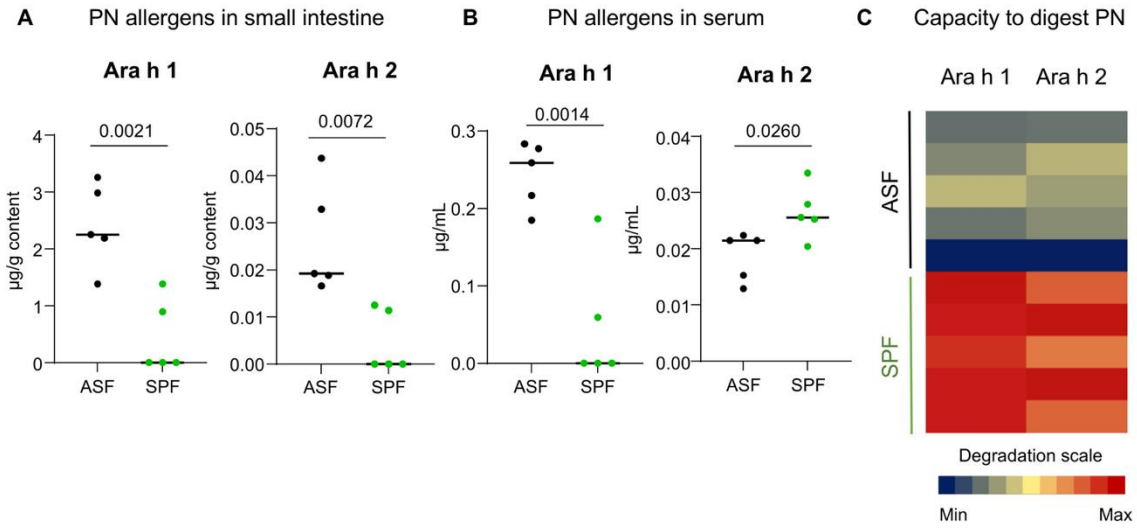

Figure S2. Peanut (PN) digestion by Altered Schaedler Flora (ASF) and specific pathogen-free (SPF) C3H-HeN mice. ASF and SPF C3H-HeN mice were provided a 24 mg bolus of PN i.g. Peripheral blood and small intestinal contents were collected 40 minutes post PN delivery for analysis. n=5 mice per group. PN allergens (Ara h 1 and 2) in small intestinal content (A) and in serum from peripheral blood (B). (C) Heatmap showing digestion capacity of ASF and SPF microbiota of C3H-HeN mice against Ara h 1 and 2. Small intestinal contents were subsequently incubated with PN allergens *in vitro* and remaining allergens were quantified after digestion. Allergen degradation capacity is expressed as the percentage of degraded allergen relative to control non-growth incubations (containing crude peanut extract (CPE)), with the color scale ranging from blue (0% degradation; minimum) to red (100% degradation; maximum). Each row represents one mouse. Significance levels: Ara h 1 SPF vs. ASF (P<0.0001), Ara h 2 SPF vs. ASF (P= 0.0001). Data are presented as mean where each dot represents an individual mouse (A-B), or each row represents one mouse (C). Displayed P values were calculated using an unpaired Student's t-test.

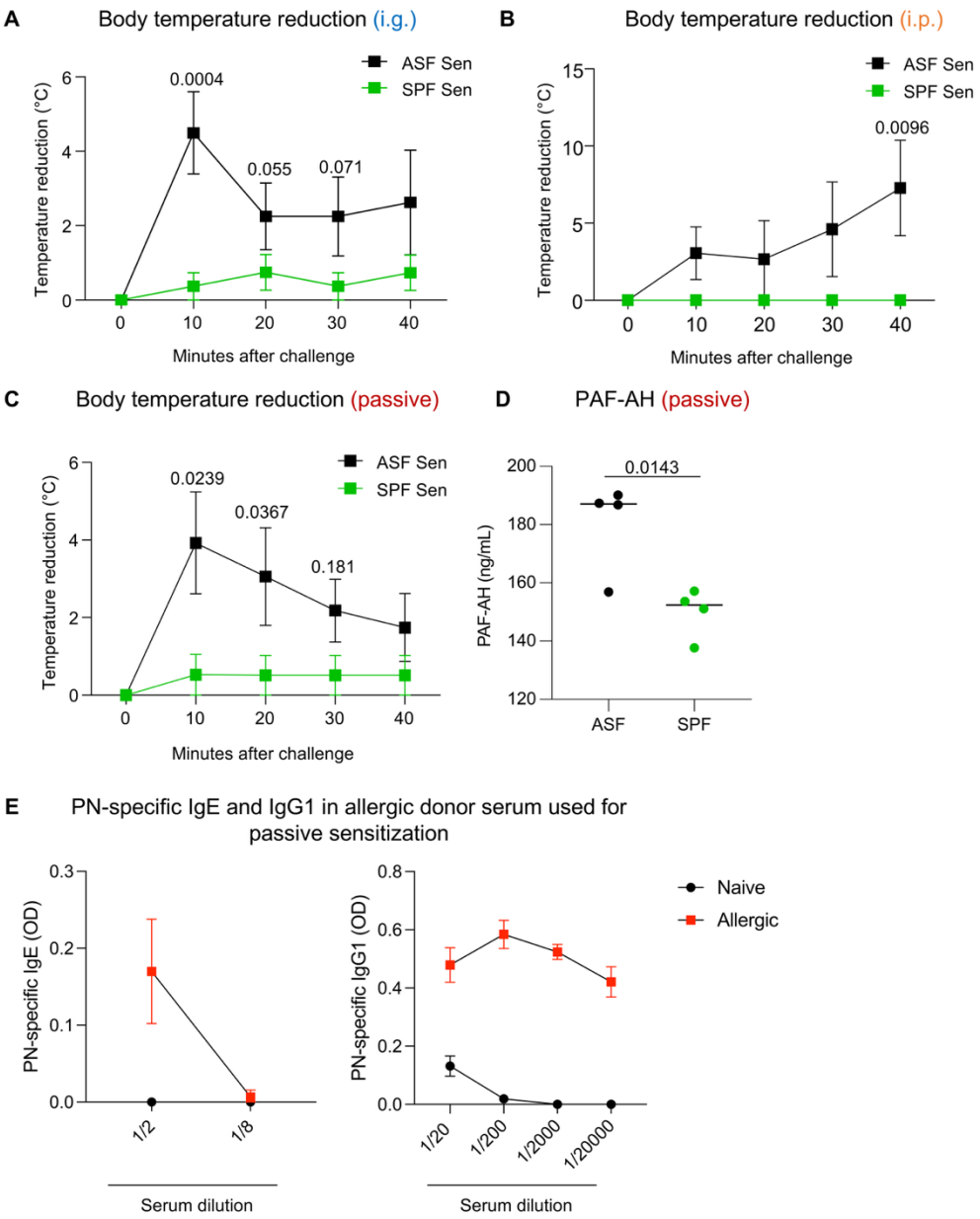

Figure S3. Body temperature reduction of Altered Schaedler Flora (ASF) and specific pathogen-free (SPF) mice in response to peanut (PN) challenge in different sensitization models, and characterization of allergic donor serum used for passive sensitization corresponding to Figure 2. (A-C) Core temperature reduction after PN challenge for intragastrically (i.g.), intraperitoneally (i.p.), and passively sensitized mice, respectively. (D) Serum platelet-activating factor-acetylhydrolase (PAF-AH) after PN challenge for passively sensitized mice. (G) PN-specific IgE and IgG1 in allergic donor serum used for passive sensitization. Data are presented as mean ± SD (A-C, E) and mean where each dot represents one mouse (D). Displayed *P* values were calculated using an unpaired Student's *t*-test.

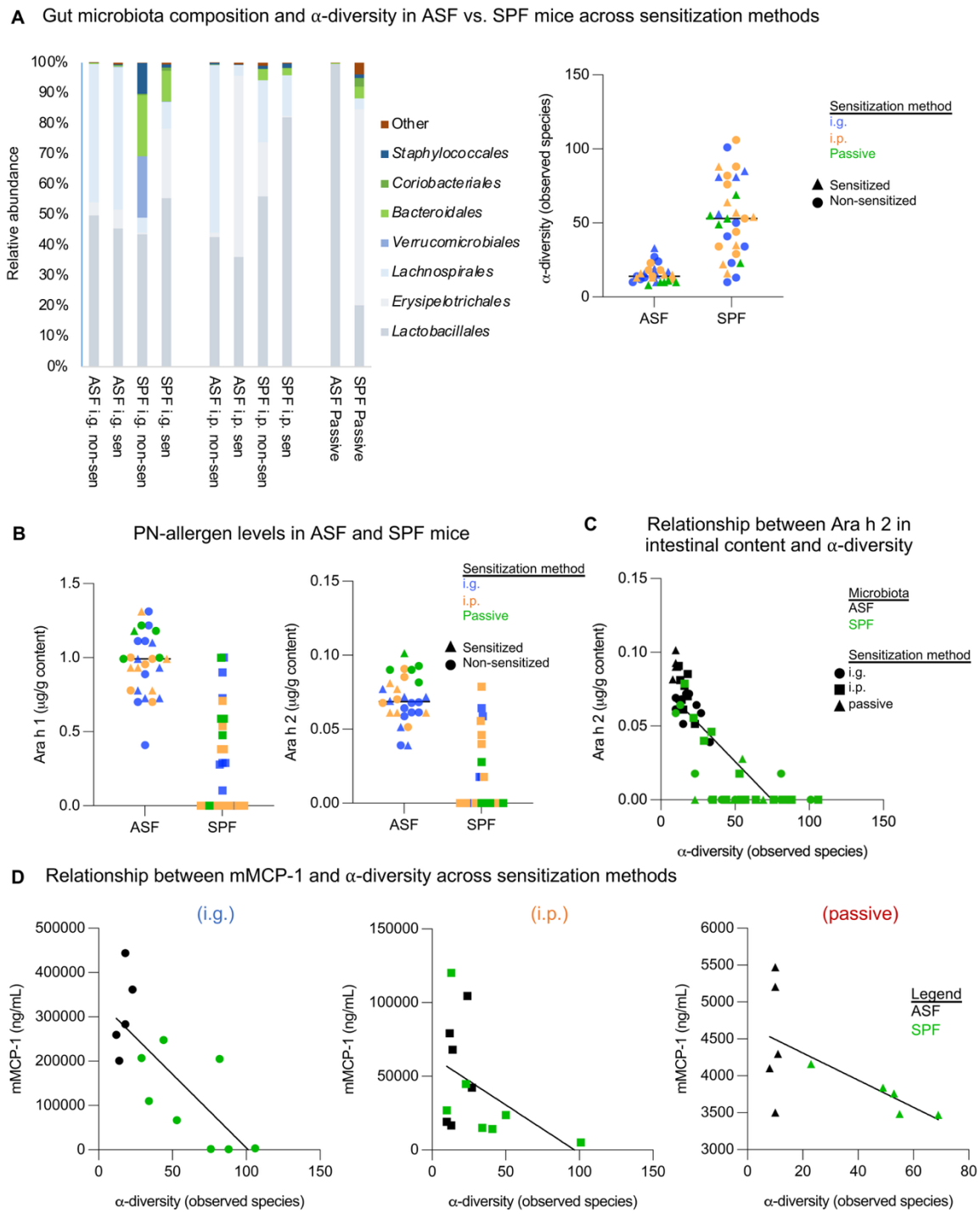

Figure S4. Gut microbiota composition and diversity of ASF and SPF C3H-HeN mice across sensitization methods, and their relationship with peanut (PN)-challenge outcomes (corresponding to Figure 2). (A) Relative abundance of bacterial orders and α-diversity (observed species) in the small intestine across intragastric (i.g.), intraperitoneal (i.p.), and passive sensitization, including sensitized non-sensitized mice. (B) Levels of Ara h 1 and 2 in intestinal content across sensitization methods, including sensitized and non-sensitized mice. (C) Correlation plot of Ara h 1 against α-diversity in small intestinal content (y=-0.001039x + 0.07793, R^2=0.6736, P<0.0001). (D) Relationship between

serum mucosal mast cell protease 1 (mMCP-1) concentrations and α-diversity across sensitization methods.

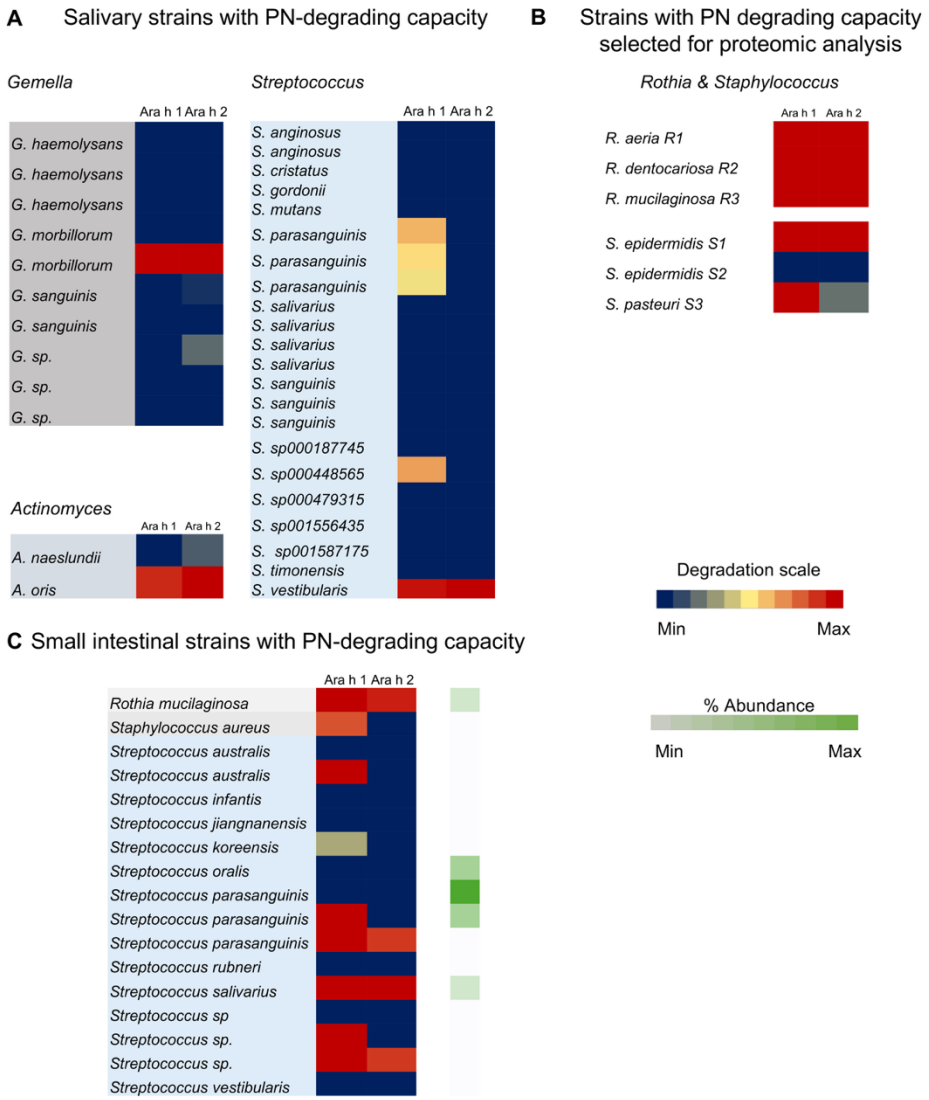

Figure S5. Characterization of peanut (PN)-degrading bacteria isolated from human saliva and small intestine. (A) Heatmap of PN allergen degradation capacity of bacterial strains isolated from saliva. (B) Degradation of Ara h 1 and 2 by bacterial strains that were further characterized in Figures 4 and 5 for their proteomic profiles and effects on mast cell activation. (C) Heatmap of PN allergen degradation capacity of bacterial strains isolated from the small intestine (jejunal aspirates). Color scale (blue-red) represents the percentage of allergen degradation relative to control non-growth incubations, with blue indicating no degradation and red indicating complete degradation. For (C), the relative abundance of each isolated strain is shown using a green scale, ranging from light green (low abundance) to dark green (high abundance), calculated as a percentage of total isolates from saliva.

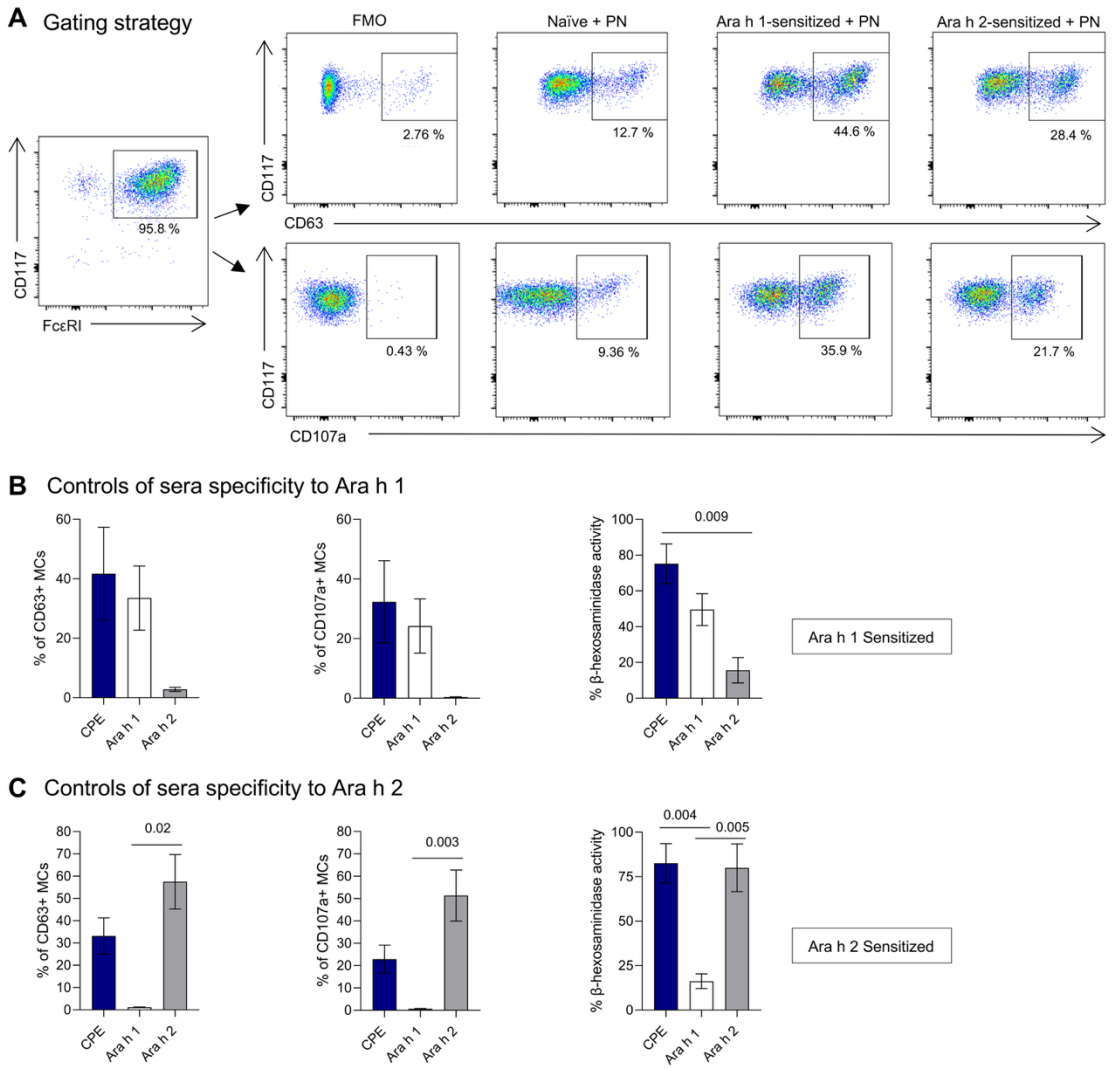

Figure S6. Characterization of sera specificity from mono-sensitized mice. (A) Gating strategy. Bone marrow-derived mast cells (MCs) co-express FcεRI and CD117. MC activation was detected by the expression of CD63 and CD107a. Gates of positive and negative controls are shown. Controls of sera specificity to (B) Ara h 1 and (C) Ara h 2. MCs were sensitized with a pool of sera from Ara h 1- or Ara h 2-allergic mice, respectively, and then challenged with undigested PN (blue), native Ara h 1 (white) or recombinant Ara h 2 (grey). Data are presented as the mean +/- SEM of each group. Displayed *P* values were calculated using a one-way ANOVA with Tukey's post-hoc test in panels B and C (CD107a and β-hexosaminidase activity) or using Kruskal-Wallis test with Dunn´s post hoc test in panel C (CD63).

Protease repertoire of *Rothia* species identified by whole genome sequencing

	Gene	Annotation
Intracellular	pepB	leucyl aminopeptidase
	pepN	aminopeptidase N
	pepP	Xaa-Pro aminopeptidase
	pepO	peptidase M13
	map	type I methionyl aminopeptidase
	pqqL	peptidase M16
	dacB	D-alanyl-D-alanine carboxypeptidase/D-alanyl-D-alanine-endopeptidase
	htpX	Zn-dependent protease with chaperone function
	argE	dipeptidase
	degQ	MarP family serine protease
	lepB	signal peptidase I
	lspA	signal peptidase II
	lAP4	M18 family aminopeptidase
	CPBP family intramembrane metalloprotease domain-containing protein	CPBP family intramembrane metalloprotease domain-containing protein
	ptrB	oligopeptidase B
	pcp	peptidase C15
	peptidase E	peptidase E
	peptidase A24	peptidase A24
	glpG	rhomboid family intramembrane serine protease
	ATP-dependent protease Clp, ATPase subunit	ATP-dependent protease Clp, ATPase subunit
	clpS	ATP-dependent Clp protease adapter ClpS
	clpX	ATP-dependent Clp protease ATP-binding subunit ClpX
	clpP	ATP-dependent Clp protease proteolytic subunit
	ftsH	ATP-dependent zinc metalloprotease FtsH
	protease/lipase ABC transporter permease/ATP-binding protein	protease/lipase ABC transporter permease/ATP-binding protein
	immA	ImmA/IrrE family metallo-endopeptidase
	peptidase M48	peptidase M48
	M23 family metallopeptidase	M23 family metallopeptidase
	prepilin peptidase	prepilin peptidase
	Membrane protein related to metalloendopeptidase	Membrane protein related to metalloendopeptidase
	Periplasmic protease	Periplasmic protease
	nlpD	Murein DD-endopeptidase MepM and murein hydrolase activator NlpD, contains LysM domain
	pepE	peptidase S51
	tonB	serine protease
	rseP	zinc metalloprotease
	Peptidase C39 domain-containing protein	Peptidase C39 domain-containing protein
	CAAX amino terminal protease family protein	CAAX amino terminal protease family protein
	CAAX protease self-immunity	CAAX protease self-immunity
	M48 family peptidase	M48 family peptidase
	Peptidase M20 domain-containing protein 2	Peptidase M20 domain-containing protein 2
	Endopeptidase La	Endopeptidase La
	Site-2 protease family protein	Site-2 protease family protein
	Peptidase family M50	Peptidase family M50
	Peptidase-M3 domain-containing protein	Peptidase-M3 domain-containing protein
	L,D-transpeptidase	L,D-transpeptidase
	Peptidase-A24 domain-containing protein	Peptidase-A24 domain-containing protein
	lspA	Lipoprotein signal peptidase
Extracellular	peptidase S8	peptidase S8
	group_294	peptidase S8
	group_1522	peptidase S8
	group_2124	Peptidase S8
	group_2125	peptidase S8
	Peptidase S8	Peptidase S8
	aprE	peptidase S8
	acm	serine protease like S8
	group_5120	peptidase S8
	Subtilisin	peptide S8
	Peptidase-S8 domain-containing protein	Peptidase-S8 domain-containing protein
	eMpr	V8-like Glu-specific endopeptidase
	Minor extracellular protease vpr	Minor extracellular protease vpr
	Extracellular basic protease	Extracellular basic protease
Both/Unknown	Di- and tripeptidase	Di- and tripeptidase
	prolyl aminopeptidase	prolyl aminopeptidase
	serine protease	serine protease
	Peptidase S1 domain-containing protein	Peptidase S1 domain-containing protein
	Peptidase-M78 domain-containing protein	Peptidase-M78 domain-containing protein
	group_2044	peptidase
	group_2073	peptidase
	zinc metalloprotease	zinc metalloprotease
	Peptidase C51 domain-containing protein	Peptidase C51 domain-containing protein
	Peptidase	Peptidase
	group_2882	Peptidase
	group_2894	peptidase
	group_2945	peptidase
	peptidase	peptidase
	group_2952	peptidase
	group_2963	peptidase
	group_2964	peptidase
	Zn-dependent proteases	Zn-dependent proteases
	group_5239	zinc metalloprotease
	group_6644	serine protease
	X-Pro dipeptidyl-peptidase (S15 family) domain protein	X-Pro dipeptidyl-peptidase (S15 family) domain protein
	Peptidase-M23 domain-containing protein	Peptidase-M23 domain-containing protein
	Peptidase C56	Peptidase C56
	Peptidase-S9 domain-containing protein	Peptidase-S9 domain-containing protein
	Pyroglutamyl-peptidase I	Pyroglutamyl-peptidase I
	Zinc-dependent metalloprotease	Zinc-dependent metalloprotease

Gene presence

No Yes

Degradation scale

Min Max

Ara h 1

Ara h 2

Allergen degradation capacity (western blotting)

Figure S7. Protease repertoire of *Rothia* species identified by whole-genome sequencing. Heatmap showing predicted proteases encoded in *Rothia* genomes, including *Rothia mucilaginosa* (R3), *Rothia dentocariosa* (R2), and *Rothia aeria* (R1), as well as additional species without specific isolate names. Rows represent protease genes grouped by subcellular localization (intracellular, extracellular, or both/unknown) with functional annotations, and columns correspond to individual *Rothia* genomes. Blue shading indicates gene presence (light blue: not present, dark blue: present). Green-highlighted labels denote duplicate recognition of the same protease across different sequence annotations. Allergen degrading capacity against Ara h 1 and Ara h 2, determined by Western blotting, is shown at the bottom right for reference and the heat map colour scale (blue-red) represents the percentage of allergen degradation relative to control non-growth incubations (crude peanut extract).

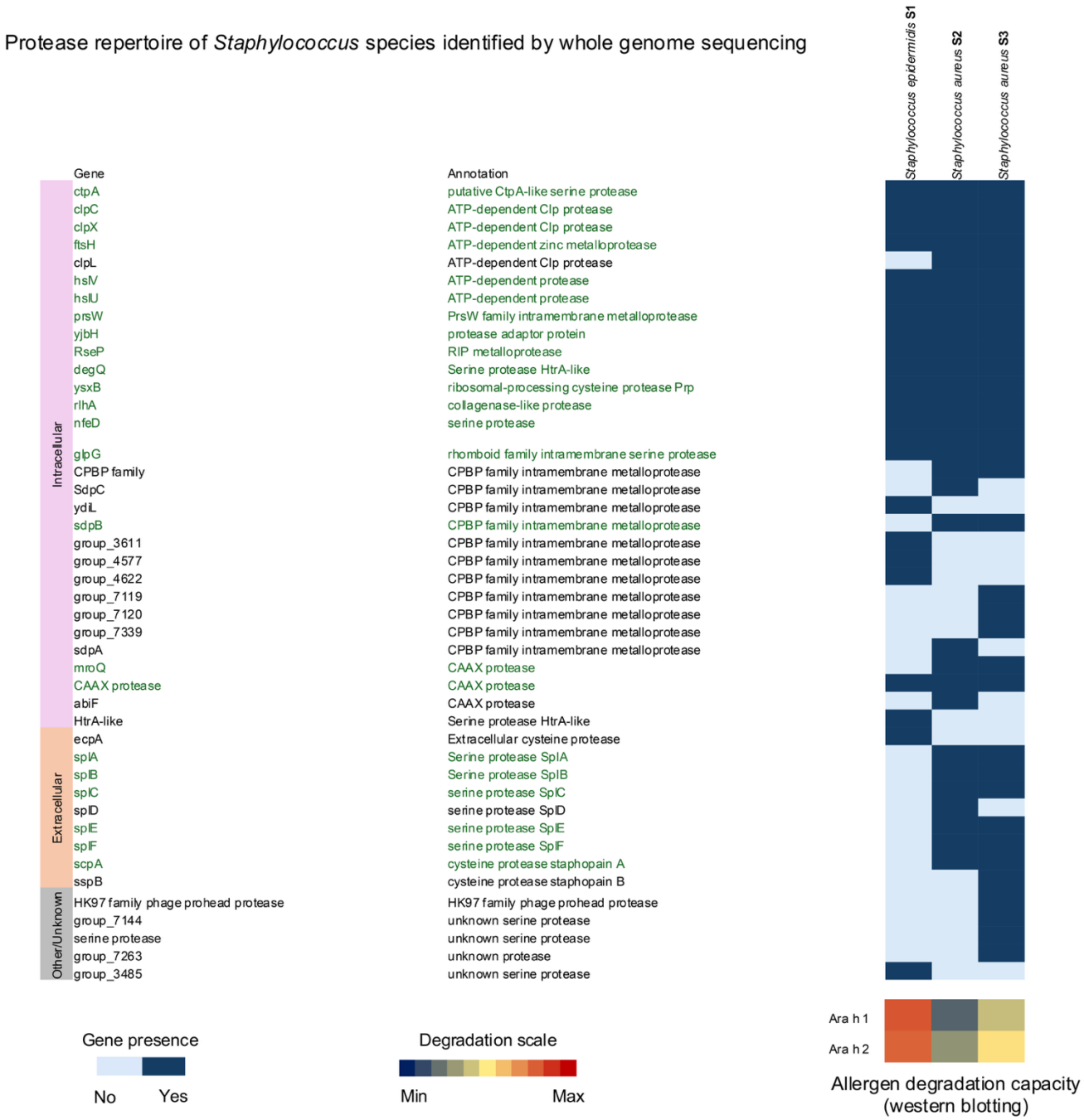

Figure S8. Protease repertoire of *Staphylococcus* species identified by whole-genome sequencing. Heatmap showing predicted proteases encoded in *Rothia* genomes, including *Staphylococcus epidermidis* (S1), *Staphylococcus aureus* (S2), and *Staphylococcus aureus* (S3). Rows represent protease genes grouped by subcellular localization (intracellular, extracellular, or both/unknown) with functional annotations, and columns correspond to individual *Staphylococcus* genomes. Blue shading indicates gene presence (light blue: not present, dark blue: present). Green-highlighted labels denote duplicate recognition of the same protease across different sequence annotations. Allergen degrading capacity against Ara h 1 and Ara h 2, determined by Western blotting,

is shown at the bottom right for reference and the heat map colour scale (blue=0%, red=100%) represents the percentage of allergen degradation relative to control non-growth incubations (crude peanut extract).

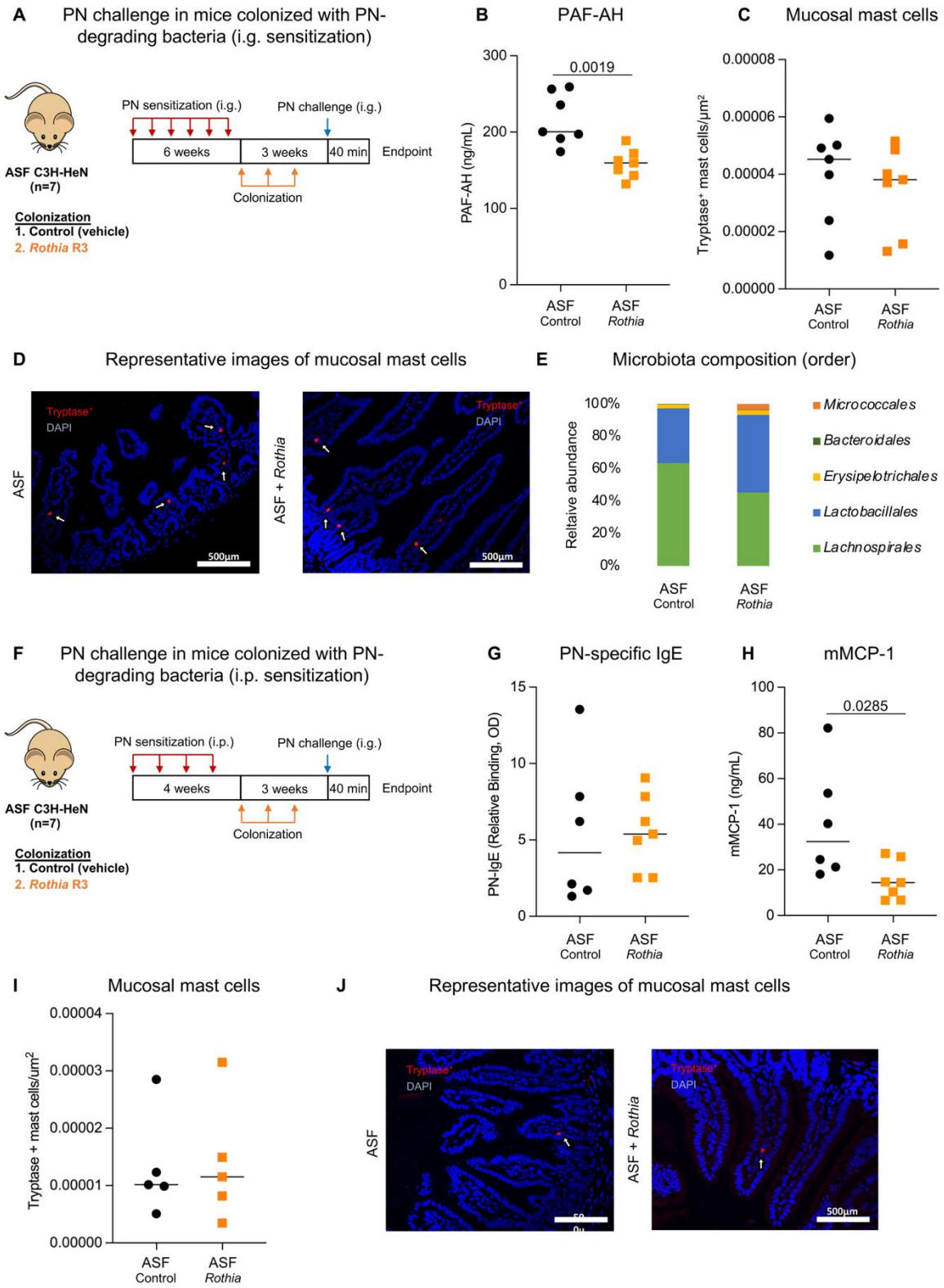

Figure S9. (A-D) Peanut (PN) intragastric sensitization and challenge in ASF-microbiota mice colonized with or without *Rothia* R3. (A) Experimental design. C3H-HeN mice with altered Schaedler flora (ASF) microbiota sensitized i.g. to PN once per week for 6 weeks.

One week after the last sensitization, mice were co-colonized with *Rothia* R3 once per week for three weeks. Mice were provided a PN bolus i.g. three weeks after the first colonization and sacrificed 40 minutes later. n=7 mice per group. (B) Serum platelet activating factor-acetylhydrolase (PAF-AH). (C) Tryptase-positive mast cells quantified in small intestinal sections. (D) Representative images of small intestinal mucosal tryptase-positive mast cells. (E) Small intestinal microbiota composition (order). (F-H) PN i.p. sensitization and challenge in ASF-microbiota mice colonized with or without *Rothia* strains. (F) Experimental design. C3H-HeN mice with ASF microbiota sensitized i.p. to PN once per week for 4 weeks. One week after the last sensitization, mice were co-colonized with *Rothia* strains once per week for three weeks. Mice were provided a PN bolus i.g. three weeks after the first colonization and sacrificed 40 minutes later. n=7 mice per group. (G) Serum PN-specific IgE before PN challenge. (H) Serum mMCP-1 after PN challenge. (I) Tryptase-positive mast cells quantified in small intestinal sections. (J) Representative images of small intestinal mucosal tryptase-positive mast cells.Displayed *P* values were calculated using an unpaired Student's *t*-test.

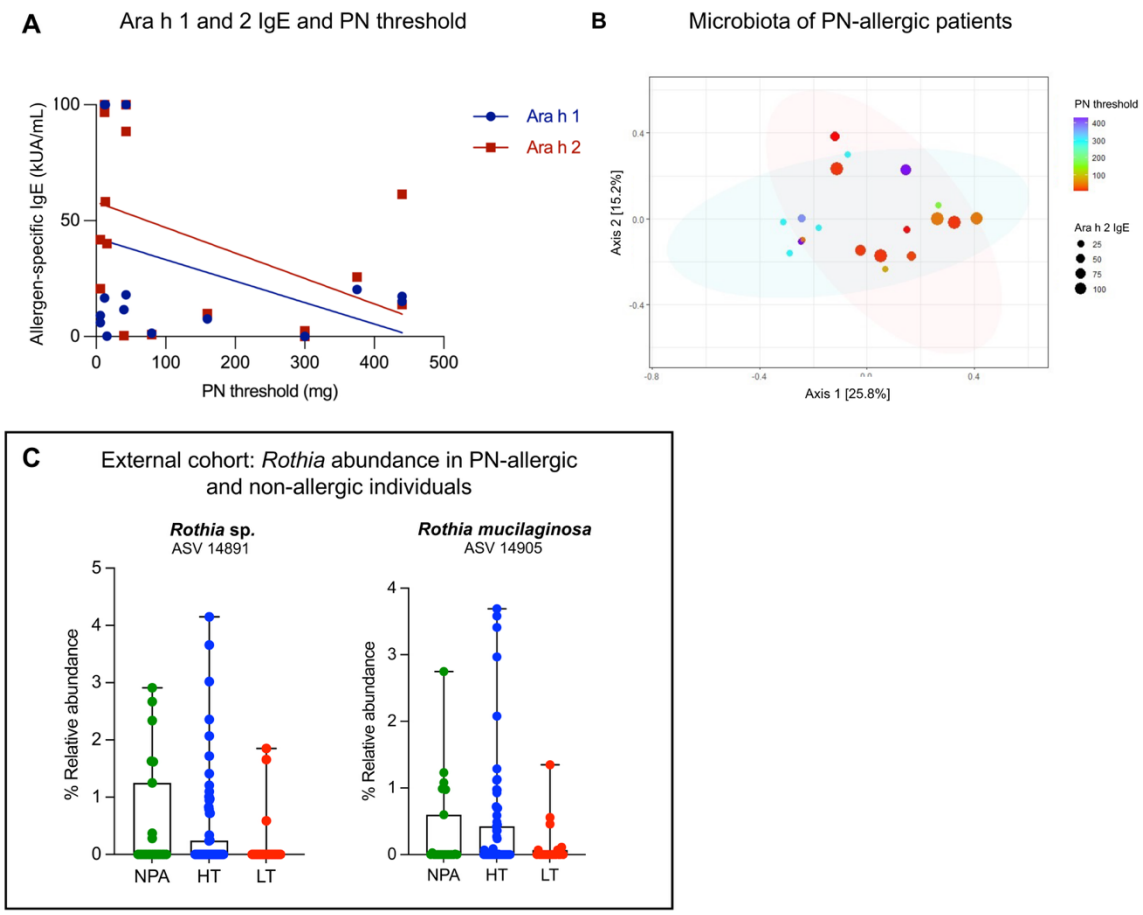

Figure S10. (A-B) Peanut (PN)-allergic patients (n=19) were tested for PN threshold using increasing PN concentrations before enrolment in oral immunotherapy. (A) Correlation plot of Ara h 1-specific IgE (y= -0.09x + 42.45, R^2 = 0.15, P=0.11) and Ara h 2-specific IgE (y= -0.11x + 58, R^2= 0.21, P=0.06) against PN threshold. (B) Bray-Curtis-tomrepresents serum Ara h 2-specific IgE levels, while dot color corresponds to the PN threshold (scales shown). (C) Abundance of *Rothia* species in saliva from analysis of 16s rRNA data from an external cohort including 120 children (23 non-PN-allergic controls (NPA), 74 PN-allergic with high PN threshold (HT; >443 mg), and 23 PN-allergic with low PN threshold (LT; <443 mg)) who underwent double-blind, placebo-controlled PN challenges. Data are presented as interquartile range (IQR) with whiskers extending to the min and max data points.

Table S1: Detailed subject demographics. Peanut, PN; Male, M; Female; F.

Status	ID	Sex	Age	Race	PN threshold (mg)	Ara h 1 IgE (kUA/mL)	Ara h 2 IgE (kUA/mL)
PN-allergic saliva	PN1	F	10	Unknown	300	0.10	1.19
	PN2	F	7	Asian	300	0.10	2.44
	PN3	F	1	White	300	0.10	0.10
	PN4	F	27	White	440	15.2	13.8
	PN5	F	6	White	375	20.3	25.7
	PN6	M	6	White	40	11.6	0.41
	PN7	M	7	White	300	N/A	N/A
	PN8	F	15	White	440	17.3	12.1
	PN9	M	9	White	12	100	25.8
	PN10	M	13	White	6	9.11	0.19
	PN11	M	10	White	43	18	88.5
	PN12	F	13	White	13	100	58.2
	PN13	F	13	White	43	100	100
	PN14	F	14	White	12	100	96.7
	PN15	M	9	White	6	5.95	20.7
	PN16	M	11	Asian	160	7.62	9.92
	PN17	F	2	Asian	80	1.41	0.84
	PN18	F	2	Black/African American	15.5	0.18	40.1
	PN19	M	4	Unknown	12	16.7	100
Non-PN-allergic saliva	HV1	M	35	White	N/A	N/A	N/A
	HV2	M	22	White			
	HV3	M	20	White			
	HV4	F	26	White			
	HV5	F	33	White			
	HV6	F	24	White			
	HV7	F	18	White			
	HV8	M	30	White			
	HV9	F	38	White			
	HV10	F	20	Black/African American			
	HV11	M	40	Asian			
	HV12	F	66	White			
	HV13	M	33	White			
Non-PN-allergic jejunal washes	HV14	M	57	White	N/A	N/A	N/A
	HV15	M	63	White			
	HV16	F	57	White			
	HV17	F	35	White			
	HV18	M	53	White			

Table S2: Serum characterization for western blotting. Peanut, PN.

Serum	Total IgE levels (kU/L)	PN IgE (kUA/mL)	rAra h 1 IgE (kUA/mL)	rAra h 2 IgE (kUA/mL)	rAra h 3 IgE (kUA/mL)	rAra h 8 IgE (kUA/mL)	rAra h 9 IgE (kUA/mL)	Sex	Age	Positive Skin Prick Test	Other hypersensitivities
A	12.49	Unknown	52.9	>100	26.6	0.02	0.02	F	30	PN, pollen of Cupressaceae, Acer pseudoplatanus, olive, grasses, Salsola, dog, cat, horse and rabbit. Minimal reaction to mites and aspergillus	Persistent moderate asthma and intermittent rhinoconjunctivitis
B	176	54.9	20.4	24.5	0	0	0	F	19	PN, chickpea, arizonica pollen, minimal reaction to pine nuts	Atopic dermatitis